UNIVERSITA' DEGLI STUDI DI PARMA

Dottorato di ricerca in FISIOPATOLOGIA SISTEMICA

Ciclo XXVI

BONE MARROW MICROENVIRONMENTAL CONTROL OF HEMATOPOIETIC STEM CELL TRAFFICKING

Coordinatore:
Chiar.mo Prof. Enrico Maria Silini

Tutor:
Chiar.mo Prof. Federico Quaini

Dottorando: Ferraro Francesca

To Marta, Renato, Stefano and Stephen

INTRODUCTION

The pathophysiology of diabetes mellitus

Diabetes Mellitus: Progression, Forms and Causes.

Diabetes mellitus (DM) is a chronic incurable disease that disrupts the physiological balancing of blood sugar metabolism and leads to acute and chronic complications that yield high morbidity and mortality. The incidence and prevalence of diabetes worldwide has reached an alarming proportion. Based on a survey of 199 countries, it has been estimated that the number of adults with diabetes has doubled within the past three decades from 153 million in 1980 to 347 million in 2008. Although 70% of the observed increase is attributed to population growth and ageing, the number also reflects the unfortunate global shift towards a western lifestyle of unhealthy diet and physical inactivity resulting in increased obesity [1].

There are two types of diabetes, classified as type 1 and type 2 diabetes, which also have multiple sub-types [2]. Type 1 is an immune-mediated form where abnormal antibodies attack and damage Langerhans cells, which are the site of insulin production in the endocrine portion of the pancreas. Unfortunately, the specific antibody or the triggering event initiating the autoimmune process underlying many cases of type I diabetes often remains unknown [2].

Type 2 diabetes, which is the most common form of diabetes accounting for >90 percent of diabetic cases, is associated with two physiological defects: insulin resistance in the insulin-targeted peripheral tissues (adipose tissue, muscle and

liver) and impaired insulin secretion. The type II disease evolves over many years and progresses through multiple stages.

Although there is some controversy about the precise sequence of events in the natural history of type 2 diabetes, the development of peripheral insulin resistance is typically an early event. To compensate for insulin resistance, pancreatic beta cells begin to increase insulin production, which causes plasma insulin levels to rise. However, because the compensation may not be complete the patient may develop impaired glucose tolerance and/or impaired fasting glucose. As the disease evolves, there is a progressive impairment in the ability of the beta cell to secrete insulin. The onset of overt diabetes begins when impaired beta cell function exceeds the ability to compensate for the preexisting insulin resistance. Once insulin resistance is complete, the magnitude of hepatic glucose production elevates fasting plasma glucose levels resulting in severe hyperglycemia and decompensated diabetes.

Although the primary (genetic) causes of insulin resistance are not known, much is known about some factors that contribute to the pathogenesis of insulin resistance. Most patients with type 2 diabetes are obese, and the increase in adiposity is believed to be an important causal factor in the development of insulin resistance. The increase in adipose tissue is associated with an increase in plasma free fatty acid levels, which promotes hepatic glucose production and inhibits peripheral glucose utilization. In addition, the diabetic state leads to a vicious cycle in which insulin deficiency and hyperglycemia both exacerbate insulin resistance

and further impair insulin secretion [3]. Impaired glucose tolerance (IGT) defines a pre-diabetic state of high glucose level that does not meet the criteria for diabetes diagnosis but it is associated with insulin resistance and increased risk of cardiovascular pathology. IGT may precede type 2 diabetes mellitus by many years. Other rare causes of diabetes accounts for the remaining 1-2% of all diabetes. Briefly, in MODY or "Maturity onset diabetes of the young" specific genetic mutations have been identified. The most common is mutation of HFN on chromosome 12, followed by mutation of glucokinase (a sensor for glucose) in chromosome 7. "Latent autoimmune diabetes of the adult" (LADA) is a form of diabetes where inflammation of the pancreatic islet causes abnormal pancreatic beta cell activity. Diabetes can also be caused by any pathologic process that leads to pancreas disruption (chronic pancreatitis, cancer, hemochromatosis etc), by drugs (.i.e. corticosteroids) and viral infection or be part of rare genetic syndrome [3].

Regardless of the underlying cause the evolution and the development of diabetes and related complications appears to be solely due poorly controlled hyperglycemia and its metabolic consequences. That is why so far, given the lack of a pathogenetic cure, the treatment for diabetes focuses of properly controlling the glycemic index, which is often very difficult to obtain[4].

The Pathophysiology of Diabetes Mellitus

DM is a systemic disease that is associated with a significantly reduced quality of life due to end stage multi organ dysfunction such as nephropathy, generalized microangiopathy and macroangiopathy with atherosclerosis, retinopathy and

neuropathy [2]. As mentioned, these complications have been traditionally attributed to the toxic effect of chronic high glucose levels on tissue parenchymal cells. These elevated glucose levels cause non-enzymatic glycosylation of proteins with production of advanced glycation end-products (AGEs) and subsequent changes in their solubility and functions). This seems to be mediated by the high concentration of reactive oxygen species (ROS) induced by the overflowing mitochondrial respiratory chain[5]. This increased production of ROS leads to the activation of damage-related signal transduction pathways that induce profound changes in vascular endothelial and smooth muscle cells and subsequent modifications of the extracellular matrix (ECM).

Consequently, DM patients have a 2-3-fold higher risk of developing cardiovascular disease (CVD), owing to the widespread endothelial dysfunction, which is considered the first step in the atherogenetic process [6,7]. Atherosclerotic vascular disease in DM is aggressive, multifocal, distal and develops earlier than in non-DM subjects. Microvascular complications, including retinopathy, nephropathy, and neuropathy, develop as a consequence of structural and functional damage to the microcirculation of target organs. Typical morphological features include thickening of the basement membrane, loss of pericyte coverage, capillary rarefaction, excess deposition of stiff EMC components leading to reduced perfusion, atrophic changes, and fibrosis [7]. All these morphological features are reflected by organ dysfunctions, including visual loss, impaired glomerular filtration or tubular resorption, reduced nerve conduction velocity.

Diabetes Mellitus and the Hematopoietic System

The hematopoietic system or blood system is also an organ that is negatively impacted by DM, however, the effect of DM on the blood has been relatively under investigated. Interestingly, nerves, vessels, ECM, all of which are damaged in DM patients, are also components of the bone marrow microenvironment or "niche" that are critical for maintaining proper hematopoiesis[8]. More recent observations have advanced the idea that diabetes alters the number, function and motility of hematopoietic stem cells (HSCs) [9-11]and causes BM neuropathy[12]. Moreover, given that various hematopoietic cell population participate in organ repair, the hypothesis that diabetes-related damage to the bone marrow and HSCs perpetuates the wide-spread organ damage found in DM patients has emerged. This notion potentially unveils new and intriguing therapeutic perspectives for prevent diabetic complications other than tight glycemic control. **Therefore, understanding precisely how diabetes affects the physiology of the bone marrow microenvironment and hematopoietic stem cell activity will provide significant insight into the physiopathology and progression of diabetes as well as open new avenues for developing novel anti-diabetic therapies.**

To clarify the features and mechanisms driving BM pathology in diabetes, we present the existing data of how complex cellular networks that comprise the bone marrow microenvironment orchestrate HSC function, survival and trafficking.

Hematopoietic system and hematopoiesis

The mammalian hematopoietic system or simply 'the blood' is a dynamic and versatile organ system that is comprised of a network of specialized cell types that regulate physiological functions such as systemic oxygen delivery, wound healing and defense against external and internal pathogens. This diverse network of cell populations are maintained by and originate from a population of multi-potent somatic stem cells called hematopoietic stem cells (HSCs).

In order for HSCs to maintain homeostasis of the hematopoietic system for the entire lifespan of an organism and they carefully balance decisions between differentiation (*commitment)* towards mature blood cell production and self-duplication (*self-renewal*) processes to replenish and maintain the HSC pool. Perturbations in HSC biology can impair basic physiological functions such as pathogen defense, wound healing, and systemic oxygen delivery, as well as contribute to the development of blood cancers[13]. Therefore, understanding the molecular cues that dictate HSC behavior under both homeostatic and physiopathological conditions will provide a foundation for developing novel therapeutic strategies for correcting disease of the blood.

In adult mammals, hematopoiesis predominantly occurs within the bone marrow, which is situated within the bone cavity. Here HSCs reside in specialized compartments called 'niches' where they are retained in a quiescent state [14]. Primitive HSCs divide giving rise to progenitor cells that can proliferate and differentiate into all the lineages of blood cells (Figure 1).

Spontaneous or induced failure at any point in the hematopoietic cascade can lead to abnormal production of blood cell lineages and eventually to a vast variety of hematopoietic disorders such as leukemia, lymphoma, anemia, thrombocytopenia. Many of these disorders still lack effective pharmacologic treatments and therefore often yield high mortality rates.

Bone marrow transplantation (BMT) is a form of regenerative medicine that is used to treat a wide variety of human hematological diseases and disorders [15-18]. Prior to bone marrow transplant, patients are administered radiation and/or chemotherapy (*conditioning*) that serve to ablate a patient's entire hematopoietic system, both healthy and diseased cells. Following conditioning therapy, patients are given either an autologous or allogeneic stem cells. For an autologous transplant, patients are infused with their own *healthy* HSCs that were collected prior to ablative conditioning. Alternatively, patients that receive an allogeneic transplant are infused with bone marrow cells taken from a healthy donor[15].

The foundation of transplantation therapy is built upon the principles of HSC trafficking. For example, HSCs have the ability to travel out the bone marrow into the peripheral blood, a process referred to a HSC mobilization and vice-versa (homing, lodgment and engraftment)[19]. This ability can be traced back to embryonic life where HSCs utilize the circulatory system to travel from specific embryonic and extra-embryonic sites to the fetal liver, and ultimately ending their developmental journey in the bone marrow (BM) where they carry out definitive lifelong hematopoiesis[20].

The emergence of the hematopoietic system.

The first site of emergence of definitive HSCs in mammals is controversial. Anatomically, the earliest sign of hematopoietic activity in both humans and mice can be found in the yolk sac around embryonic day 7[21-23]. Definitive HSCs originate at E8.5 from an intraembryonic site near the aorta, the para-aortic splanchnopleura (P-Sp) that becomes the aorta-gonad-mesonephros (AGM) region[24]. Other authors identified the allantoic mesoderm of the placenta, an extraembryonic site as a site for multipotent HSCs in the early embryo between E8.5 and E9.5[25-27]. This has been corroborated by studies in heartbeat deficient Ncx1−/- embryos, which do not survive beyond E10.5 due to the absence of functional circulation, suggest that HSCs may be independently generated in the placenta[28]. When the circulatory system becomes operative, definitive HSCs and myeloerythroid progenitors are capable to migrate from the embryonic hematopoietic sites through the circulation, starting their migratory journey by colonizing fetal liver at E10.5[29]. From the fetal liver, HSCs migrate to the BM and definitively establish their home shortly before birth at day E17.5 [30] However, functional HSCs will only exit the fetal liver and migrate when the BM environment is able to support their engraftment and self-renewal. Mechanisms regulating trafficking of HSCs before birth are not well known. However, none of the knockout animals deficient in a single molecule mediating adhesion events of HSCs/progenitors under flow during fetal or adult life (e.g. selectins and α4 integrins) display deficits in fetal liver colonization, suggesting redundancy of adhesion mechanisms mediating embryonic HSC migration [31].

In adult life, a small number of HSCs continue their travel from bone marrow to the blood and back for reasons that are not yet clear. Circulating HSCs can "home" to the bone marrow and lodge into specific microenvironments termed the "niche" that allow their survival, and regulate their self-renewal and proliferation[32,33]. Conversely, BM HSCs egress constitutively into the bloodstream by a reverse phenomenon. As we mentioned above, clinical HSC transplantation capitalizes on this natural phenomenon through the enforced release of stem cells (referred to as "mobilization") by cytokines, such as G-CSF, and/or chemotherapy to facilitate their collection in blood by leukapheresis (ref stembook). This point is exemplified by the fact that following simple intravenous infusion HSCs/progenitors are be able to "find their way" to the BM niche and reconstitute the BM hematopoietic reservoir. These therapies significantly improve the clinical outcome of patients with a variety of oncologic and non-oncologic diseases.

The hematopoietic stem cell niche and its components

HSC trafficking is in large part influenced by the bone marrow microenvironment also known as the HSC niche. The niche concept, as an HSC-regulatong entity, was first introduced ain 1978 by Ray Schoefield[34]. Since this seminal report an enormous amount of data has been generated to precisely characterize the niche components that are critical to maintain HSCs homeostasis and trafficking. In figure 2 we summarized the niche components that have been identified and characterized so far. Each component is described in more details in the text below.

The Endosteal Hematopoietic Niche

Given that HSCs line the endosteum, it was initially proposed that osteolineage cells were a potential supportive component of the HSC niche. Intriguingly, one of the very first studies describing cells that behaved like osteogenic-cell was actually seeking to determine why hematopoiesis was located in the bone. Tavassoli and Crosby [35] placed bone marrow fragments into non-bony tissues to see if the addition on non-hematopoietic bone cells could enable engraftment of hematopoietic cells in those tissues. Hematopoiesis occurred only if a bony ossicle with microcirculation formed. Within the bone marrow, the endosteal surfaces of bone were recognized as a rich source of primitive hematopoietic cells by studies that analyzed preserved tissue at progressive distances from the endosteum [36,37].

These studies suggested that endosteum was a site of enrichment for hematopoietic stem/progenitor cells (HSPCs) and therefore, the location of the HSC niche. This issue is controversial, however. A number of histologic studies have indicated that HSC are perivascular in the unmanipulated mouse bone marrow[38-41]. Several different imaging approaches have demonstrated that HSCs localize to endosteal surfaces shortly after transplant, while more mature hematopoietic progenitor cells (HPCs) localize further away[42-45].. Hematopoietic stem cells that were closely associated with the endosteum were also shown to have a greater ability to reconstitute hematopoiesis in lethally ablated recipient mice than those HSCs contained in the central marrow cavity[46]. When HSCs were acquired from aged donors, it was found that they localize to sites further away from the endosteum

than HSCs from younger donors[42], suggesting that HSC localization within the bone may be a mediator of the difference in HSC function observed with the aging process.

Studies by Taichman and colleagues[47-49] demonstrated that osteolineage cells produce many supportive growth factors including granulocyte colony stimulating factor (G-CSF), granulocyte macrophage colony stimulating factor (GM-CSF), interleukin 1 (IL-1), IL-6, and transforming growth factor beta (TGF-β). *In vivo* genetic approaches have also demonstrated that osteolineage cells are a significant regulatory component of hematopoiesis[50-53]. Specifically, transgenic mice selectively expressing a constitutively active PTH/PTHrP receptor in osteolineage cells enhanced HSC expansion by increasing the expression of the Notch ligand, Jagged1. Notch signaling regulates cell fate decisions including HSC self-renewal[53-55] thus by changing self-renewal versus differentiation decisions, Notch can increase HSC number without differentiation or increase in HPC or mature cells[54-56]. This regulatory relationship of Notch ligand expression by osteolineage cells may restricted to situations of increased PTH/PTHrP receptor activation, as subsequent studies have shown that Notch signaling is not mandatory for the maintenance of adult HSC function[55].

Within the endosteal niche, HSCs are retained through a variety of adhesion molecule interactions, many of which appear to be redundant systems. Early studies exploring the role of osteolineage cells in maintaining HSCs suggested that N-cadherin interactions positively effected HSCs[55], however more recent studies

have contradicted these findings[56]. Numerous other adhesion molecules have been implicated as contributors of HSC and HPC tethering, including, but not limited to, the integrins α4β1 – very late antigen-4 (VLA-4)[57-62],α5β1 – very late antigen-5 (VLA-5)[63], α4β7 – lymphocyte Peyer's patch adhesion molecule-1 (LPAM-1)[64], the alpha 6 integrins (Laminins)[65,66], CD44[67], E-selectins[68-70], the angiopoietin receptor tyrosine kinase with immunoglobulin-like and EGF-like domains-2 (Tie-2)[51], endolyn (CD164)[71], the calcium-sensing receptor (CaR)[72], stromal derived factor-1α SDF-1α[73], and osteopontin (OPN)[74-76]. OPN is also a negative regulator of HSC pool size within the bone marrow niche[76], and knockout of OPN in mice results in endogenous hematopoietic mobilization to the periphery and increases the mobilization response to G-CSF[74]. Recently, osteolineage cells were also found to express agrin, which mediates cell-cell contact with short term HSCs and initiates proliferation, perhaps functioning as an opposing signal to OPN[77]. These results suggest that OPN, a target for modulation of the endosteal HSC niche, and that agrin receptors, a target on HSCs, may serve as future therapeutic strategies to modify and enhance hematopoietic transplant and recovery, in line with previously described strategies targeting other adhesion interactions in the niche[78-83].

Up to this point the focus has been on the role of osteolineage cells and their associated regulation of hematopoietic cells. However, cells of hematopoietic origin also support and regulate osteolineage cells. For example, cell-to-cell contact between osteolineage cells and hematopoietic progenitor cells (HPC) has been shown to be important for HPC survival[84]. Using an *in vitro* system, Gillette et al. demonstrated that human $CD34^+$ cells (an HPC/HSC population of cells) co-cultured

with osteolineage cells made cell-cell contact and exchanged a portion of their membrane with the osteolineage cells, creating a signaling endosome[85]. This signaling endosome caused osteolineage cells to down-regulate Smad signaling and increase production of SDF-1α, suggesting that hematopoietic cells may instruct osteolineage cells to create a more habitable environment, allowing them to directly affect their own microenvironment. These results may suggest that HSCs help to create their own niches, perhaps by instructing neighboring stromal cells to produce supportive factors.

The Endosteal Niche and HSPC trafficking

Administration of G-CSF causes HSCs and HPCs egress (i.e. mobilize) from of the bone marrow and into the peripheral blood, where they can subsequently be collected by apheresis and used in hematopoietic transplantation. Treatment with G-CSF causes significant suppression of osteolineage cells[86-88], causing apoptosis[89] and a characteristic "flattening" of osteolineage cells[88] suggesting that osteolineage cells actively participate to the mobilization process. Recently, Winkler et al.[86] reported that a population of macrophage cells, characterized as F4/80$^+$ Ly-6G$^+$ CD11b$^+$ and termed “osteomacs”[89], line the endosteal surfaces of bone and that G-CSF treatment resulted in a trafficking, and reduction in number, of osteomacs. Presumably, this reduction in osteomacs was responsible for the attenuation of function of osteolineage cells. Confirming this hypothesis, macrophages depletion using either the Mafia transgenic mice, which allows for inducible deletion of macrophages, or with clodronate-loaded liposomes (Clo-lip) treatment, which

selectively kill macrophages, results in significant mobilization of HSC and HPC. A similar report from Chow et al. also demonstrated that depletion of macrophages with Clo-lip treatment results in hematopoietic mobilization[90], describing a Gr-1^{negative} F4/80^{+} CD115^{mid} CD169^{+} macrophage population as a regulator of osteolineage cells. Similar to the osteomac population, the authors suggest that the CD169^{+} macrophages express a soluble, yet to be identified, factor(s), which positively supports niche cells. In comparable studies by Christopher et al., a soluble factor produced by monocyte/macrophage populations supported osteolineage function[91], suggesting that manipulation of monocyte/macrophage populations or the factor(s) produced by them is a future therapeutic strategy to manipulate the endosteal niche, and possibly suggest a novel strategy for therapeutically manipulating bone cells.

Osteoclasts are also monocyte-derived cells, which are present along endosteal surfaces of bone. Osteoblasts and osteoclasts regulate both bone formation and bone resorption, respectively, within the bone marrow niche, and pre-osteoclasts cause retraction of osteoblasts[92], theoretically creating transient "holes" in the HSC supporting endosteal niche. Given that treatment with G-CSF causes increases in osteoclast number and activity[93-96] it was hypothesized that osteoclasts may regulate the endosteal niche and alter HSC retention and localization. In line with this notion, increasing osteoclast activity by administering RANK ligand correlates with a moderate increase in HPC mobilization[95]. Correspondingly, stress models such as bleeding or LPS treatment also increased the number of osteoclasts in the endosteal niche and HPC in the peripheral blood,

supporting a role for osteoclasts in niche regulation. Kollet et al. suggested that osteoclast-derived proteolytic enzymes, such as Cathepsin K, degraded important niche retention molecules, thereby facilitating egress of HSC and HPC[94]. Follow-up studies by the same laboratory showed decreased osteoclast maturation and activity in CD45 knockout mice, with reduced mobilization to RANK ligand and G-CSF[97] further suggesting osteoclasts are important in the regulation of the endosteal niche. In contrast to these studies, Takamatsu et al. reported earlier that while G-CSF treatment increased osteoclast number and bone resorption in both BALB/c mice and humans, the increase in osteoclasts did not occur until 10-15 days or 6-8 days, respectively, after treatment with G-CSF[93] whereas niche clearance by G-CSF is typically observed 4 to 5 days after treatment, and therefore the importance of osteoclasts remains unclear. Similarly, treatment of mice with osteoclast inhibiting bisphosphonates does not impair HSC mobilization in response to G-CSF and in fact increases HSC egress[98]. Intriguingly, the endosteal surface of bone, specifically underneath resorbing osteoclasts, there is a significant source of soluble extracellular calcium that previous studies have demonstrated that HSC expression of calcium sensing receptors mediates a chemoattraction to soluble Ca^{2+} [72]Genetic ablation of the calcium sensing receptor in mice reduces HSC content within the bone marrow niche and increases HSC numbers in the peripheral blood[99,100]. These results might suggest that the bone resorbing, and subsequent Ca^{2+} releasing activity of osteoclasts, may be involved in niche retention

Prior to hematopoietic transplant patients are conditioned with chemotherapeutic agents and/or irradiation to remove resident HSCs and HPCs,

which is essential for successful engraftment of donor HSCs. However, these agents also affect niche cells. A recent study from Dominici et al. demonstrated that following a lethal dose of irradiation megakaryocytes migrate toward the endosteal surface and induce a 2-fold expansion in osteolineage cells, presumably increasing the available niches for subsequent HSC engraftment[101]. These results are in close alignment with other studies in which mice deficient in GATA-1 and NF-E2 transcription factors had significantly increased megakaryocyte production, leading to a 6-fold expansion of osteolineage cells[102], a process requiring direct cell-cell contact between megakaryocytes and osteolineage cells[103,104]. Further support of blood cells impacting bone biology are the observations that excessive blood loss, which stresses the hematopoietic system, leads to osteoporosis in mice[105] and that splenectomy in mice results in an expansion of megakaryocytes with reduced GATA-1 expression and increased bone formation[106]. These intriguing findings suggest that there is much remains to be learned about the bi-directional regulatory relationship between blood and bone. Further exploration of these is clearly warranted particularly since there is a substantial prevalence of bone disorders following hematopoietic transplantation and its associated conditioning regimens[107-114].

Ageing and Turnover of the Endosteal Niche

The endosteal surface of bone, as described earlier, is a dynamic tissue with a high turnover rate of osteoblasts that are continually replenished by early osteogenic precursors and skeletal stem cells. Several reports, using *in vitro* co-

culture studies have shown that HSCs cultured on primitive osteolineage cells have a higher reconstituting capacity than those cultured on more mature osteoblasts[115,116], suggesting that the maturational status of osteolineage cells may be a key determinate of HSC support. Indeed, several studies conducted *in vivo* have revealed that disrupting immature osteolineage cells, which resemble mesenchymal stem and progenitor cells[117] withers HSC maintenance, whereas ablation of differentiated-more mature osteoblasts are ablated, hematopoiesis was unaffected[118-119]. These findings suggest that immature osteolineage cell subset is an essential component of the HSC niche. The Nestin$^+$ multipotent-mesenchymal stem cells express high levels of hematopoietic-supportive molecules, suggesting that this cell subset is also unique constituent of the bone marrow niche[120]. Intriguingly, Nestin$^+$ cells were found to wrap around endothelial cells within the bone marrow near the endosteum, but also towards the central marrow, implying that an alternate HSC niche localization exists that is located further from the endosteum, commonly referred to as the vascular niche.

The Vascular Niche: Vascular and Perivascular Cells

While it is clear that HSCs reside and thrive within the endosteal bone marrow niche, other studies have identified the perivascular region as an alternative HSC niche[120,121,38,40,41]. The dichotomy is partially reconciled by recent finding from our laboratory that osteoblasts are perivascular[43], but the reverse need not be true: there may be a perivascular niche that is not located near osteoblasts. Stem cell localization studies utilizing two-photon *in vivo* imaging have uncovered

that while HSCs, on average, are near the endosteum, they are not exclusively adjacent to osteolineage cells[42,46]. Studies assessing the localization of progenitor cells that also display the signaling lymphocyte activation molecule (SLAM; $CD150^+$, $CD48^-$ and $CD244^-$) expression pattern, which are highly enriched for HSCs, have shown that these SLAM cells are adjacent to bone marrow sinusoidal blood vessels as oppose to the endosteum, suggesting the existence of a "vascular niche" for HSCs[121] This is supported by the observation that endothelial cells, very similarly to osteolineage cells, can support hematopoiesis both *in vitro* and *in vivo*[122-125]. We have also described small endothelial microdomains, which express E-selectin and SDF-1α, and act as a point of entry for HSC after transplantation[126]. Regeneration of sinusoidal endothelial cells has been reported to be essential for hematopoietic reconstitution following myelosuppression[127], and bone marrow endothelial cells support the growth and expansion of HSC through angiocrine factors[128]. Interestingly, similar to the HSC cell to cell contact with osteolineage cells altering the endosteal niche function[84], Slayton et al. reported that donor hematopoietic cells migrated to sites of vascular sinusoidal injury within bones and contributed to repair following transplantation[129], further highlighting the complexity and interconnectedness of the bone marrow microenvironment[130]

While it is not completely clear what factors influence the particular niche location of HSCs, the fact that reticular cells with high production of SDF-1α are present in both the endosteal and vascular niches, may provide a common mechanism of HSC support in both niches[125]. A recent report has demonstrated that shortly after transplantation into non-myeloablated recipients, HSCs preferentially

localize to the endosteum in metaphyseal regions of bone in close association with blood vessels[131]. Given that the endosteal region is itself highly vascularized may suggest that the HSC niche actually encompasses overlapping regions within the bone.

Nervous System Mediators of the HSC Niche

While it is clear that cellular and molecular constituents within the microenvironment interact and co-regulate each other, the question arises as to whether there is a global regulator of the entire bone system, able to rapidly alter numerous components of the niche to respond as needed. The recently described nestin$^+$ MSCs are highly intriguing, as nestin, an intermediate filament protein, is normally restricted to nerve cells. Interstingly, the same laboratory has also demonstrated that HSC and HPC mobilization by G-CSF requires peripheral β_2-adrenergic signals[88]. Specifically, the authors found that blocking β_2-adrenergic signaling in mice by chemical sympathectomy (using 6-hydroxydopamine) or administering the β-blocker propanolol or genetically ablating dopamine β-hydroxylase (Dbh), an enzyme that converts dopamine into norepinephrine, diminished the ability of G-CSF to induce HSC mobilaization. Moreover, the authors were able to reverse the Dbh knockout phenotype by treating mice mice with the β_2-adrenergic agonist, Clenbuterol[88]. Circadian rhythms also regulate HSC niche retention[132,133]. Specifically, pharmacological inhibition of β_3-adrenergic signaling disrupts rhythmic oscillations, which then lead to uncontrolled norepinephrine release, increased CXCR4 expression, and enhanced SDF-1α production and

therefore causing regular transient trafficking from the bone marrow niche. Nervous system signaling has also been demonstrated to have direct effects on HSC, as human $CD34^+$ hematopoietic cells express β_2-adrenergic and dopamine receptors and neurotransmitters, such as norepinephrine, serve as direct chemoattractants for HSCs[134], underscoring the global control the nervous system has over the hematopoietic ecologic system. A recent report showed that β_2-adrenergic signaling causes up-regulation of the vitamin D receptor (VDR) on osteolineage cells and that VDR signaling was necessary for osteolineage responses to G-CSF treatment[135]. VDR expression is also regulated by circadian rhythms[136] providing a possible interconnection between the nervous system and the bone microenvironmental system.

Recently, Yamazaki et al. described a population of non-myelinating Schwann cells which ensheath sympathetic nerves in the bone marrow[137]. These cells are primary producers of TGF-β, which promotes HSC quiescence[138,139], and therefore when the bone is denervated, the loss of TGF-β signaling correlates with a reduction in the HSC pool[137]. Given that TGF-β is also capable of attracting skeletal stem cells[140], this may suggest that the nervous system can coordinate skeletal stem cell trafficking and migration to sites of need, though further exploration is required.

The role of adipose tissue in the HSC Niche

Recently, adipose tissue was also identified as an important mediator of hematopoiesis. Adipose, or "yellow marrow" is a major constituent of the bone marrow niche, but until recently was thought to play a passive role as a space-filler

in the bone marrow cavity. By quantifying and characterizing the properties of hematopoietic progenitors from distinct vertebrae that differ in adipocyte content, Naveiras et al determined that increased niche adiposity correlates to decreased net hematopoietic cellularity, and decreased number and activity of hematopoietic progenitors. This phenomenon was subsequently examined in a transplant setting by performing bone marrow transplant on 'fatless' A-ZIP/F1 mice that lack adipocytes. These mice showed significantly improved engraftment, white blood cell recovery, and donor chimerism post-transplantation relative to wildtype controls[141].

The described results suggest that suppressing adipocyte number in a transplant setting could provide important therapeutic benefits by providing a better environment for HSC engraftment. Naveiras et al singled out PPAR-γ as a putative target that could be pharmacologically recapitulate the engraftment phenotype of A-ZIP/F1 mice in wildtype animals. PPAR-γ is a member of the Peroxisome Proliferator-Activated Receptor family of nuclear hormone receptors that has been identified as a tissue-specific master regulator of adipogenesis. In the presence of ligands such as steroids, cholesterol byproducts, and fatty acids, PPAR-γ forms a heterodimer with Retinoid X Receptor (RXR) to bind to DNA to the expression of regulate transcription of genes related to lipid and carbohydrate metabolism and initiate the differentiation of mesenchymal stem cells (MSCs) to adipocytes[142,143]. The necessity of PPAR-γ for adipocyte differentiation has been established by several experiments. PPAR-γ-/- mouse ES cells fail to differentiate into adipocytes in culture, while normal adipogenesis can be rescued in these cells

by viral reinsertion of the PPAR-γ gene[144]. Furthermore, retroviral insertion of PPAR-γ into wild type fibroblasts promotes differentiation into adipocytes[142], an effect that can be recapitulated pharmacologically by treatment with thiazolidinediones, which are PPAR-γ agonists[145]. Conditional knockout of PPAR-γ in cells expressing the adipocyte-specific promoter aP2 show significant morphogenic defects and reduced body mass due to progressive lipodystrophy[146]. Collectively, these data establish justification for targeting PPAR-γ to inhibit adipogenesis.

Interplay between the Adipose and Endosteal niches

Adipocytes and osteoblasts are both descendants of mesenchymal stem cells (MSCs), however, the rates of osteogenesis and adipogenesis inversely correlate during development and aging[147-149]. Specifically, histological analysis of individuals with osteoporosis and aplastic anemia reveals that these patients display increased adiposity that is associated with decreased bone formation and impaired hematopoiesis[150,151]. Moreover, samples of rat bone marrow stromal cell cultures show a similar inverse relationship[152]. These observations suggest that adipogenesis and osteogenesis could be antagonistic processes that are inversely related to one another. According to this model MSCs go through a developmental branchpoint, where niche-mediated cues dictate whether MSCs commit to adipogenesis or osteogenesis.

Consistent with this hypothesis, several observations suggest that PPAR-γ is a critical mediator of MSC lineage fate by not only stimulating adipogenesis but also

actively suppressing osteogenesis in the bone marrow niche. This notion was initially proposed based on the finding that a single nucleotide polymorphism in the PPAR-γ gene is associated with decreased bone mineral density[153]. Future studies showing that several other PPAR-γ polymorphisms are associated with osteoporosis strengthened this relationship[154]. Additionally, MSCs from patients with aplastic anemia express significantly higher levels of PPAR-γ compared to control individuals[155]. Concurrent with the aforementioned decrease in adipogensis, PPARgamma-/- embryonic stem cells demonstrate enhanced osteogenesis in culture[144]. Furthermore, mice with heterozygous (PPAR-γ+/-) or homozygous hypomorphic (PPAR-γhyp/hyp) mutations both display increased osteogenesis through an expansion of the osteoblast population via stromal precursors[144,156]. Recent *in vitro* studies of human osteoblasts have shown that TNF-α signaling stimulates bone mineralization via downregulation of PPAR-γ in the osteoblast compartment[144]. Perhaps the most interesting finding is that pharmacological activation of PPAR-γ with thiazolidinediones, a class of commonly used anti-diabetes drugs, results in decreased bone mineral density, concomitant with an overall increase in adipogenesis[154,157-159] . This suggests that prolonged pharmacological modulation of PPAR-γ alone is sufficient to alter the bone-adipose equilibrium, though it is not clear at what rate. Given the role of osteoblasts in HSC engraftment mentioned above and mobilization PPAR-γ inhibition, on an acute timescale, could have important therapeutic benefits in bone marrow transplant.

The impact of Diabetes Mellitus on the HSCs and the bone marrow microenvironment

For long time, the status of BM in patients with DM has been often overlooked, however it has recently been established that BM HSCs of diabetic mice compared to controls display elevated markers of oxidative stress, DNA damage and apoptosis Furthermore, side population (SP) HSPCs are mis-localized in diabetic bone marrow[160]. In humans, a reduction in CD34+ HSCs was found in BM aspirates of diabetic compared to non-diabetic subjects. Extensive anatomical, histological and cell composition analyses of BM from non-diabetic and type 2 diabetic subjects display microvascular and hematopoietic cell rarefaction as well as fat deposition [161].

Many of the known cellular components of the HSC niche (endosteal, perivascular, vascular and neuro-vascular) show some degree of disruption in experimental models of diabetes. For example, it has been reported that diabetes disrupts BM innervation. Specifically, a reduced number of tyrosine hydroxylase (TyrOH)-immunoreactive nerve endings was detected in the BM of type 2 diabetic rats[12]. In addition to microangiopathy, neuropathy and stem cell rarefaction, the diabetic BM is characterized by extensive fatty infiltration (Figure 3), which as mentioned above negatively impacts HSCs and the HSC niche. Collectively, these data establish that diabetes negatively impacts the bone marrow micro-environment and HSC biology, however the precise physiological and molecular mechanisms for these defects remain unresolved.

The central thesis of this project was further elucidate the physiological and molecular events that lead to BM dysfunction in diabetes.

RATIONALE

The foundation of this project was built upon our initial observations made during an analysis of a caseload of patients treated with G-CSF to induce hematopoietic stem cell (HSC) mobilization at the Parma Bone Marrow Transplant Centre between 1st January 2004 and 30th October 2008. Within this dataset we observed an overall mobilization failure rate of 22.6% (14/62), defined as <20 $CD34^+$ and <3000 polymorphonuclear (PMNs) cells/ml; <5,000 leukocytes/ml; <50,000 platelets/ml blood at the beginning of leukapheresis. Strikingly, within these data we found that of the 14 patients who were classified as 'poor mobilizers', 7 (50%) had been previously diagnosed with diabetes mellitus (DM). On the contrary only 25% (12/48) of 'good or sufficient mobilizers' had previously diagnosed with DM. The observed difference in poor versus good mobilizers amongst diabetic patients was independent of age, gender and cycles of prior chemotherapy (Figure 4a).

Moreover, of the 48 patients that were able to sufficiently mobilize, the number of $CD34^+$ cells/kg was significantly lower in diabetic individuals compared to non-diabetic individuals (p=0.014, Figure 4b). Glucose levels were also significantly higher in poor mobilizers (p=0.002, Figure 4c) irrespective of a DM diagnosis.

We also observed a trend of slower neutrophil recovery (p=0.146) and significantly reduced platelet recovery (p=0.006) in diabetic patients following peripheral blood stem cell transplantation (p=0.146 and 0.006 respectively, Figure

3d). Finally, we also found that within patients classified as 'poor mobilizers', diabetic patients displayed a significant delay in both neutrophil and platelet recovery versus non-diabetic patients (p=0.002 and p=0.003, respectively; Figure 3e). These data were our first evidence that diabetes mellitus may negatively impact the cell migratory patterns of hematopoietic stem and progenitor cells (HSPCs).

In addition to our clinical observations, other groups have found that patients with diabetes mellitus have altered cell migratory patterns under both homeostatic and stressful conditions as well as other tissues such as: 1) diabetics have a lower proportion of circulating haematopoietic progenitors[162] and a reduced homing capacity of medullary mononuclear cells in the ischemic myocardium **[163];** 2) gestational diabetes is associated with a statistically significant risk of fetal malformation[164]; 3) wound healing is impaired in diabetic subjects[165]; 4) diabetics are more infection-prone[166].

The healing of wounds, repair of organ damage, embryogenesis, neovascularisation and immune response presuppose a preserved directional migration capacity of certain types of cell attracted by a gradient (chemotaxis).

As diabetes influences the processes based on the cells' chemotactic/migratory capacity, the assumption underlying the project is that mobilization and stem cell engraftment regulation mechanisms are also altered by diabetes during HSC transplantation.

Based on these collective observations, our central thesis is that many of the pathophysiological complications of diabetes are due to a common systemic stem

and progenitor cell trafficking problem and therefore diabetes can be re-examined as a stem cell disease. By extension this hypothesis presupposes that correcting these cell migratory failings will uncover new opportunities for designing an alternative class of anti-diabetic therapies.

Therefore, the collective aims of this project was to determine the underlying physiological and molecular aberrations that cause defective HSPC trafficking in diabetes and examine whether these defects could be corrected. The results of the proposed experiments would not only provide novel mechanistic insights into how HSPC biology but would also establish the paradigm that diabetes, and possibly other chronic degenerative diseases, can be viewed as hematopoietic stem cell diseases.

MATERIALS & METHODS

Analysis of Mobilization Patient Caseload

Sixty-two patients treated with G-CSF to induce hematopoietic stem cell (HSC) mobilization at the Parma Bone Marrow Transplant Centre between 1st January 2004 and 30th October 2008 we assessed for overall mobilization failure rate as defined as <20 $CD34^+$ and <3000 polymorphonuclear (PMNs) cells/ml; <5,000 leukocytes/ml; <50,000 platelets/ml blood at the beginning of leukapheresis.

Nineteen cases of diabetes mellitus were identified (mean 57±7 yrs of age; 10 males) following the guidelines of the American Diabetes Association[167]. The interval from the documentation of diabetes to transplantation ranged from 6 months to 5.3 years. High levels of blood glucose, HbA1c > 7 gm% (PID 5 HBA1C=6.8, PID17 HBA1C=6.7, PID1,8,9,12 HBA1C missing) and need for insulin treatment were documented. In two cases (11%), diabetes mellitus was associated with the use of corticosteroids, whereas in the remaining cases type I or II diabetes were present. Controls consisted of 43 non-diabetic subjects (52±12 yrs; 24 males). The principal needs for autologous peripheral blood stem cell transplantation were clinical remission of multiple myeloma (42%), lymphoma (32%) and acute myeloid leukemia (26%).

Parameters for inducing and enumerating HSC mobilization

$CD34^+$ cells were counted using a Becton-Dickinson FACSCalibur after erythrocyte lysis (EDTA-ammonium chloride solution) and direct incubation for 30

minutes with phycoerythrin (PE) conjugated monoclonal anti-CD34 (HPCA2, Becton-Dickinson, San Jose, Ca, USA). $CD34^+$ cell counts were performed following ISHAGE logical gate protocol. A negative control for non specific fluorescence (Simultest; Becton Dickinson, Erembodegem-Aalsi, Belgium) was used with unstained cells; the minimal number of events acquired for each determination was 70,000 and the entire procedure was performed at 4 °C. In all cases only the $CD34^+$ cell count performed in the lymphomonocyte gate was considered for data analysis.

Chemotherapy included high-dose of cyclophosphamide (7 g/m^2), ifosfamide, carboplatin, etoposide (ICE) [168] or high-dose Ara-C and dexamethasone (DHAP)[169] regimens, which were equally employed in the two groups (See supplementary table 1). Starting 24 hrs after the discontinuation of chemotherapy, G-CSF (10 ug/kg/day, Roche, Basel, Switzerland) was subcutaneously given until leukapheresis. From day 9 after priming, circulating $CD34^+$ cells were monitored daily. The following parameters were used as criteria for the beginning of leukapheresis: $CD34^+$ cells ≥ 20/uL and/or PMNs ≥ 3000/uL, leukocyte count ≥ 5,000/uL, platelet count ≥ 50,000/uL.

Mouse models of Diabetes – Type I Diabetes

For our mouse model of type I diabetes, C57BL/6 male mice were treated for five consecutive days with a single intraperitoneal injection of streptozotocin (STZ) diluted in citrate pH 4.5 (50 mg/kg/die in one daily dose). Mice injected with citrate buffer were used as controls. STZ is a glucose analog that is taken up by and kills pancreatic beta cells, which subsequently causes a decline of systemic insulin levels

with a concomitant increase in blood glucose levels. Therefore, successful induction of diabetes following STZ-treatment was determined by measuring blood insulin and glucose levels by ELISA (R&D System) and Glucometer (One Touch Ultra®).

Mouse models of Diabetes – Type II Diabetes

The mutant leptin receptor (*db*) mice were purchased from the Jackson laboratories (Bar Harbor, ME) and heterozygous (*db/+*) mice were bred together to generate homozygous (*db/db)* mice. Mice were genotyped using the protocol recommended by Jackson Laboratories. Homozygous (*db/db)* mice become obese by 4-6 weeks and develop diabetes shortly thereafter. The diabetic status of mice was determined by measuring insulin and glucose levels by ELISA (R&D System) and Glucometer (One Touch Ultra®), respectively. Wild type littermates were used as controls against *db/db* mice.

Bone marrow cell isolation

Mice were sacrificed via CO_2 asphyxia; tibiae, femurs, and spine were removed and excess soft tissue was eliminated. Using a pestle and mortar, the bones were crushed and washed in PBS with 0.5% FBS and passed through a 40μm filter into a collection tube. Cells were spun at 1500rpm for 5 minutes; the supernatant was removed, and cells were then further processed for staining, sorting or for transplantation.

Transplantation assay

All bone marrow transplantations were performed by tail vein injection. The C57BL/6 background expresses the CD45.2 congenic polymorphism on all hematopoietic tissues. Both of our Type I (i.e. STZ-induced) and Type II (i.e. *db/db* mice) models used mice of the C57BL/6 background and are therefore express the CD45.2 congenic marker. C57BL/6.SJL mice (available from Jackson Laboratories) express the CD45.1 congenic marker. All transplantation assays involved transplanting bone marrow (BM) cells from C57BL/6 mice (CD45.2+) into SJL recipient mice (CD45.1+), which allows us to distinguish between BM cells generate by the donor versus the recipient. Moreover, for competitive transplantation assays we used donor BM that was CD45.2+ and both the competitor and the recipients BM cells were derived from SJL mice (CD45.1). Prior to transplantation, all recipient mice were conditioned with 9.5cGy of irradiation to lethally ablate the recipient bone marrow cells – this is particularly important because this dose of irradiation kills resident recipient HSCs and evacuates the niche, which provides space for engraftment of donor HSCs. Mice are then administered acidic water supplemented with antibiotics for 21 days. To assess the engraftment contribution of both donor and competitor BM cells, either peripheral blood (extracted from the retro-orbital vein) or bone marrow (taken from the long bones) were first lysed to remove red blood cells and the remaining mono-nuclear cells (MNCs) were then stained with fluorescently labeled antibodies that specifically recognize CD45.1 and CD45.2. Labeled MNCs cells were then analysed by flow cytometry to determine the percent contribution of donor and/or competitor populations.

HSC mobilization in mice

To induce HSPC mobilization, mice were administered 8 injections of human recombinant 125 mg/Kg/day G-CSF (Filgastrim, Amgen) every 12 hours intra-peritoneal (i.p.). Three hours following the final G-CSF injection, peripheral blood (PB) was extracted from the retro-orbital vein of mice. Mobilized progenitors were quantified as described below.

Enumeration of mobilized HSPCs

We quantified the number of hematopoietic stem and progenitor cells (HSPCs) using both in vitro and in vivo methods. For in vitro enumeration of HSPCs: 50ul of PB was plated in methylcellulose supplemented with recombinant murine GM-CSF, IL-3, IL-6 and EPO (M3434, Stem Cell Technologies, British Columbia, CA) culture for 7 days and then assessed for colony formation– each colony representing an HSPC (CFU-C assay). For in vivo analysis: 100-150uL of mobilized blood was injected into lethally irradiated (9.5 Gy) the SJL congenic strain of C57BL/6 – SJL mice (as described above). HSPC engraftment was monitored weekly by determining the percent donor CD45+ cells in the recipient PB by FACS analysis (as described above).

Immunophenotypic analysis of BM

Mice were sacrificed via CO_2 asphyxia and then tibias, femurs, and spinal bones were removed and excess soft tissue was eliminated. Using a pestle and mortar, the bones were crushed and washed in PBS with 0.5% FBS and passed

through a 40μm filter into a collection tube. Cells were spun at 1500rpm for 5 minutes; the supernatant was removed, and cells were then further processed for either staining, sorting or for bone marrow transplantation. Hematopoietic stem progenitors were identified based on their expression of lineage markers as well as c-Kit, Sca-1 and CD48, CD150 or CD34, CD135 (Flk-2) expression. Lineage staining was performed using a cocktail of biotinylated anti-mouse antibodies against Mac-1 (CD11b), Gr-1 (Ly-6G and Ly-6C), Ter119 (Ly-76), CD3 , CD4, CD8a (Ly-2), and B220 (CD45R) (BD Biosciences). For detection we used lineage-streptavidin conjugated with PacOrange (Invitrogen) fluorescent mareker and then subsequently stained with c-Kit-APC (CD117), Sca1-APC-Cy7 and either CD48-FITC + CD150-PE (CD135) – for SLAM HSC analysis or CD34-FITC + Flk2-PE for alternative LT-HSCs immunophenotyping (BD Biosciences). For congenic strain discrimination, anti-CD45.1-APC and anti-CD45.2 FITC antibodies (BD Biosciences) were used. Compensation and data analysis were performed with Flowjo 8.5.3. For cell cycle staining cells were fixed overnight in 70% ethanol, washed twice in PBS and stained with a solution containing propidium iodide, RNAse A in Triton X 0.1%.

Flow cytometric analysis of adhesion molecules

To examine the cell surface expression of the adhesion molecules CXCR4, CD49D, CD49E, CD62L on HSPCs, bone marrow mono-nuclear cells (BM-MNCs) were recovered form both STZ-treated and control mice and stained with lineage, cKIT and Sca-1 antibodies as described above. Stained BM-MNCs from each experimental condition were divided into 4 tubes and separately stained with PE-

conjugated forms of CXCR4, CD49D, CD49E or CD62L antibodies (eBioscience). Stained cells were then subjected to flow cytometry and analyzed as described above.

Transwell migration assays (Modified Boyden chamber assay)

For migration assays, 2 × 10^3 FACS-sorted LSK cells were suspended in 500 μl of RPMI and seeded in triplicate in the upper chamber of 24-well, 5-μm Transwell plates (Corning). Cells were incubated for 1 hour at 37°C in the presence or absence of SDF-1α (stromal cell–derived factor 1α also known as CXCL12), after which the supernatant was removed and the wells were washed once with PBS to remove nonadherent cells. Adherent cells were harvested by treatment with cell dissociation buffer, enzyme-free (Invitrogen), and plated in methylcellulose (CFC-U assay described above).

Adhesion Assay

For adhesion assays, 2 × 10^3 FACS-sorted LSK cells were plated in triplicate on 24-well culture dishes precoated with fibronectin for 4 hours. Next, the adherent fraction was dissociated by treatment with cell dissociation buffer, enzyme-free (Invitrogen), collected, and plated in MethoCult media (M3434, Stemcell Technologies). Progenitor adhesion was determined as the percentage of CFU-C in the adherent fractions relative to the frequency of CFU-C in the input sample.

Assessment of cellular and secreted Cxcl12

CXCL12 labeling was performed using Monoclonal Anti-human/mouse CXCL12 Antibody Clone 79018 after fixation and permeabilization (BD cytofix/cytoperm kit) followed by secondary goat anti-mouse IgG-PE (both from R&D systems). Both peripheral blood and bone marrow SDF1 levels were quantified using ELISA (R&D System).

RNA isolation and quantitative real time RT-PCR

Nestin and Col2.3 cells were FACS sorted for GFP protein directly into lysis buffer and RNA isolation was performed using the Dynabeads mRNA DIRECT ™ Micro kit (Invitrogen). Primer sequences and RT-PCR procedure used have been previously described[120].

Adhesion and migration assays

For adhesion assays: 2 x 10^3 FACS sorted LSK cells were plated in triplicate on 24-well culture-dishes pre-coated with fibronectin. The adherent fraction was dissociated by treatment with Cell Dissociation Buffer, enzyme-free (Invitrogen), collected and plated in MethoCult media (M3434, Stem cell technologies). Progenitor adhesion was determined as the percentage of CFU-C in the adherent fractions, relative to the frequency of CFU-C in the input sample.

For migration assays: 2 x 10^3 FACS sorted LSK cells were suspended in 500 uL of RPMI and seeded in triplicate in the upper chamber of 24-well, 5-um Transwell plates (Corning, Lowell, MA). Cells were incubated for 1 h at 37ºC in the absence or presence of SDF1-α, after which the supernatant was removed and the wells were

washed once with PBS to remove non-adherent cells. Adherent cells were harvested by treatment with Cell Dissociation Buffer, enzyme-free (Invitrogen) and plated in methylcelullose. Progenitor adhesion was determined as above mentioned.

Imaging of the HSC niche

Mice were anesthetized and prepared for in vivo imaging as previously described[43]. FACS-sorted HSCs were stained in PBS for 15 min at 37°C with DiD (Invitrogen) or DiI (Invitrogen) using a 1:200 dilution and injected into lethally irradiated recipients. An about 4 × 6–mm area of the calvarium comprising the central sinus and the surrounding bone marrow cavities within the left and right frontal bones was scanned. When using Col2.3GFP and Nestin-GFP reporter mice, three-dimensional models of the osteoblastic or nestin cells and the bone (second-harmonic generation) were developed through Z-stack reconstruction. Using the Pythagoric theorem, we determined the location of stained HSCs injected in relation to the bone and the GFP^+ cells. The images were analyzed with ImageJ software (National Institutes of Health; http://rsbweb.nih.gov/ij/).

Immunostaining of mice calvaria

Calvaria from diabetic and control mice were fixed in 4% paraformaldehyde for 1 hour and subsequently washed twice in PBS. Blocking of unspecific binding and permeabilization were achieved with 20% goat serum and 0.5% Triton X-100 in PBS overnight. Endogenous biotin was blocked with Vector Kit (catalog number Sp-2001) following the manufacturer's instructions. Primary antibody (Chemicon rabbit anti–tyrosine hydroxylase; BD Pharmingen APC-conjugated anti-CD31) was

applied at 1:100 in 20% goat serum and 0.1% Triton X-100 in PBS and incubated for 2 to 3 days. Samples were washed with 0.1% Triton X-100 in PBS and incubated overnight with a secondary biotinylated goat anti-rabbit antibody (1:200) in 20% goat serum and 0.1% Triton X-100 in PBS. After washing with 0.1% Triton X-100 in PBS, samples were incubated for 2 hours with ABC kit (Vector PK-6100) prepared 30 min before use. After washes with PBS, samples were incubated with Cy3-tyramide (Perkin Elmer) (1:200) in diluent reagent for 30 min, washed with PBS, and visualized by fluorescence microscopy. Projections of Z-stacks (100 to 200 μm) of calvaria bone marrow were analyzed with the SlideBook software (Intelligent Imaging Innovations).

Drugs administration

A single injection of isoproterenol (Sigma; 5 mg/kg: i.p.) was administered to diabetic and control mice. SR 59230A (Sigma; 5 mg/kg: i.p) was administered daily for 10 days to diabetic mice.

Mice treated with saline were used as a control. Animals were sacrificed 2 hours after injection by CO_2 asphyxia and the femora were flushed with 200 uL of PBS. Trizol (Invitrogen) was used for total RNA extraction.

Osteoblastic cell deletion

Mice in which expression of Cre-recombinase was driven by Osteocalcin promoter were crossed with mice harboring an inducible Difteria Toxin Receptor transgene (iDTR)[170,171]. In the double transgenic, Cre-mediated removal of a

transcriptional STOP cassette allows the expression of DT receptor. Upon DT administration efficient ablation of the target population was achieved. Mice with only one transgene were used as controls. Both double and single transgenic mice were treated with either STZ for diabetes induction or with saline. After 5 weeks, DT was administered at the dose of 100 ng per mouse twice a day for 14 days. Nine days after starting the toxin administration G-CSF was administered (8 injections of 125 ugr/kg every 12 hrs). At days 14, blood was collected and used for flow and transplantation assays.

ELISA

CXCL12 protein levels were assessed in bone marrow supernatant and PB plasma. Briefly femurs from diabetic and control mice were flushed 4 times using 100 uL of PBS (total volume) in Eppendorf tubes. PB was collected via retroorbital bleeding in Eppendorf tubes without adding anti-coagulant. The samples were then incubated at 37ºC for 1 hr and spun at 4.6 rpm for 5 min. Plasma was then collected and used for CXCL12 evaluation with ELISA kit (Ray Biosystem) following manufacturer instructions.

Insulin levels were assessed in PB plasma with ELISA kit (Crystal Chem. Inc) following manufacturer instructions.

Western blot

Nestin-GFP cells were sorted using FACS-aria. Western blot was performed using antibody antPhopho-PKA (Invitrogen) following manufacturer instruction.

Statistical analysis

Mice: Unless otherwise specified, unpaired, 2-tailed Student's t test was used and data have been plotted as average ± s.e.m. Statistical significance is indicated by * ($p<0.05$) or ** ($p<0.01$) or *** ($p<0.001$).

Human: Fisher's exact test was used to compare the frequency of diabetes between poor and good mobilizers. The Wilcoxon two-sample test was used to compare the distribution of $CD34^+$ cell/kg and glucose levels between patient groups. Neutrophil recovery and platelet engraftment were measured from the day of transplantation with peripheral blood stem cells or bone marrow harvested cells. The cumulative incidence of engraftment was estimated using the Kaplan-Meier method, and the difference between diabetic and non- diabetic patients was assessed by the logrank test. All p-values were based on a two-sided hypothesis and were computed using SAS 9.2. (SAS Inst.).

RESULTS

After reviewing a caseload of patients mobilized with G-CSF in the Parma Bone Marrow Transplant Centre between 1st January 2004 and 30th October 2008, we observed a mobilization failure rate of 22.6% (n=62) (Figure 3). Seven of the 14 'poor-mobilizers' were diabetic whereas only 25% of 'good mobilizers' were diabetic. To determine the cellular and molecular underpinnings of the increased frequency of poor G-CSF-mediated mobilization observed in diabetic patients our first goal was to recapitulate the phenotype in a small animal model of diabetes.

We elected to utilize two murine models of diabetes that separately recapitulate both types of human diabetes. To mimic type I diabetes, where in humans the primary defect is the lack of production of insulin by the pancreatic beta cells, we treated mice with streptozotocin, which is an analogue of glucose that is taken up by pancreatic cells and subsequently kill them. To model type II diabetes, where the primary defect in humans is a cell resistance to the insulin, we used mice that lack the leptin receptor (db/db mice), which promotes insulin resistance in adipose and muscle tissues.

As mentioned in the rationale section, we observed that poor mobilization in response to G-CSF correlated with an increased frequency of diabetes as well as increased serum glucose levels (Figure 4a-c). Therefore, we first measured the glucose levels (described in the materials & methods) of all STZ-treated and db/db mice and reassigned mice into 4 experimental groups based on serum glucose

levels: Group A (<150mg/dl), Group B (150-200mg/dl), Group C (200-300mg/dl) and Group D (>300mg/dl). Mice from each group were then administered 8 doses of 62.5mg/kg G-CSF, separated by 12 hours each (see materials & methods). Following the last G-CSF treatment, peripheral blood (PB) was extracted from mice and either cultured in cytokine-enriched methylcellulose to enumerate mobilized functional HSPCs or assessed by flow cytometry to quantify immunophenotypic HSPCs. From these assays we observed an inverse correlation of serum glucose to G-CSF mediated HSPC mobilization as measured by either flow cytometry or colony forming units – statistically validated by both two-tailed, non-parametric student T test as well as a Jonckheere-Terpstra test, which an additional test reputed to be more robust for evaluating cohorts of different size. (Figures 5a-b).

Since type I (STZ-induced) and type 2 (db/db) diabetes, are characterized by insulin deficiency and hyperinsulinemia, respectively we also examined whether there was a correlation between insulin levels and the efficacy of G-CSF-induced HSPC mobilization. Insulin levels varied according to the model (low in STZ and high in db/db), but we did not observe any significant correlation between insulin levels and HSPC mobilization. However, we did find that plasma insulin concentrations were low/absent (0.1± 0.2 ng/ml) or high (30±8 ng/ml) in the poorest mobilizer groups of STZ-induced and db/db mice, respectively. Mice from either model that had lower glycemic levels showed plasma insulin levels within the normal range (1.1±0.3 ng/ml). These results suggest that the rate of reduction in HSPC mobilization caused by diabetes is proportional to glucose levels but independent of insulin concentration.

Although the causes of the two different types of diabetes vary, both diseases lead to the development of similar vascular and neural complications, which are related to the chronic hyperglycemia observed in both diseases. Since we observed a similar mobilization defects in both mice models, we elected to use the STZ mouse model to elucidate the mechanism at the bases of the mobilization defect.

Concamitant with the reduction in mobilized HSPCs we observed using the in vitro CFU-C model, we also observed in vivo when we transplanted mobilized blood into lethally irradiated syngeneic recipient mice (Figure 6a-c) (see Materials & Methods for technical details).

We hypothesized that the observed reduction in HSPC mobilization could be due to either a global reduction HSPC content in the BM of diabetic mice or a primary defect in migratory properties of HSPCs as well as a combination of both. Consistent with the former notion, the HSPC content is reduced in the BM of diabetic rats [7,172]. Therefore, we quantified the number of immunophenotypic LT-HSCs in the BM of STZ-treated diabetic mice using both SLAM markers (Lineage^{low}, cKit+, Sca-1+, CD150+, CD48-) as well as CD34 and Flk2 (Lineagelow, cKit+, Sca-1+, CD34-, Flk2-) (methods for extracting BM, antibody staining and flow cytometry are described in materials & methods). Much to our surprise and in contrast to those observations made in diabetic rates we found that diabetic mice displayed an increased number of LSK progenitors per femur while the total number of LT-HSCs was not significantly different in diabetic and non-diabetic marrow (Figure 7a-d). However, it is possible that LT-HSC function could be affected without a significant

change in immunophenotype. Therefore, we took mononuclear cells (MNCs) from both diabetic and non-diabetic mice and separately examined their ability to reconstitute hematopoiesis in lethally irradiated recipient mice in competition with normal unconditioned BM (Figure 7e). As predicted, recipient mice transplanted with a 1:1 mixture of non-diabetic BM MNCs (CD45.2) and competitor BM MNCs (CD45.2) displayed a 50% hematopoietic contribution from non-diabetic BM (%CD45.2 – Figure 6f). Consistent with the increased number of immunophenotypic HSPCs we observed in the BM of diabetic mice, we also observed that MNCs derived from diabetic mice have an enhanced ability to competitively reconstitute hematopoiesis in lethally irradiated recipient mice (%CD45.2 – Figure 7f). These results suggest that the primary cause of reduced stem cell mobilization in response to G-CSF treatment in diabetes could be a consequence of altered migratory signals/ability. Interestingly, when analyzing the donor (CD45.1) chimerism in these transplants we found that 80% of the donor derived peripheral blood cells were of myeloid lineage (CD45.1, Gr1+, Mac1+). In contrast, myeloid cells constitute only 40% of the total PB cells when donor cells were derived form non-diabetic animals. This result suggests that diabetic stem progenitor cells are skewed toward the myeloid lineage (data not shown).

Given that our results that stem cell trafficking might be altered in diabetes and that HSPC migration is regulated by signals from the niche we hypothesized that diabetes could be disturbing the microenvironment signals that mediate stem cell motion. Before proceeding to test this hypothesis we first wanted to confirm that the diabetic process did not primarily affect HSCs.

HSPC mobility is largely influenced by chemokine gradients and the presence of adhesion molecules that anchor HSPCs – two factors that are not necessarily mutually exclusive. CXCR4, CD49D, CD49E and CD62L are cell surface proteins known to influence both HSPC adhesion and migration. Therefore, we first examined the expression of these cell surface markers on HSPCs from both diabetic and non-diabetic mice. From these analyses, we found that HSPCs purified from diabetic mice displayed a significant increase in CD62L (also known as L-selectin) expression compared to control HSPCs (Figure 8a,c). However, We did not observe a significant difference in the expression of CXCR4, CD49D or CD49E between the two conditions (Figure 8a,c) nor did we find any significant difference in the frequency HSPCs that express CXCR4, CD49D, CD49E or CD62L between the two experimental conditions (Figure 8b).

Next, we aimed to evaluate whether the cell mobility properties of HSPCs from both diabetic and non-diabetes mice possessed differing abilities to migrate toward the HSPC chemo-attractant SDF-1a (also referred to as Cxcl12). To address this question, HSPCs FACS-purified from each experimental condition were subjected to an in vitro transwell migration assay (see Material & Methods). From this analysis we found that HSPCs (i.e. LSKs) sorted from diabetic mice displayed a significant decrease in the ability to migrate a SDF-1a gradient (Figure 8d).

Since we observed that HSPCs from diabetic mice had impaired migration towards Cxcl12 without a change in the expression of Cxcr4 – the cognate receptor of Cxcl12 – we inferred that the downstream intracellular signaling of Cxcl12-Cxcr4 binding may be altered in diabetic HSPCs compared to control mice. Therefore, we evaluated

the calcium flux of diabetic and control LSK cells after CXCL12 exposure. No difference in calcium flux was observed between the two groups, suggesting that the disease did not affect CXCR4 down stream signaling (data not shown).

Next, we examined the ability of diabetic HSPCs to adhere to the extracellular matrix component fibronectin using an in vitro adhesion assay (see materials & Methods). Contrary to impaired migration, we observed that HSPCs isolated from STZ-treated mice demonstrated increased adhesion to fibronectin ex vivo (Figure 8e). Overall, changes in HSPC migratory and adhesive activities were documented that could contribute to the observed phenotype.

To determine whether the observed changes in HSPC migration, adhesion and antigen expression profile in STZ-treated mice persisted in a normal host, recipient mice transplanted 16 weeks earlier with CD45.2 bone marrow cells from STZ- or saline-treated mice were treated with G-CSF (Figure 9a). However, no difference in CFU-C mobilized into the blood was observed (Figure 9b). Also, transplantation of irradiated animals with mobilized blood revealed that the contribution of the chimeric fractions (CD45.1/CD45.2 ratio) was equivalent in the two groups (Figure 9c,d). These data indicate that cell autonomous alterations in chemotactic properties were not persistent or were reverted in a non-diabetic host suggesting a role for the bone marrow (BM) microenvironment in the diabetes-induced mobilization defect. Further, they exclude a direct, durable effect of STZ on HSPC accounting for their mobilization abnormality and argue against STZ damage to HSPC causing the mobilization abnormality. Furthermore, STZ has a serum half-life of ~15 minutes with complete clearance by 4 hours[173] arguing against durable

presence of STZ rather than its effect on glucose control as the basis for the observed effect.

From these data we postulated that the failed HSPC mobilization in diabetic animals could be due to alterations in the bone marrow (BM) microenvironment. To assess whether the BM microenvironment was sufficient to induce the alterations in HSPC numbers and the poor G-CSF response observed in diabetic mice, we transplanted equivalent numbers of wild-type CD45.1 bone marrow cells into lethally irradiated diabetic and control mice (Figure 10a). Sixteen weeks post engraftment, bone marrow LSK were increased (Figure 10b) with a trend to increased LT-HSC in diabetic recipients (Figure 10c-d) similar to the results we obtained in non-transplanted diabetic mice. Furthermore, when G-CSF was administered to these animals, the number of circulating CFU-C was lower in diabetic mice transplanted with WT cells (Figure 10e). Collectively, these results indicate that HSPC exposure to STZ was not required for the abnormalities in their function. Rather, persistent extrinsic signals from the abnormal, diabetic microenvironment or a rapidly reversible change in HSPC function are responsible for maintaining the mobilization defect associated with diabetes.

Diabetes mediated disruption of the osteoblastic niche contributes to the mobilization defect

The mechanism of action of G-CSF has been widely studied in murine models. The CXCL12 chemokine has been highly preserved through evolution and in fact just one amino acid distinguishes the protein sequence in humans and mice, which

makes the murine model particularly useful for understanding human haematopoietic regulatory mechanisms. In the murine bone marrow, CXCR4 is expressed by the HSC and its ligand CXCL12 by the osteoblasts, medullary endothelial cells and stromal cells[174].

G-CSF, in part, promotes HSPC mobilization G-CSF induce stem cell mobilization by decreasing bone marrow SDF-1 and up regulating CXCR-4 on HSPC[175-177] it has also been shown that the mobilization effect lies in the capacity of G-CSF to differentially modify the SDF1 gradient (CXCL12) between the bone marrow and the peripheral blood[175,177]. Some studies suggest that suppression of CXCL-12 production by bone marrow osteoblasts is critical step for cytokine-induced mobilization[87,178]. Administration of G-CSF does alter osteoblast morphology along with an oseteoblast-dependent down regulation of CXCL-12[88]. However osteoblastic cells are heterogeneous population and the aforementioned studies have defined osteoblastic cells based on the expression of non-specific surface receptor profiles [178,179] or immunostaining[88].

Osteoblastic cells, which are a heterogeneous mixture of bone-rleated progenitor and mature cells, originate from a common mesenchymal progenitor. The maturation of differentiated bone cells from mesenchymal progenitors, commences with increased expression of the transcription factors runx2 and osterix followed by the expression of more mature markers of osteoblastogenesis such as alkaline phosphatase, collagen type I and eventually osteocalcin [180]. This differentiation is gradual and progresses through several intermediate functional

stages that are currently undetermined due to a lack of well-defined surface markers. Despite a lack of known surface markers, different osteolineage cell populations in mice can be distinguished by the expression of Osterix (Osx), Osteocalcin or both. To determine whether one of these specific subsets of osteolineage cells are selectively altered by the administration of G-CSF, we bred a mouse models whereby osteoblastic subsets are differentially labeled with fluorescent proteins enabling their visualization and perspective isolation in the same animal. To visualize Osx+ cells, Cre recombinase was expressed as a fusion protein with a modified estrogen receptor (ERt) allowing for time specific activation of the recombinase by administration of the estrogen analogue, tamoxifen[181]. Osterix-CreERt2 (Osx-Cre) animals[182] were crossed with Rosa26-loxP-stop-loxP-mcherry (Rosa-mCh) mice so that osterix expressing cells begin to express mCherry at the time of tamoxifen injection and then their progeny are permanently labeled for the remainder of the cell's lifespan. Clearance of tamoxifen from the cells mediates the return of the CreERt complex to the inactive state, thus creating a time window for gene modulation as well as cell population tracking[183]. To label the intermediate populations and the mature populations we then crossed Osx-Cre^{+}/Rosa-mCh mice with mice expressing the green fluorescent protein, GFP, driven by the osteocalcin promoter (OC-GFP mice). In this triple transgenic model the more mature osteocalcin-producing cells are green, the most immature are red whereas the intermediate population that differentiated after the injection of tamoxifen are double positive for green and red (Figure 11a). To examine how G-CSF affected each of these populations, triple transgeneic mice were first

administered Tamoxifen to activate expression of mCherry in cells expressing Osx-CreER. Following Tamoxifen treatment mice were given G-CSF as described above. From this analysis, we observed that more mature osteocalcin producing osteoblasts are selectively inhibited and both ++ and Osx+ populations ($p<0.01$ and 0.001 respectively) are significantly expanded by the administration of G-CSF (Figure 11b).

Based on these results we wanted to determine whether depeletion/inhibition of osteocalcin-expressing osteoblastic cells is a functionally critical step in the ability of G-CSF to promote HSPC mobilization. Therefore, we employed a mouse model where we could selectively deplete osteocalcin positive cells. Specifically, mice bearing a transgene that expresses Cre recombinase under the regulation of osteoblast specific promoter osteocalcin (OCN-Cre) was crossed with mice that ubiquitously express a flox-stop-flox-diptheria toxin receptor (iDTR)[171]. In the compound transgenic animals, Cre-mediated removal of a transcriptional STOP cassette allows for constitutive expression of DT receptor in Osteocalcin+ osetoblastic cells. Mice were then administered diphtheria toxin (DT) – wild type mice do not carry the DTR - to induce efficient ablation of the target population. Mice with only one transgene were used as controls. Diabetes was induced as previously described in both double transgenic (Oc-CRE-iDTR) and controls (Oc-CRE or iDTR). After deletion mice were treated with G-CSF or saline. Mobilized peripheral blood was transplanted in lethally irradiated congenic recipients along with support cells (Figure 12a). Peripheral blood chimerism analysis at 4 weeks was used to define progenitor mobilization. Baseline levels of

LSK were assessed to exclude a potential effect of DT administration on progenitor mobilization and no difference was found (data not shown). The treatment with DT was maintained over the entire length of G-CSF administration to exclude the possibility of residual osteoblastic cell function.

The data from these experiments uncovered several novel observations. First, loss of osteoblasts increased the number of progenitors in the blood regardless of G-CSF treatment indicating that osteoblasts are critical for retaining HSPCs in the bone marrow under homeostatic conditions. Second, G-CSF mediated-mobilization of HSPCs was compromised by osteoblast depletion in non-diabetic control mice. Third, in the presence of diabetes, osteoblast depletion completely abolished any residual mobilizing potential of G-CSF (Figure 12b).

However, we postulated that additional cell populations contribute to the G-CSF-dependent HSPC mobilization defect in diabetic animals given that osteoblast depletion without diabetes did not have the same degree of compromise as the setting of osteoblast depletion and diabetes. Moreover, it is known that several cell populations of distinct tissue origin found in the BM microenvironment contribute G-CSF-mediated HSPC mobilization. Therefore, we hypothesized that non-osteoblasts are also a part of the STZ-induced mobilization defects and prompted us to further charactherize the role of osteoblast and analyze the perivascular compartment in diabetic animals.

Following transplantation into irradiated recipients, LT-HSCs are visualized near osteoblastic cells and sinusoidal vessels[43]. LT-HSCs are retained in the BM by

interactions with molecules such as kit ligand or stem cell factor (SCF) present on osteoblastic cells[184-186] and CXCL12 on a variety of cell types, including perivascular cells and as we have mentioned throughout, modulating CXCL12 levels is thought to be a requisite aspect of HSPC mobilization from the BM into the blood[187-189]. Consequently, we examined microanatomic relationships between osteoblastic and perivascular cells, HSPC and kit ligand, CXCL12 levels in the bone marrow in the setting of diabetes. Mice carrying a transgene in which GFP is driven under the osteoblast-specific *Col2.3kb* promoter[190] or the *Nestin* promoter[191] (labeling mesenchymal stem cells) were used to locate these cells throughout the microenvironment topography.

We then performed high-resolution confocal microscopy and two-photon video imaging in *Nes-Gfp* and *Col2.3-Gfp* transgenic mice after injection of LT-HSCs. Briefly, calvarial BM was visualized following the injection of 5,000 dye-labeled LT-HSCs. The total number of HSCs and measurements of their distance relative to osteoblastic cells, the endosteal surface and Nes-GFP$^+$ cells were quantified in diabetic and control mice. The first observation we made from these analyses, was that higher numbers of LT-HSCs were observed 24hrs after injection in diabetic mice compared to their controls (Figure 13a). Clusters of 2, 3 or more DiD labeled cells were also observed at higher proportion in diabetic mice (Figure 13b). To assess whether these events could be attributed to an increased chemoattractive ability of the diabetic marrow causing cell accumulation or to induce HSPC proliferation, we injected a 1:1 mixture of FACS sorted LT-HSCs stained with the lipophilic cyanine dyes DiD or DiI. We found that cells in clusters were exclusively

stained with one dye, consistent with migration and proliferation of a single cell, rather than co-localization of multiple injected HSCs (Figure 13c). Further evaluation was conducted *in vitro* using DsRed-stained LSK CD48$^-$ cells cultured over a layer of stromal cells derived from control or diabetic mice. Despite several days of normoglycemic culture conditions (5.5 mM), diabetic stroma still promoted a 20% increase in HSPC growth compared to normal stroma (Figure 13d). Together with the higher fraction of cycling bone marrow cells found in diabetic mice (data not shown) and increased cell number detected by FACS and two photon video imaging, these data indicate that the diabetic stroma fosters HSPC proliferation.

We also found that LT-HSCs were found in closer proximity to osteoblastic cells and to the endosteal surface in diabetic mice 24-48 hrs after transplantation (Figure 13d). However, we did not observe any difference in HSPC location relative to nestin expressing perivascular cells in diabetic versus non-diabetic mice. Assessment of mRNA levels of niche-related genes (CXCL12, V-cam1, SCF and angiopoietin-1) in osteoblastic cells revealed that, under steady state, the expression of SCF, previously associated with HSPC lodgment in the endosteal region[186], was ~2-fold higher in diabetic mice (Figure 13e), consistent with the observed closer proximity of HSPCs**.** These data suggest that the diabetic microenvironment alters the lodgment and proliferation of normal HSCs.

Previous studies have shown that G-CSF-induced HSPC mobilization requires down-regulation of CXCL12 in the BM[177,192,193]. In steady state, Nes-GFP$^+$ cells are reportedly a major contributor of CXCL12 in mouse bone marrow[120]. In control

mice, *Cxcl12* mRNA levels were over 10-fold higher in Nes-GFP$^+$cells compared to osteoblastic cells (Figure 13g). *Cxcl12* mRNA levels in Nes-GFP$^+$ cells were reduced by ~2-fold in diabetic animals compared with controls (Figure 14a). Exposure to G-CSF had minimal impact on *Cxcl12* mRNA levels in Nes-GFP+ cells in the setting of diabetes while *Cxcl12* mRNA levels were efficiently down regulated in control mice (Figure 14a). Thus, the magnitude of *Cxcl12* mRNA change following G-CSF administration was dramatically lower in diabetic animals compared to controls (92% versus 38%). This was the consequence of both lower baseline *Cxcl12* levels and failure of G-CSF to induce sufficient *Cxcl12* mRNA down-regulation. The lower mRNA level in diabetic mice was accompanied by a decrease in Cxcl12 protein in Nes-GFP+ cells by flow cytometry (Figure 14b – measurement of intracellular Cxcl12 is described in Materials & Methods). Despite these changes in cell type-specific mRNA levels, CXCL12 protein content in bone marrow extracellular fluids did not change (Figure 14c) whereas we observed higher CXCL12 protein levels in the peripheral blood of diabetic mice ($p<0.05$, data not shown). Together, these data suggest that CXCL12 expression dynamics are changed in the diabetic microenvironment in a cell specific manner.

Increased sympathetic innervation and impaired response to β-adrenergic stimulation in diabetic bone marrow.

Sympathetic nervous system (SNS) cells also participate in G-CSF-induced HSPC mobilization. Specifically, treatment with G-CSF was noted in prior studies to increase sympathetic activity in the BM, leading to *Cxcl12* mRNA downregulation in

perivascular nestin^{+} mesenchymal stem cells and HSPC release[88,120]. Therefore, to survey for additional potential mechanisms that explain the compromised mobilization found in diabetic animals, we evaluated the function of SNS cells in diabetic and control mice. To do so, we first performed immunostaining for tyrosine hydroxylase, the rate-limiting enzyme in catecholamine synthesis, in the skull of diabetic and control mice. We observed that catecholaminergic nerve terminals were increased by >2-fold in the calvarial bone marrow of diabetic mice (Figure 15a-b). To determine whether increased catecholaminergic innervation was associated with altered sensitization of β-adrenergic receptors in Nes-GFP^{+} cells, we treated diabetic and control *Nes-Gfp* transgenic mice with the β-adrenergic receptor agonist isoproterenol and measured *Cxcl12* mRNA levels two hours later (Figure 15c). Reduced *Cxcl12* mRNA levels in diabetic Nes-GFP^{+} cells were confirmed under steady state. Further, the decrease in *Cxcl12* mRNA levels after isoproterenol treatment in control animals was markedly blunted in diabetic mice (Figure 14c). Similar results were obtained from unsorted bone and trabecular bone marrow cells (Figure 15d).

Activation of the β-adrenergic receptor is known to induce c-AMP-dependent protein kinase A (PKA) phosphorylation of the Threonine 197 (T197) residue in the catalytic subunit of PKA. Therefore, we assessed the level of phospho-PKA^{T179} in sorted Nes-GFP^{+} cells from control and diabetic mice both under baseline conditions and following isoproterenol administration. Western analysis using anti-phospho-T197-PKAα/β revealed that isoproterenol markedly increased (~2.5 fold) the level of active PKA in non-diabetic mice (Figure 14e,f). Conversely, we observed higher

baseline levels of phospho-PKA in diabetic mice, whereas isoproterenol induced only minor changes (Figure 15e,f).

β-adrenergic signaling in Nes-GFP$^+$ cells is mediated by binding to and activation of β3 adrenoreceptor, selectively expressed on nestin cells and absent on osteoblastic cells[133]. Therefore, we administered a selective β3 adrenergic blocker (SR59230A, Sigma) to diabetic mice and compared Cxcl12 level to that of saline injected diabetic mice. Cxcl12 levels in sorted Nes-GFP$^+$ cells were restored by β3 adrenergic blockade supporting the model of sympathetic hyperactivity causing aberrant CXCL12 regulation (Figure 15g). These results are consistent with diabetes related sympathetic nervous system dysfunction perturbing the molecular axis governing HSPC mobilization by G-CSF.

SNS-independent HSPC mobilization is preserved in diabetes.

All of our evidence to this point suggested that the impairment in stem cell mobilization in diabetic mice observed upon G-CSF challenging is in large part due to imbalances in the Cxcl12 bone marrow gradient. Moreover, our data suggests that diabetes-related damage to the SNS disrupts the ability of Nestin+ cells to appropriately down-regulate Cxcl12 in response to G-CSF and thus leading to inappropriate HSPC retention. Therefore, if elevated concentrations of Cxcl12 in the diabetic bone marrow was blocking HSPC mobilization, then we hypothesized that blocking the ability of Cxcl12 to activate Cxcr4 signaling on HSPCs would restore normal HSPC mobilization in response to G-CSF. To address this notion we took advantage of the FDA-approved mobilization drug AMD3100, which is a clinically

used bicyclam antagonist that reversibly blocks the interaction between CXCL12 and CXCR4[82,194-196]. Both diabetic and non-diabetic control mice were injected with a single dose of AMD3100 (5 mg/kg). One hour after the administration of AMD3100, equal volumes of blood from each condition were separately transplanted in lethally irradiated non-diabetic recipients, together with competitor cells. Evaluation of chimerism at 4 weeks showed that AMD3100 alone was able to mobilize an equal number of HSPCs in both diabetic and non-diabetic mice as no significant differences in engraftment between mobilized diabetic and control HSPC were observed (Figure 15h). Since AMD3100 alone is a weak mobilizer compared to G-CSF[197,198] we concomitantly administered G-CSF and AMD3100 together and found that co-administration of AMD3100 was able to completely mitigate the G-CSF-dependent HSPC mobilization defects observed in diabetic mice (Figure 15i). These data are consistent with CXCL12 modulation in cells of the marrow microenvironment being the primary basis for the diabetes-induced mobilization defect.

DISCUSSION

By reviewing a caseload of patients who were administered G-CSF to mobilize HSPCs we found that people with diabetes are less likely to mobilize sufficient HSPCs or in other words diabetics are more likely to be poor mobilizers. Interestingly, from the same review of patient data we observed a significant inverse correlation between the number of mobilized HSPCs and blood glucose levels. In order to gain insight into the cellular and molecular abnormalities that lead to this phenomena, we utilized two established mouse models of diabetes that separately recapitulate type I and type II diabetes and both displayed impaired HSPC mobilization when administered G-CSF. Our results demonstrate that this mobilization defect is not the consequence of reduced bone marrow HSPC content or an intrinsic HSPC defect but are rather the result of damage to non-hematopoietic niche cells that lose their ability to modulate CXCL12 levels in the BM microenvironment. Importantly, we were also able to pharmacologically reverse the defect with the FDA-approved drug AMD3100, which directly inhibit the CXCL12-CXCR4 interaction.

Our findings has been subsequently strongly substantiated by a prospective clinical trial in which DM and control subjects were subjected to a single low-dose G-CSF administration to study stem/progenitor cell mobilization. Compared to healthy subjects, patients with type 1 or type 2 diabetes showed a marked inability to mobilize CD34+ cells and other progenitor and pro-angiogenic phenotypes 24h after G-CSF [199].

Taken together, these studies indicate that the diabetic BM fails to mobilize stem/progenitor cells after G-CSF and tissue ischemia, a pathological condition now deemed as "mobilopathy"[200].

This mobilopathy cannot be simply attributed to a reduction in the number of intramarrow HSPC or EPC that can be mobilized. In animal models of diabetes, the number of BM stem cells was found to be decreased, unaffected or even increased[160,172], according to the DM model type and duration. In humans, BM CD34+ stem cells seem to be reduced[161,201,202], but defective mobilization takes place before baseline circulating stem cell levels decline[199]

The Effects of Diabetes on HSCs and Bone Marrow Microenvironment

We documented some hematopoietic cell autonomous changes in diabetes such as reduced migratory ability and increased adherence to extracellular matrix components. Similar findings have been reported for other cell types in diabetic settings[165,203-205]. These properties of diabetic HSPC might participate in the altered mobilization capacity, however they were not retained after transplantation into non-diabetic hosts suggesting that the phenotype may be rapidly reversible. We therefore focused on whether abnormalities in the microenvironment were present. It has been described that hyperglycemia induces persistent epigenetic changes in stromal cells, such as those of the endothelial lineage[206]. Correspondingly, we found that HSPC proliferation induced by diabetic bone marrow stromal cells was maintained even when cultured in normal glucose media for over 10 days. We also observed that diabetes derived stem cells gave rise to differentiated progenitor

skewed towards the myeloid phenotype. HSCs undergo dramatic changes with aging. An increase in absolute numbers of HSCs along with a functional deficit in reconstitution potential and a shift toward production of myeloid cells are the hallmarks of murine hematopoietic aging.

These changes have been attributed to cell intrinsic, epigenetic and microenvironmental changes. This molecular profile resembles the elevated inflammatory state previously described in older mice ("inflamm-aging")

In our model these observations might suggest that diabetes could be responsible for accelerated aging of the stem cell compartment with a first phase of proliferation followed eventually by a burnout of HSPC. Moreover, we showed that diabetic microenvironment is sufficient per se to induce early proliferation of transplanted wild type LT-HSC and this phenomenon is accompanied by changes in their localization. LT-HSCs tend to localize closer to the osteoblastic cells and the endosteal surface in diabetes at all time points examined. Importantly, diabetes reduced the number of osteoblastic cells supporting the notion that bone formation is impaired in patients affected by the disease. By selectively depleting osteoblasts, we showed that they participate in the residual ability of diabetic animals to mobilize to G-CSF, but that other cell types also contribute.

Communication between the SNS and Nestin+ cells is disrupted in Diabetes

We hypothesized and found that nestin+ mesenchymal stem cells that we defined have a defect in CXCL12 response to G-CSF in diabetes. Down-regulation of CXCL12 is a critical event in G-CSF-induced HSPC mobilization[88,133,207].

Mechanistically, it has been purported that G-CSF down-regulates Cxcl12 levels by altering SNS activity. SNS nerve terminals in the bone marrow are mainly located along arterioles and innervate perivascular cells[208,209]. Perivascular nestin$^+$ mesenchymal stem cells, which are also innervated by SNS fibers, serve as a major source of CXCL12 in the mouse bone marrow, and downregulate *Cxcl12* in response to G-CSF or adrenergic stimulation[209]. Even we found that the overall content of Cxcl12 in the bone marrow parenchyma was unchanged in STZ-treated animals, Cxcl12 mRNA and protein levels in steady-state diabetic mice were reduced in stromal nestin$^+$ cells. Furthermore, the profound suppression of Cxcl12 synthesis in nestin$^+$ cells following G-CSF administration disappeared in diabetic mice, suggesting that the loss of the chemokine directional gradient may be responsible for the defect in mobilization observed in diabetic settings. We also observed increased SNS terminals in diabetic calvaria bone marrow, associated with blunted response of nestin$^+$ cells to β-adrenergic agonists. It is known that diabetes is associated with increased sympathetic neural drive in humans[210,211]. These results strongly suggest that diabetes-related dysautonomia contribute to the impaired function of nestin$^+$ cells, leading to defective HSPC mobilization. However, given that G-CSF acts through multiple pathways to elicit HSPC mobilization[207], we cannot exclude the participation of additional mechanisms in the mobilization defect.

Pharmacological Targeting of the HSC niche restores HSPC mobilization in Diabetic mice

Patients that are unable to sufficiently mobilize HSPCs following G-CSF treatment must undergo bone marrow aspiration to recover the appropriate number of HSPCs. However, patients that are autologously transplanted with bone marrow-derived stem cells display delayed engraftment, which leaves patients susceptible to life-threatening complications such as sepsis and bleeding. Therefore, given that our results indicate that diabetic patients are more likely to be poor mobilizers, it is of significant importance to identify pharmacological methods for improving HSPC mobilization.

We have found that normal HSPC mobilization can be restored in diabetic mice using AMD3100, which directly blocks CXCR4-CXCL12 binding, and this demonstrates that the disease does not affect this specific interaction providing a pathophysiologic rationale for the use of AMD3100 in the mobilization of HSPC for patients with diabetes. Finally, we found that nestin^{+} cells with similar morphology and distribution to the murine ones are also present in the human bone marrow, suggesting a possible similar role in human disease. Although the short-term diabetes model used may not reflect the late consequences of diabetes encountered in many patients, these studies serve as a guide for a more extensive evaluation of diabetic patients and provide a strong rationale for the use of alternatives to G-CSF for stem cell mobilization in patients with diabetes.

FUTURE DIRECTIONS:

The Possible Role of Inflammation and Macrophages in HSPC mobilization in Diabetes

Alterations in BM monocyte/macrophage cells may represent another inflammatory drive of HSPC retention versus mobilization in DM. In type 2 diabetic patients, the BM/PB gradient of M1 (inflammatory) and M2 (anti-inflammatory) monocyte subtypes suggests that M2 cells are stuck in the BM. In addition, while we have observed that G-CSF fails to mobilize HSPCs in diabetic patients, it has been shown that it induces an efflux of M2 from the diabetic BM[212]. We have preliminary data in mice that indicate that diabetes induces excess in BM macrophages, which are not adequately suppressed by G-CSF, thus also possibly contributing to reduced HSPC mobilization (Figure 16a-b). The mechanisms linking hyperglycemia to augmented myelogenesis have been recently at least partially clarified and involve the excess production of RAGE ligands by neutrophils[213].

The Impact of the Extracellular matrix in HSPC mobilization and Diabetes

As mentioned in the introduction, extracellular matrix and cell surface-associated macromolecules such as heparan sulfate Proteoglycans are the core structural scaffolds of BM niches. Ext-1 is a glycosyltransferase, critical for the biosynthesis of glucosaminoglycans such as heparan sulfate (HS) and therefore, HS containing proteoglycans (HSPG) such as syndecans, betaglycans (type III TGFb receptors), glypicans and some isoforms of the hyaluronan receptor, CD44. These molecules are critical for growth factor binding and generating extra-cellular

gradients of key chemokines by regulating their localization and stability and as a result affect HSPC trafficking.

Interestingly, we have observed that mice that lack the Ext-1 gene specifically in osteolineage-commmitted mesenchymal progenitors - Mx1-Cre was recently shown to delete floxed alleles in this population in addition to hematopoietic cells[214] - restores normal HSPC mobilization in response to G-CSF (Figure 17). do not exhibit hematopoietic stem cells mobilization defect in response to G-CSF. These mice also display reduced retention of HSCs in the bone marrow and increased amount of HSPCs in blood and spleen (Figure 17a-c).

Reasoning that poor retention in the setting of genetic deletion of EXT1 could indicate a novel means of enhancing stem cell mobilization, we tested heparin and protamine that are pharmacologic inhibitors of the EXT1 product heparan sulfate.

Our preliminary data (Figure 18) indicate that these inhibitors are capable of inducing HSPC mobilization. They do so in a manner additive to mobilization with G-CSF, the current clinical standard. Further, they are capable of inducing mobilization in a clinically relevant context of poor mobilization in response to G-CSF represented by diabetes.

Results of engraftment into irradiated recipients of the blood from diabetic mice treated with heparan sulfate inhibitor heparin in combination with G-CSF results in a higher level of engraftment than blood from the animals treated with G-CSF alone (Figure 18). These observations prompt us to hypothesize that Ext-1 deletion could slow the progression of diabetic disease by improving stem cell mediated organ

repair**.** As mentioned previously, non enzymatic glycosylation contribute to many pathologic processes in DM. Lack of Ext-1 mediated glycosyl transferase activity could reduce organ damage in a stem cell-independent manner by means of slowing the progression of advance glycation end product (AGEs) formation. We are in the process of assessing organ dysfunction in kidney and peripheral nerves of diabetic mice bearing Ext-1 deletion versus diabetic control animal. We have observed that the compromised response to G-CSF was fully corrected in Type I diabetic mice lacking *Ext1* expression in Mx1+ mesenchymal cells (Figure 19a). Furthermore, combination of heparin with G-CSF resulted in normal mobilization of long term reconstituting cells in diabetic animals as measured by PB competitive transplantation into lethally irradiated congenic mice (Figure 19b). These data demonstrate that functional competitive inhibition of endogenous HSPGs rescues the mobilization abnormalities noted in animals with pharmacologically induced diabetes.

These data would provide a proof of concept that developing pharmacological inhibition of this signaling pathway is a legitimate strategy for slowing the progression of end terminal organ dysfunction in diabetes.

CONCLUSION

We have presented our data indicating that the BM is a major target of diabetic damage. Diabetes compromises BM architecture and affects its function, especially impairing the mobilization of immature cells into the bloodstream, thus impairing its regenerative capacity. In addition, diabetes negatively affects the activity of mobilized cells by altering multiple components of the HSC niche. BM derived progenitors are involved in the pathophysiology and natural history of diabetes and its multiorgan complications. This previously unrecognized function of the BM is lost in diabetic patients. Using murine selective Knockouts models we are now exploring novel therapeutic strategies directed to restore BM function and HSPC motility possibly slowing diabetic complications.

REFERENCES

1. Danaei G, Finucane MM, Lu Y, et al. National, regional, and global trends in fasting plasma glucose and diabetes prevalence since 1980: systematic analysis of health examination surveys and epidemiological studies with 370 country-years and 2.7 million participants. *Lancet*. 2011;378(9785):31-40.
2. Diagnosis and classification of diabetes mellitus. *Diabetes Care*. 2004;27 Suppl 1:S5-S10.
3. Kadowaki T. Insights into insulin resistance and type 2 diabetes from knockout mouse models. *J Clin Invest*. 2000;106(4):459-465.
4. Brownlee M. The pathobiology of diabetic complications: a unifying mechanism. *Diabetes*. 2005;54(6):1615-1625.
5. Avogaro A, Fadini GP, Gallo A, Pagnin E, de Kreutzenberg S. Endothelial dysfunction in type 2 diabetes mellitus. *Nutr Metab Cardiovasc Dis*. 2006;16 Suppl 1:S39-45.
6. Avogaro A, de Kreutzenberg SV, Fadini G. Endothelial dysfunction: causes and consequences in patients with diabetes mellitus. *Diabetes Res Clin Pract*. 2008;82 Suppl 2:S94-S101.
7. Oikawa A, Siragusa M, Quaini F, et al. Diabetes mellitus induces bone marrow microangiopathy. *Arterioscler Thromb Vasc Biol*. 2010;30(3):498-508.
8. Krause DS, Scadden DT, Preffer FI. The hematopoietic stem cell niche--home for friend and foe? *Cytometry B Clin Cytom*. 2013;84(1):7-20.
9. Fadini GP, Sartore S, Schiavon M, et al. Diabetes impairs progenitor cell mobilisation after hindlimb ischaemia-reperfusion injury in rats. *Diabetologia*. 2006;49(12):3075-3084.
10. Ceradini DJ, Yao D, Grogan RH, et al. Decreasing intracellular superoxide corrects defective ischemia-induced new vessel formation in diabetic mice. *J Biol Chem*. 2008;283(16):10930-10938.
11. Bento CF, Pereira P. Regulation of hypoxia-inducible factor 1 and the loss of the cellular response to hypoxia in diabetes. *Diabetologia*. 2011;54(8):1946-1956.
12. Busik JV, Tikhonenko M, Bhatwadekar A, et al. Diabetic retinopathy is associated with bone marrow neuropathy and a depressed peripheral clock. *J Exp Med*. 2009;206(13):2897-2906.
13. Papayannopoulou T, Scadden DT. Stem-cell ecology and stem cells in motion. *Blood*. 2008;111(8):3923-3930.
14. Purton LE, Scadden DT. The hematopoietic stem cell niche. StemBook. Cambridge (MA); 2008.
15. Appelbaum FR. Hematopoietic-cell transplantation at 50. *N Engl J Med*. 2007;357(15):1472-1475.
16. Thomas ED, Buckner CD, Sanders JE, et al. Marrow transplantation for thalassaemia. *Lancet*. 1982;2(8292):227-229.
17. Lucarelli G, Polchi P, Galimberti M, et al. Marrow transplantation for thalassaemia following busulphan and cyclophosphamide. *Lancet*. 1985;1(8442):1355-1357.

18. Lucarelli G, Galimberti M, Polchi P, et al. Marrow transplantation in patients with advanced thalassemia. *N Engl J Med*. 1987;316(17):1050-1055.
19. Magnon C, Frenette PS. Hematopoietic stem cell trafficking. StemBook. Cambridge (MA); 2008.
20. Orkin SH, Zon LI. Hematopoiesis: an evolving paradigm for stem cell biology. *Cell*. 2008;132(4):631-644.
21. Moore MA, Metcalf D. Ontogeny of the haemopoietic system: yolk sac origin of in vivo and in vitro colony forming cells in the developing mouse embryo. *Br J Haematol*. 1970;18(3):279-296.
22. Samokhvalov IM, Samokhvalova NI, Nishikawa S. Cell tracing shows the contribution of the yolk sac to adult haematopoiesis. *Nature*. 2007;446(7139):1056-1061.
23. Palis J, Robertson S, Kennedy M, Wall C, Keller G. Development of erythroid and myeloid progenitors in the yolk sac and embryo proper of the mouse. *Development*. 1999;126(22):5073-5084.
24. Godin I, Cumano A. The hare and the tortoise: an embryonic haematopoietic race. *Nat Rev Immunol*. 2002;2(8):593-604.
25. Alvarez-Silva M, Belo-Diabangouaya P, Salaun J, Dieterlen-Lievre F. Mouse placenta is a major hematopoietic organ. *Development*. 2003;130(22):5437-5444.
26. Gekas C, Dieterlen-Lievre F, Orkin SH, Mikkola HK. The placenta is a niche for hematopoietic stem cells. *Dev Cell*. 2005;8(3):365-375.
27. Ottersbach K, Dzierzak E. The murine placenta contains hematopoietic stem cells within the vascular labyrinth region. *Dev Cell*. 2005;8(3):377-387.
28. Rhodes KE, Gekas C, Wang Y, et al. The emergence of hematopoietic stem cells is initiated in the placental vasculature in the absence of circulation. *Cell Stem Cell*. 2008;2(3):252-263.
29. Mikkola HK, Orkin SH. The journey of developing hematopoietic stem cells. *Development*. 2006;133(19):3733-3744.
30. Mendes SC, Robin C, Dzierzak E. Mesenchymal progenitor cells localize within hematopoietic sites throughout ontogeny. *Development*. 2005;132(5):1127-1136.
31. Arroyo AG, Yang JT, Rayburn H, Hynes RO. Alpha4 integrins regulate the proliferation/differentiation balance of multilineage hematopoietic progenitors in vivo. *Immunity*. 1999;11(5):555-566.
32. Martinez-Agosto JA, Mikkola HK, Hartenstein V, Banerjee U. The hematopoietic stem cell and its niche: a comparative view. *Genes Dev*. 2007;21(23):3044-3060.
33. Morrison SJ, Spradling AC. Stem cells and niches: mechanisms that promote stem cell maintenance throughout life. *Cell*. 2008;132(4):598-611.
34. Schofield R. The relationship between the spleen colony-forming cell and the haemopoietic stem cell. *Blood Cells*. 1978;4(1-2):7-25.
35. Tavassoli M, Crosby WH. Transplantation of marrow to extramedullary sites. *Science*. 1968;161(3836):54-56.
36. Gong JK. Endosteal marrow: a rich source of hematopoietic stem cells. *Science*. 1978;199(4336):1443-1445.

37. Lord BI, Testa NG, Hendry JH. The relative spatial distributions of CFUs and CFUc in the normal mouse femur. *Blood*. 1975;46(1):65-72.
38. Ding L, Saunders TL, Enikolopov G, Morrison SJ. Endothelial and perivascular cells maintain haematopoietic stem cells. *Nature*. 2012;481(7382):457-462.
39. Kunisaki Y, Bruns I, Scheiermann C, et al. Arteriolar niches maintain haematopoietic stem cell quiescence. *Nature*. 2013;502(7473):637-643.
40. Poulos MG, Guo P, Kofler NM, et al. Endothelial Jagged-1 is necessary for homeostatic and regenerative hematopoiesis. *Cell Rep*. 2013;4(5):1022-1034.
41. Ding L, Morrison SJ. Haematopoietic stem cells and early lymphoid progenitors occupy distinct bone marrow niches. *Nature*. 2013;495(7440):231-235.
42. Kohler A, Schmithorst V, Filippi MD, et al. Altered cellular dynamics and endosteal location of aged early hematopoietic progenitor cells revealed by time-lapse intravital imaging in long bones. *Blood*. 2009;114(2):290-298.
43. Lo Celso C, Fleming HE, Wu JW, et al. Live-animal tracking of individual haematopoietic stem/progenitor cells in their niche. *Nature*. 2009;457(7225):92-96.
44. Nilsson SK, Johnston HM, Coverdale JA. Spatial localization of transplanted hemopoietic stem cells: inferences for the localization of stem cell niches. *Blood*. 2001;97(8):2293-2299.
45. Xie Y, Yin T, Wiegraebe W, et al. Detection of functional haematopoietic stem cell niche using real-time imaging. *Nature*. 2009;457(7225):97-101.
46. Haylock DN, Williams B, Johnston HM, et al. Hemopoietic stem cells with higher hemopoietic potential reside at the bone marrow endosteum. *Stem Cells*. 2007;25(4):1062-1069.
47. Calvi LM, Adams GB, Weibrecht KW, et al. Osteoblastic cells regulate the haematopoietic stem cell niche. *Nature*. 2003;425(6960):841-846.
48. Taichman RS, Reilly MJ, Emerson SG. Human osteoblasts support human hematopoietic progenitor cells in vitro bone marrow cultures. *Blood*. 1996;87(2):518-524.
49. Zhang J, Niu C, Ye L, et al. Identification of the haematopoietic stem cell niche and control of the niche size. *Nature*. 2003;425(6960):836-841.
50. Visnjic D, Kalajzic Z, Rowe DW, Katavic V, Lorenzo J, Aguila HL. Hematopoiesis is severely altered in mice with an induced osteoblast deficiency. *Blood*. 2004;103(9):3258-3264.
51. Arai F, Hirao A, Ohmura M, et al. Tie2/angiopoietin-1 signaling regulates hematopoietic stem cell quiescence in the bone marrow niche. *Cell*. 2004;118(2):149-161.
52. Stier S, Cheng T, Dombkowski D, Carlesso N, Scadden DT. Notch1 activation increases hematopoietic stem cell self-renewal in vivo and favors lymphoid over myeloid lineage outcome. *Blood*. 2002;99(7):2369-2378.
53. Varnum-Finney B, Brashem-Stein C, Bernstein ID. Combined effects of Notch signaling and cytokines induce a multiple log increase in precursors with lymphoid and myeloid reconstituting ability. *Blood*. 2003;101(5):1784-1789.
54. Karanu FN, Murdoch B, Gallacher L, et al. The notch ligand jagged-1 represents a novel growth factor of human hematopoietic stem cells. *J Exp Med*. 2000;192(9):1365-1372.

55. Bigas A, Espinosa L. Hematopoietic stem cells: to be or Notch to be. *Blood*. 2012;119(14):3226-3235.
56. Kiel MJ, Radice GL, Morrison SJ. Lack of evidence that hematopoietic stem cells depend on N-cadherin-mediated adhesion to osteoblasts for their maintenance. *Cell Stem Cell*. 2007;1(2):204-217.
57. Zanjani ED, Flake AW, Almeida-Porada G, Tran N, Papayannopoulou T. Homing of human cells in the fetal sheep model: modulation by antibodies activating or inhibiting very late activation antigen-4-dependent function. *Blood*. 1999;94(7):2515-2522.
58. Vermeulen M, Le Pesteur F, Gagnerault MC, Mary JY, Sainteny F, Lepault F. Role of adhesion molecules in the homing and mobilization of murine hematopoietic stem and progenitor cells. *Blood*. 1998;92(3):894-900.
59. Peled A, Kollet O, Ponomaryov T, et al. The chemokine SDF-1 activates the integrins LFA-1, VLA-4, and VLA-5 on immature human CD34(+) cells: role in transendothelial/stromal migration and engraftment of NOD/SCID mice. *Blood*. 2000;95(11):3289-3296.
60. Papayannopoulou T, Priestley GV, Nakamoto B, Zafiropoulos V, Scott LM. Molecular pathways in bone marrow homing: dominant role of alpha(4)beta(1) over beta(2)-integrins and selectins. *Blood*. 2001;98(8):2403-2411.
61. Levesque JP, Leavesley DI, Niutta S, Vadas M, Simmons PJ. Cytokines increase human hemopoietic cell adhesiveness by activation of very late antigen (VLA)-4 and VLA-5 integrins. *J Exp Med*. 1995;181(5):1805-1815.
62. Levesque JP, Takamatsu Y, Nilsson SK, Haylock DN, Simmons PJ. Vascular cell adhesion molecule-1 (CD106) is cleaved by neutrophil proteases in the bone marrow following hematopoietic progenitor cell mobilization by granulocyte colony-stimulating factor. *Blood*. 2001;98(5):1289-1297.
63. van der Loo JC, Xiao X, McMillin D, Hashino K, Kato I, Williams DA. VLA-5 is expressed by mouse and human long-term repopulating hematopoietic cells and mediates adhesion to extracellular matrix protein fibronectin. *J Clin Invest*. 1998;102(5):1051-1061.
64. Katayama Y, Hidalgo A, Peired A, Frenette PS. Integrin alpha4beta7 and its counterreceptor MAdCAM-1 contribute to hematopoietic progenitor recruitment into bone marrow following transplantation. *Blood*. 2004;104(7):2020-2026.
65. Qian H, Tryggvason K, Jacobsen SE, Ekblom M. Contribution of alpha6 integrins to hematopoietic stem and progenitor cell homing to bone marrow and collaboration with alpha4 integrins. *Blood*. 2006;107(9):3503-3510.
66. Qian H, Georges-Labouesse E, Nystrom A, et al. Distinct roles of integrins alpha6 and alpha4 in homing of fetal liver hematopoietic stem and progenitor cells. *Blood*. 2007;110(7):2399-2407.
67. Schmits R, Filmus J, Gerwin N, et al. CD44 regulates hematopoietic progenitor distribution, granuloma formation, and tumorigenicity. *Blood*. 1997;90(6):2217-2233.
68. Sackstein R. The bone marrow is akin to skin: HCELL and the biology of hematopoietic stem cell homing. *J Invest Dermatol*. 2004;122(5):1061-1069.
69. Katayama R, Koike S, Sato S, Sugimoto Y, Tsuruo T, Fujita N. Dofequidar fumarate sensitizes cancer stem-like side population cells to chemotherapeutic

drugs by inhibiting ABCG2/BCRP-mediated drug export. *Cancer Sci*. 2009;100(11):2060-2068.
70. Katayama Y, Hidalgo A, Furie BC, Vestweber D, Furie B, Frenette PS. PSGL-1 participates in E-selectin-mediated progenitor homing to bone marrow: evidence for cooperation between E-selectin ligands and alpha4 integrin. *Blood*. 2003;102(6):2060-2067.
71. Forde S, Tye BJ, Newey SE, et al. Endolyn (CD164) modulates the CXCL12-mediated migration of umbilical cord blood CD133+ cells. *Blood*. 2007;109(5):1825-1833.
72. Adams GB, Chabner KT, Alley IR, et al. Stem cell engraftment at the endosteal niche is specified by the calcium-sensing receptor. *Nature*. 2006;439(7076):599-603.
73. Ponomaryov T, Peled A, Petit I, et al. Induction of the chemokine stromal-derived factor-1 following DNA damage improves human stem cell function. *J Clin Invest*. 2000;106(11):1331-1339.
74. Grassinger J, Haylock DN, Storan MJ, et al. Thrombin-cleaved osteopontin regulates hemopoietic stem and progenitor cell functions through interactions with alpha9beta1 and alpha4beta1 integrins. *Blood*. 2009;114(1):49-59.
75. Nilsson SK, Johnston HM, Whitty GA, et al. Osteopontin, a key component of the hematopoietic stem cell niche and regulator of primitive hematopoietic progenitor cells. *Blood*. 2005;106(4):1232-1239.
76. Stier S, Ko Y, Forkert R, et al. Osteopontin is a hematopoietic stem cell niche component that negatively regulates stem cell pool size. *J Exp Med*. 2005;201(11):1781-1791.
77. Mazzon C, Anselmo A, Cibella J, et al. The critical role of agrin in the hematopoietic stem cell niche. *Blood*. 2011;118(10):2733-2742.
78. Ramirez P, Rettig MP, Uy GL, et al. BIO5192, a small molecule inhibitor of VLA-4, mobilizes hematopoietic stem and progenitor cells. *Blood*. 2009;114(7):1340-1343.
79. Papayannopoulou T, Priestley GV, Nakamoto B. Anti-VLA4/VCAM-1-induced mobilization requires cooperative signaling through the kit/mkit ligand pathway. *Blood*. 1998;91(7):2231-2239.
80. Kikuta T, Shimazaki C, Ashihara E, et al. Mobilization of hematopoietic primitive and committed progenitor cells into blood in mice by anti-vascular adhesion molecule-1 antibody alone or in combination with granulocyte colony-stimulating factor. *Exp Hematol*. 2000;28(3):311-317.
81. Craddock CF, Nakamoto B, Andrews RG, Priestley GV, Papayannopoulou T. Antibodies to VLA4 integrin mobilize long-term repopulating cells and augment cytokine-induced mobilization in primates and mice. *Blood*. 1997;90(12):4779-4788.
82. Broxmeyer HE, Orschell CM, Clapp DW, et al. Rapid mobilization of murine and human hematopoietic stem and progenitor cells with AMD3100, a CXCR4 antagonist. *J Exp Med*. 2005;201(8):1307-1318.
83. Broxmeyer HE, Hangoc G, Cooper S, Campbell T, Ito S, Mantel C. AMD3100 and CD26 modulate mobilization, engraftment, and survival of hematopoietic stem

and progenitor cells mediated by the SDF-1/CXCL12-CXCR4 axis. *Ann N Y Acad Sci*. 2007;1106:1-19.
84. Jung Y, Wang J, Havens A, et al. Cell-to-cell contact is critical for the survival of hematopoietic progenitor cells on osteoblasts. *Cytokine*. 2005;32(3-4):155-162.
85. Gillette JM, Larochelle A, Dunbar CE, Lippincott-Schwartz J. Intercellular transfer to signalling endosomes regulates an ex vivo bone marrow niche. *Nat Cell Biol*. 2009;11(3):303-311.
86. Winkler IG, Sims NA, Pettit AR, et al. Bone marrow macrophages maintain hematopoietic stem cell (HSC) niches and their depletion mobilizes HSCs. *Blood*. 2010;116(23):4815-4828.
87. Semerad CL, Christopher MJ, Liu F, et al. G-CSF potently inhibits osteoblast activity and CXCL12 mRNA expression in the bone marrow. *Blood*. 2005;106(9):3020-3027.
88. Katayama Y, Battista M, Kao WM, et al. Signals from the sympathetic nervous system regulate hematopoietic stem cell egress from bone marrow. *Cell*. 2006;124(2):407-421.
89. Chang MK, Raggatt LJ, Alexander KA, et al. Osteal tissue macrophages are intercalated throughout human and mouse bone lining tissues and regulate osteoblast function in vitro and in vivo. *J Immunol*. 2008;181(2):1232-1244.
90. Chow A, Lucas D, Hidalgo A, et al. Bone marrow CD169+ macrophages promote the retention of hematopoietic stem and progenitor cells in the mesenchymal stem cell niche. *J Exp Med*. 2011;208(2):261-271.
91. Christopher MJ, Rao M, Liu F, Woloszynek JR, Link DC. Expression of the G-CSF receptor in monocytic cells is sufficient to mediate hematopoietic progenitor mobilization by G-CSF in mice. *J Exp Med*. 2011;208(2):251-260.
92. Perez-Amodio S, Beertsen W, Everts V. (Pre-)osteoclasts induce retraction of osteoblasts before their fusion to osteoclasts. *J Bone Miner Res*. 2004;19(10):1722-1731.
93. Takamatsu Y, Simmons PJ, Moore RJ, Morris HA, To LB, Levesque JP. Osteoclast-mediated bone resorption is stimulated during short-term administration of granulocyte colony-stimulating factor but is not responsible for hematopoietic progenitor cell mobilization. *Blood*. 1998;92(9):3465-3473.
94. Kollet O, Dar A, Shivtiel S, et al. Osteoclasts degrade endosteal components and promote mobilization of hematopoietic progenitor cells. *Nat Med*. 2006;12(6):657-664.
95. Cho KA, Joo SY, Han HS, Ryu KH, Woo SY. Osteoclast activation by receptor activator of NF-kappaB ligand enhances the mobilization of hematopoietic progenitor cells from the bone marrow in acute injury. *Int J Mol Med*. 2010;26(4):557-563.
96. Watanabe T, Yatomi Y, Sunaga S, et al. Characterization of prostaglandin and thromboxane receptors expressed on a megakaryoblastic leukemia cell line, MEG-01s. *Blood*. 1991;78(9):2328-2336.
97. Shivtiel S, Kollet O, Lapid K, et al. CD45 regulates retention, motility, and numbers of hematopoietic progenitors, and affects osteoclast remodeling of metaphyseal trabecules. *J Exp Med*. 2008;205(10):2381-2395.

98. Christopher MJ, Link DC. Granulocyte colony-stimulating factor induces osteoblast apoptosis and inhibits osteoblast differentiation. *J Bone Miner Res*. 2008;23(11):1765-1774.
99. Hirbe AC, Uluckan O, Morgan EA, et al. Granulocyte colony-stimulating factor enhances bone tumor growth in mice in an osteoclast-dependent manner. *Blood*. 2007;109(8):3424-3431.
100. Miyamoto K, Yoshida S, Kawasumi M, et al. Osteoclasts are dispensable for hematopoietic stem cell maintenance and mobilization. *J Exp Med*. 2011;208(11):2175-2181.
101. Dominici M, Rasini V, Bussolari R, et al. Restoration and reversible expansion of the osteoblastic hematopoietic stem cell niche after marrow radioablation. *Blood*. 2009;114(11):2333-2343.
102. Kacena MA, Shivdasani RA, Wilson K, et al. Megakaryocyte-osteoblast interaction revealed in mice deficient in transcription factors GATA-1 and NF-E2. *J Bone Miner Res*. 2004;19(4):652-660.
103. Ciovacco WA, Goldberg CG, Taylor AF, et al. The role of gap junctions in megakaryocyte-mediated osteoblast proliferation and differentiation. *Bone*. 2009;44(1):80-86.
104. Ciovacco WA, Cheng YH, Horowitz MC, Kacena MA. Immature and mature megakaryocytes enhance osteoblast proliferation and inhibit osteoclast formation. *J Cell Biochem*. 2010;109(4):774-781.
105. Gurevitch O, Khitrin S, Valitov A, Slavin S. Osteoporosis of hematologic etiology. *Exp Hematol*. 2007;35(1):128-136.
106. Martelli F, Verrucci M, Migliaccio G, et al. Removal of the spleen in mice alters the cytokine expression profile of the marrow micro-environment and increases bone formation. *Ann N Y Acad Sci*. 2009;1176:77-86.
107. Savani BN, Donohue T, Kozanas E, et al. Increased risk of bone loss without fracture risk in long-term survivors after allogeneic stem cell transplantation. *Biol Blood Marrow Transplant*. 2007;13(5):517-520.
108. Yao S, McCarthy PL, Dunford LM, et al. High prevalence of early-onset osteopenia/osteoporosis after allogeneic stem cell transplantation and improvement after bisphosphonate therapy. *Bone Marrow Transplant*. 2008;41(4):393-398.
109. Lee SJ, Seaborn T, Mao FJ, et al. Frequency of abnormal findings detected by comprehensive clinical evaluation at 1 year after allogeneic hematopoietic cell transplantation. *Biol Blood Marrow Transplant*. 2009;15(4):416-420.
110. Petropoulou AD, Porcher R, Herr AL, et al. Prospective assessment of bone turnover and clinical bone diseases after allogeneic hematopoietic stem-cell transplantation. *Transplantation*. 2010;89(11):1354-1361.
111. Baker KS, Ness KK, Weisdorf D, et al. Late effects in survivors of acute leukemia treated with hematopoietic cell transplantation: a report from the Bone Marrow Transplant Survivor Study. *Leukemia*. 2010;24(12):2039-2047.
112. Hautmann AH, Elad S, Lawitschka A, et al. Metabolic bone diseases in patients after allogeneic hematopoietic stem cell transplantation: report from the Consensus Conference on Clinical Practice in chronic graft-versus-host disease. *Transpl Int*. 2011;24(9):867-879.

113. McClune B, Majhail NS, Flowers ME. Bone loss and avascular necrosis of bone after hematopoietic cell transplantation. *Semin Hematol*. 2012;49(1):59-65.
114. Shanis D, Merideth M, Pulanic TK, Savani BN, Battiwalla M, Stratton P. Female long-term survivors after allogeneic hematopoietic stem cell transplantation: evaluation and management. *Semin Hematol*. 2012;49(1):83-93.
115. Cheng YH, Chitteti BR, Streicher DA, et al. Impact of maturational status on the ability of osteoblasts to enhance the hematopoietic function of stem and progenitor cells. *J Bone Miner Res*. 2011;26(5):1111-1121.
116. Chitteti BR, Cheng YH, Streicher DA, et al. Osteoblast lineage cells expressing high levels of Runx2 enhance hematopoietic progenitor cell proliferation and function. *J Cell Biochem*. 2010;111(2):284-294.
117. Omatsu Y, Sugiyama T, Kohara H, et al. The essential functions of adipo-osteogenic progenitors as the hematopoietic stem and progenitor cell niche. *Immunity*. 2010;33(3):387-399.
118. Corral DA, Amling M, Priemel M, et al. Dissociation between bone resorption and bone formation in osteopenic transgenic mice. *Proc Natl Acad Sci U S A*. 1998;95(23):13835-13840.
119. Raaijmakers MH, Mukherjee S, Guo S, et al. Bone progenitor dysfunction induces myelodysplasia and secondary leukaemia. *Nature*. 2010;464(7290):852-857.
120. Mendez-Ferrer S, Michurina TV, Ferraro F, et al. Mesenchymal and haematopoietic stem cells form a unique bone marrow niche. *Nature*. 2010;466(7308):829-834.
121. Kiel MJ, Yilmaz OH, Iwashita T, Yilmaz OH, Terhorst C, Morrison SJ. SLAM family receptors distinguish hematopoietic stem and progenitor cells and reveal endothelial niches for stem cells. *Cell*. 2005;121(7):1109-1121.
122. Yao L, Yokota T, Xia L, Kincade PW, McEver RP. Bone marrow dysfunction in mice lacking the cytokine receptor gp130 in endothelial cells. *Blood*. 2005;106(13):4093-4101.
123. Ohneda O, Fennie C, Zheng Z, et al. Hematopoietic stem cell maintenance and differentiation are supported by embryonic aorta-gonad-mesonephros region-derived endothelium. *Blood*. 1998;92(3):908-919.
124. Li W, Johnson SA, Shelley WC, Yoder MC. Hematopoietic stem cell repopulating ability can be maintained in vitro by some primary endothelial cells. *Exp Hematol*. 2004;32(12):1226-1237.
125. Sugiyama T, Kohara H, Noda M, Nagasawa T. Maintenance of the hematopoietic stem cell pool by CXCL12-CXCR4 chemokine signaling in bone marrow stromal cell niches. *Immunity*. 2006;25(6):977-988.
126. Sipkins DA, Wei X, Wu JW, et al. In vivo imaging of specialized bone marrow endothelial microdomains for tumour engraftment. *Nature*. 2005;435(7044):969-973.
127. Hooper AT, Butler JM, Nolan DJ, et al. Engraftment and reconstitution of hematopoiesis is dependent on VEGFR2-mediated regeneration of sinusoidal endothelial cells. *Cell Stem Cell*. 2009;4(3):263-274.

128. Kobayashi H, Butler JM, O'Donnell R, et al. Angiocrine factors from Akt-activated endothelial cells balance self-renewal and differentiation of haematopoietic stem cells. *Nat Cell Biol*. 2010;12(11):1046-1056.
129. Slayton WB, Li XM, Butler J, et al. The role of the donor in the repair of the marrow vascular niche following hematopoietic stem cell transplant. *Stem Cells*. 2007;25(11):2945-2955.
130. Kiel MJ, Morrison SJ. Uncertainty in the niches that maintain haematopoietic stem cells. *Nat Rev Immunol*. 2008;8(4):290-301.
131. Ellis SL, Grassinger J, Jones A, et al. The relationship between bone, hemopoietic stem cells, and vasculature. *Blood*. 2011;118(6):1516-1524.
132. Lucas D, Battista M, Shi PA, Isola L, Frenette PS. Mobilized hematopoietic stem cell yield depends on species-specific circadian timing. *Cell Stem Cell*. 2008;3(4):364-366.
133. Mendez-Ferrer S, Lucas D, Battista M, Frenette PS. Haematopoietic stem cell release is regulated by circadian oscillations. *Nature*. 2008;452(7186):442-447.
134. Spiegel A, Shivtiel S, Kalinkovich A, et al. Catecholaminergic neurotransmitters regulate migration and repopulation of immature human CD34+ cells through Wnt signaling. *Nat Immunol*. 2007;8(10):1123-1131.
135. Kawamori Y, Katayama Y, Asada N, et al. Role for vitamin D receptor in the neuronal control of the hematopoietic stem cell niche. *Blood*. 2010;116(25):5528-5535.
136. Cho Y, Noshiro M, Choi M, et al. The basic helix-loop-helix proteins differentiated embryo chondrocyte (DEC) 1 and DEC2 function as corepressors of retinoid X receptors. *Mol Pharmacol*. 2009;76(6):1360-1369.
137. Yamazaki S, Ema H, Karlsson G, et al. Nonmyelinating Schwann cells maintain hematopoietic stem cell hibernation in the bone marrow niche. *Cell*. 2011;147(5):1146-1158.
138. Larsson J, Karlsson S. The role of Smad signaling in hematopoiesis. *Oncogene*. 2005;24(37):5676-5692.
139. Yamazaki S, Iwama A, Takayanagi S, Eto K, Ema H, Nakauchi H. TGF-beta as a candidate bone marrow niche signal to induce hematopoietic stem cell hibernation. *Blood*. 2009;113(6):1250-1256.
140. Tang Y, Wu X, Lei W, et al. TGF-beta1-induced migration of bone mesenchymal stem cells couples bone resorption with formation. *Nat Med*. 2009;15(7):757-765.
141. Naveiras O, Nardi V, Wenzel PL, Hauschka PV, Fahey F, Daley GQ. Bone-marrow adipocytes as negative regulators of the haematopoietic microenvironment. *Nature*. 2009;460(7252):259-263.
142. Tontonoz P, Hu E, Spiegelman BM. Stimulation of adipogenesis in fibroblasts by PPAR gamma 2, a lipid-activated transcription factor. *Cell*. 1994;79(7):1147-1156.
143. Yanase T, Yashiro T, Takitani K, et al. Differential expression of PPAR gamma1 and gamma2 isoforms in human adipose tissue. *Biochem Biophys Res Commun*. 1997;233(2):320-324.

144. Akune T, Ohba S, Kamekura S, et al. PPARgamma insufficiency enhances osteogenesis through osteoblast formation from bone marrow progenitors. *J Clin Invest*. 2004;113(6):846-855.
145. Gimble JM, Robinson CE, Wu X, et al. Peroxisome proliferator-activated receptor-gamma activation by thiazolidinediones induces adipogenesis in bone marrow stromal cells. *Mol Pharmacol*. 1996;50(5):1087-1094.
146. He W, Barak Y, Hevener A, et al. Adipose-specific peroxisome proliferator-activated receptor gamma knockout causes insulin resistance in fat and liver but not in muscle. *Proc Natl Acad Sci U S A*. 2003;100(26):15712-15717.
147. Meunier P, Aaron J, Edouard C, Vignon G. Osteoporosis and the replacement of cell populations of the marrow by adipose tissue. A quantitative study of 84 iliac bone biopsies. *Clin Orthop Relat Res*. 1971;80:147-154.
148. Park SR, Oreffo RO, Triffitt JT. Interconversion potential of cloned human marrow adipocytes in vitro. *Bone*. 1999;24(6):549-554.
149. Pittenger MF, Mackay AM, Beck SC, et al. Multilineage potential of adult human mesenchymal stem cells. *Science*. 1999;284(5411):143-147.
150. Burkhardt R, Kettner G, Bohm W, et al. Changes in trabecular bone, hematopoiesis and bone marrow vessels in aplastic anemia, primary osteoporosis, and old age: a comparative histomorphometric study. *Bone*. 1987;8(3):157-164.
151. Wen JQ, Feng HL, Wang XQ, Pang JP. Hemogram and bone marrow morphology in children with chronic aplastic anemia and myelodysplastic syndrome. *World J Pediatr*. 2008;4(1):36-40.
152. Beresford JN, Bennett JH, Devlin C, Leboy PS, Owen ME. Evidence for an inverse relationship between the differentiation of adipocytic and osteogenic cells in rat marrow stromal cell cultures. *J Cell Sci*. 1992;102 (Pt 2):341-351.
153. Ogawa S, Urano T, Hosoi T, et al. Association of bone mineral density with a polymorphism of the peroxisome proliferator-activated receptor gamma gene: PPARgamma expression in osteoblasts. *Biochem Biophys Res Commun*. 1999;260(1):122-126.
154. Harslof T, Tofteng CL, Husted LB, et al. Polymorphisms of the peroxisome proliferator-activated receptor gamma (PPARgamma) gene are associated with osteoporosis. *Osteoporos Int*. 2011;22(10):2655-2666.
155. Xu Y, Takahashi Y, Wang Y, et al. Downregulation of GATA-2 and overexpression of adipogenic gene-PPARgamma in mesenchymal stem cells from patients with aplastic anemia. *Exp Hematol*. 2009;37(12):1393-1399.
156. Cock TA, Back J, Elefteriou F, et al. Enhanced bone formation in lipodystrophic PPARgamma(hyp/hyp) mice relocates haematopoiesis to the spleen. *EMBO Rep*. 2004;5(10):1007-1012.
157. Grey A, Bolland M, Gamble G, et al. The peroxisome proliferator-activated receptor-gamma agonist rosiglitazone decreases bone formation and bone mineral density in healthy postmenopausal women: a randomized, controlled trial. *J Clin Endocrinol Metab*. 2007;92(4):1305-1310.
158. Lazarenko OP, Rzonca SO, Suva LJ, Lecka-Czernik B. Netoglitazone is a PPAR-gamma ligand with selective effects on bone and fat. *Bone*. 2006;38(1):74-84.

159. Lencel P, Delplace S, Hardouin P, Magne D. TNF-alpha stimulates alkaline phosphatase and mineralization through PPARgamma inhibition in human osteoblasts. *Bone*. 2011;48(2):242-249.
160. Hazra S, Jarajapu YP, Stepps V, et al. Long-term type 1 diabetes influences haematopoietic stem cells by reducing vascular repair potential and increasing inflammatory monocyte generation in a murine model. *Diabetologia*. 2013;56(3):644-653.
161. Spinetti G, Cordella D, Fortunato O, et al. Global remodeling of the vascular stem cell niche in bone marrow of diabetic patients: implication of the microRNA-155/FOXO3a signaling pathway. *Circ Res*. 2013;112(3):510-522.
162. Fadini GP, Pucci L, Vanacore R, et al. Glucose tolerance is negatively associated with circulating progenitor cell levels. *Diabetologia*. 2007;50(10):2156-2163.
163. Jimenez-Quevedo P, Silva GV, Sanz-Ruiz R, et al. [Diabetic and nondiabetic patients respond differently to transendocardial injection of bone marrow mononuclear cells: findings from prospective clinical trials in "no-option" patients]. *Rev Esp Cardiol*. 2008;61(6):635-639.
164. Passarge E. Congenital Malformations and Maternal Diabetes. *Lancet*. 1965;1(7380):324-325.
165. Lan CC, Liu IH, Fang AH, Wen CH, Wu CS. Hyperglycaemic conditions decrease cultured keratinocyte mobility: implications for impaired wound healing in patients with diabetes. *Br J Dermatol*. 2008;159(5):1103-1115.
166. Fernandez-Real JM, Pickup JC. Innate immunity, insulin resistance and type 2 diabetes. *Trends Endocrinol Metab*. 2008;19(1):10-16.
167. Akhter J. The American Diabetes Association's Clinical Practice Recommendations and the developing world. *Diabetes Care*. 1997;20(6):1044-1045.
168. Jerkeman M, Leppa S, Kvaloy S, Holte H. ICE (ifosfamide, carboplatin, etoposide) as second-line chemotherapy in relapsed or primary progressive aggressive lymphoma--the Nordic Lymphoma Group experience. *Eur J Haematol*. 2004;73(3):179-182.
169. Velasquez WS, Cabanillas F, Salvador P, et al. Effective salvage therapy for lymphoma with cisplatin in combination with high-dose Ara-C and dexamethasone (DHAP). *Blood*. 1988;71(1):117-122.
170. Zhang M, Xuan S, Bouxsein ML, et al. Osteoblast-specific knockout of the insulin-like growth factor (IGF) receptor gene reveals an essential role of IGF signaling in bone matrix mineralization. *J Biol Chem*. 2002;277(46):44005-44012.
171. Buch T, Heppner FL, Tertilt C, et al. A Cre-inducible diphtheria toxin receptor mediates cell lineage ablation after toxin administration. *Nat Methods*. 2005;2(6):419-426.
172. Orlandi A, Chavakis E, Seeger F, Tjwa M, Zeiher AM, Dimmeler S. Long-term diabetes impairs repopulation of hematopoietic progenitor cells and dysregulates the cytokine expression in the bone marrow microenvironment in mice. *Basic Res Cardiol*. 2010;105(6):703-712.
173. Adolphe AB, Glasofer ED, Troetel WM, Weiss AJ, Manthei RW. Preliminary pharmacokinetics of streptozotocin, an antineoplastic antibiotic. *J Clin Pharmacol*. 1977;17(7):379-388.

174. Dar A, Kollet O, Lapidot T. Mutual, reciprocal SDF-1/CXCR4 interactions between hematopoietic and bone marrow stromal cells regulate human stem cell migration and development in NOD/SCID chimeric mice. *Exp Hematol*. 2006;34(8):967-975.
175. Lapidot T, Petit I. Current understanding of stem cell mobilization: the roles of chemokines, proteolytic enzymes, adhesion molecules, cytokines, and stromal cells. *Exp Hematol*. 2002;30(9):973-981.
176. Levesque JP, Hendy J, Takamatsu Y, Simmons PJ, Bendall LJ. Disruption of the CXCR4/CXCL12 chemotactic interaction during hematopoietic stem cell mobilization induced by GCSF or cyclophosphamide. *J Clin Invest*. 2003;111(2):187-196.
177. Petit I, Szyper-Kravitz M, Nagler A, et al. G-CSF induces stem cell mobilization by decreasing bone marrow SDF-1 and up-regulating CXCR4. *Nat Immunol*. 2002;3(7):687-694.
178. Christopher MJ, Liu F, Hilton MJ, Long F, Link DC. Suppression of CXCL12 production by bone marrow osteoblasts is a common and critical pathway for cytokine-induced mobilization. *Blood*. 2009;114(7):1331-1339.
179. Aubin JE LFtol. The osteoblast lineage. Principles of bone biology: Academic Press. ; 1996.
180. Aubin JE, Liu F. The osteoblasts lineage. In: Bilezikian JP, Raisz LG, Rodan GA, eds. Principles of bone biology. San Diego: Academic Press; 1996:51–67.
181. Metzger D, Clifford J, Chiba H, Chambon P. Conditional site-specific recombination in mammalian cells using a ligand-dependent chimeric Cre recombinase. *Proc Natl Acad Sci U S A*. 1995;92(15):6991-6995.
182. Maes C, Kobayashi T, Selig MK, et al. Osteoblast precursors, but not mature osteoblasts, move into developing and fractured bones along with invading blood vessels. *Dev Cell*;19(2):329-344.
183. Feil R, Brocard J, Mascrez B, LeMeur M, Metzger D, Chambon P. Ligand-activated site-specific recombination in mice. *Proc Natl Acad Sci U S A*. 1996;93(20):10887-10890.
184. Huang EJ, Nocka KH, Buck J, Besmer P. Differential expression and processing of two cell associated forms of the kit-ligand: KL-1 and KL-2. *Mol Biol Cell*. 1992;3(3):349-362.
185. Driessen RL, Johnston HM, Nilsson SK. Membrane-bound stem cell factor is a key regulator in the initial lodgment of stem cells within the endosteal marrow region. *Exp Hematol*. 2003;31(12):1284-1291.
186. Ogawa M, Matsuzaki Y, Nishikawa S, et al. Expression and function of c-kit in hemopoietic progenitor cells. *J Exp Med*. 1991;174(1):63-71.
187. Czechowicz A, Kraft D, Weissman IL, Bhattacharya D. Efficient transplantation via antibody-based clearance of hematopoietic stem cell niches. *Science*. 2007;318(5854):1296-1299.
188. Wright DE, Bowman EP, Wagers AJ, Butcher EC, Weissman IL. Hematopoietic stem cells are uniquely selective in their migratory response to chemokines. *J Exp Med*. 2002;195(9):1145-1154.
189. Imai K, Kobayashi M, Wang J, et al. Selective secretion of chemoattractants for haemopoietic progenitor cells by bone marrow endothelial cells: a possible role in

homing of haemopoietic progenitor cells to bone marrow. *Br J Haematol*. 1999;106(4):905-911.
190. Kalajzic I, Kalajzic Z, Kaliterna M, et al. Use of type I collagen green fluorescent protein transgenes to identify subpopulations of cells at different stages of the osteoblast lineage. *J Bone Miner Res*. 2002;17(1):15-25.
191. Mignone JL, Kukekov V, Chiang AS, Steindler D, Enikolopov G. Neural stem and progenitor cells in nestin-GFP transgenic mice. *J Comp Neurol*. 2004;469(3):311-324.
192. Thomas J, Liu F, Link DC. Mechanisms of mobilization of hematopoietic progenitors with granulocyte colony-stimulating factor. *Curr Opin Hematol*. 2002;9(3):183-189.
193. Levesque JP, Hendy J, Takamatsu Y, Williams B, Winkler IG, Simmons PJ. Mobilization by either cyclophosphamide or granulocyte colony-stimulating factor transforms the bone marrow into a highly proteolytic environment. *Exp Hematol*. 2002;30(5):440-449.
194. Hatse S, Princen K, Bridger G, De Clercq E, Schols D. Chemokine receptor inhibition by AMD3100 is strictly confined to CXCR4. *FEBS Lett*. 2002;527(1-3):255-262.
195. Liles WC, Broxmeyer HE, Rodger E, et al. Mobilization of hematopoietic progenitor cells in healthy volunteers by AMD3100, a CXCR4 antagonist. *Blood*. 2003;102(8):2728-2730.
196. Shen H, Cheng T, Olszak I, et al. CXCR-4 desensitization is associated with tissue localization of hemopoietic progenitor cells. *J Immunol*. 2001;166(8):5027-5033.
197. DiPersio JF, Stadtmauer EA, Nademanee A, et al. Plerixafor and G-CSF versus placebo and G-CSF to mobilize hematopoietic stem cells for autologous stem cell transplantation in patients with multiple myeloma. *Blood*. 2009;113(23):5720-5726.
198. Flomenberg N, Devine SM, Dipersio JF, et al. The use of AMD3100 plus G-CSF for autologous hematopoietic progenitor cell mobilization is superior to G-CSF alone. *Blood*. 2005;106(5):1867-1874.
199. Fadini GP, Albiero M, Vigili de Kreutzenberg S, et al. Diabetes impairs stem cell and proangiogenic cell mobilization in humans. *Diabetes Care*. 2013;36(4):943-949.
200. DiPersio JF. Diabetic stem-cell "mobilopathy". *N Engl J Med*. 2011;365(26):2536-2538.
201. Fadini GP, Albiero M, Seeger F, et al. Stem cell compartmentalization in diabetes and high cardiovascular risk reveals the role of DPP-4 in diabetic stem cell mobilopathy. *Basic Res Cardiol*. 2013;108(1):313.
202. Fadini GP, Boscaro E, de Kreutzenberg S, et al. Time course and mechanisms of circulating progenitor cell reduction in the natural history of type 2 diabetes. *Diabetes Care*. 2010;33(5):1097-1102.
203. Bhatwadekar AD, Glenn JV, Li G, Curtis TM, Gardiner TA, Stitt AW. Advanced glycation of fibronectin impairs vascular repair by endothelial progenitor cells: implications for vasodegeneration in diabetic retinopathy. *Invest Ophthalmol Vis Sci*. 2008;49(3):1232-1241.

204. Loughlin DT, Artlett CM. 3-Deoxyglucosone-collagen alters human dermal fibroblast migration and adhesion: implications for impaired wound healing in patients with diabetes. *Wound Repair Regen*. 2009;17(5):739-749.
205. Azcutia V, Abu-Taha M, Romacho T, et al. Inflammation determines the pro-adhesive properties of high extracellular d-glucose in human endothelial cells in vitro and rat microvessels in vivo. *PLoS One*;5(4):e10091.
206. El-Osta A, Brasacchio D, Yao D, et al. Transient high glucose causes persistent epigenetic changes and altered gene expression during subsequent normoglycemia. *J Exp Med*. 2008;205(10):2409-2417.
207. Papayannopoulou T. Current mechanistic scenarios in hematopoietic stem/progenitor cell mobilization. *Blood*. 2004;103(5):1580-1585.
208. Yamazaki K, Allen TD. Ultrastructural morphometric study of efferent nerve terminals on murine bone marrow stromal cells, and the recognition of a novel anatomical unit: the "neuro-reticular complex". *Am J Anat*. 1990;187(3):261-276.
209. Mendez-Ferrer S, Michurina T, Ferraro F, et al. Stem cell pairs, mesenchymal and hematopoietic, form a unique niche in the bone marrow. *Nature*. 2010.
210. Rosengard-Barlund M, Bernardi L, Fagerudd J, et al. Early autonomic dysfunction in type 1 diabetes: a reversible disorder? *Diabetologia*. 2009;52(6):1164-1172.
211. Straznicky NE, Eikelis N, Lambert EA, Esler MD. Mediators of sympathetic activation in metabolic syndrome obesity. *Curr Hypertens Rep*. 2008;10(6):440-447.
212. Fadini GP, de Kreutzenberg SV, Boscaro E, et al. An unbalanced monocyte polarisation in peripheral blood and bone marrow of patients with type 2 diabetes has an impact on microangiopathy. *Diabetologia*. 2013;56(8):1856-1866.
213. Nagareddy PR, Murphy AJ, Stirzaker RA, et al. Hyperglycemia promotes myelopoiesis and impairs the resolution of atherosclerosis. *Cell Metab*. 2013;17(5):695-708.
214. Park D, Spencer JA, Koh BI, et al. Endogenous bone marrow MSCs are dynamic, fate-restricted participants in bone maintenance and regeneration. *Cell Stem Cell*. 2012;10(3):259-272.

FIGURES

Figure 1:

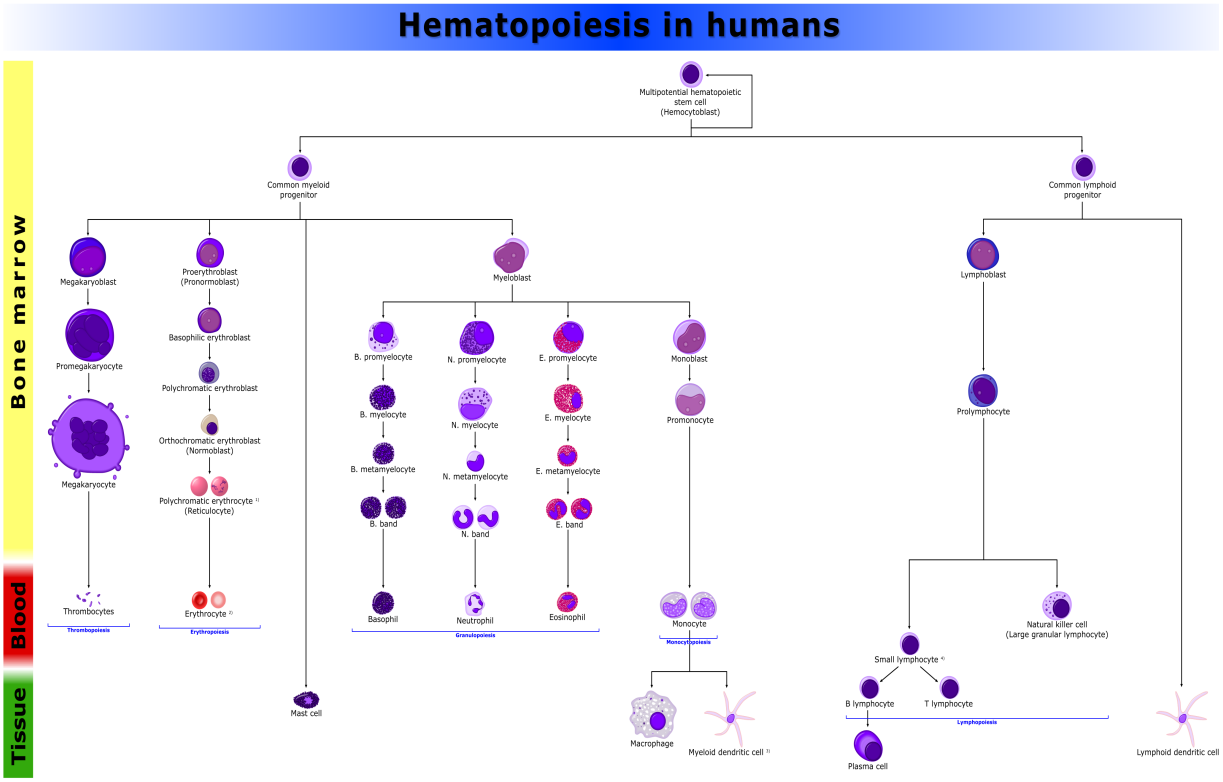

Figure 1 – Simplified hierarchic view of hematopoiesis. Long-term HSCs (LT-HSC) give rise to short term HSCs (ST-HSC) which give rise to progenitor cells. The progenitor cells proliferate and differentiate into different lineages of terminally differentiated cells. (Figure adapted Wikipedia [C. Pina, 2007]).

Figure 2:

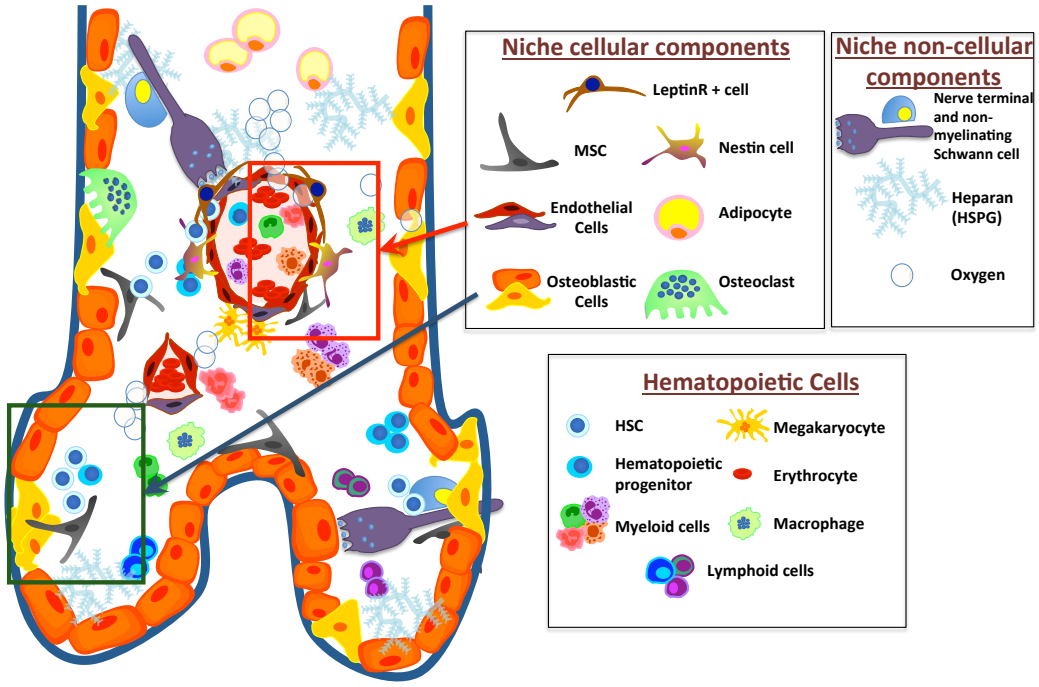

Figure 2: Schematic depicting the microanatomy of the normal hematopoietic stem cell niche. The normal bone marrow microenvironment consists of a variety of cell types including osteoblasts, osteoclasts, mesenchymal stem cells, adipocytes, endothelial cells, perivascular reticular cells, sympathetic neurons, macrophages, and other hematopoietic cells. The location, proliferation, differentiation, and quiescence of hematopoietic stem cells are regulated by cytokines secreted by constituents of the bone marrow microenvironment, the extracellular matrix, the oxygen tension, and the nervous system

Figure 3

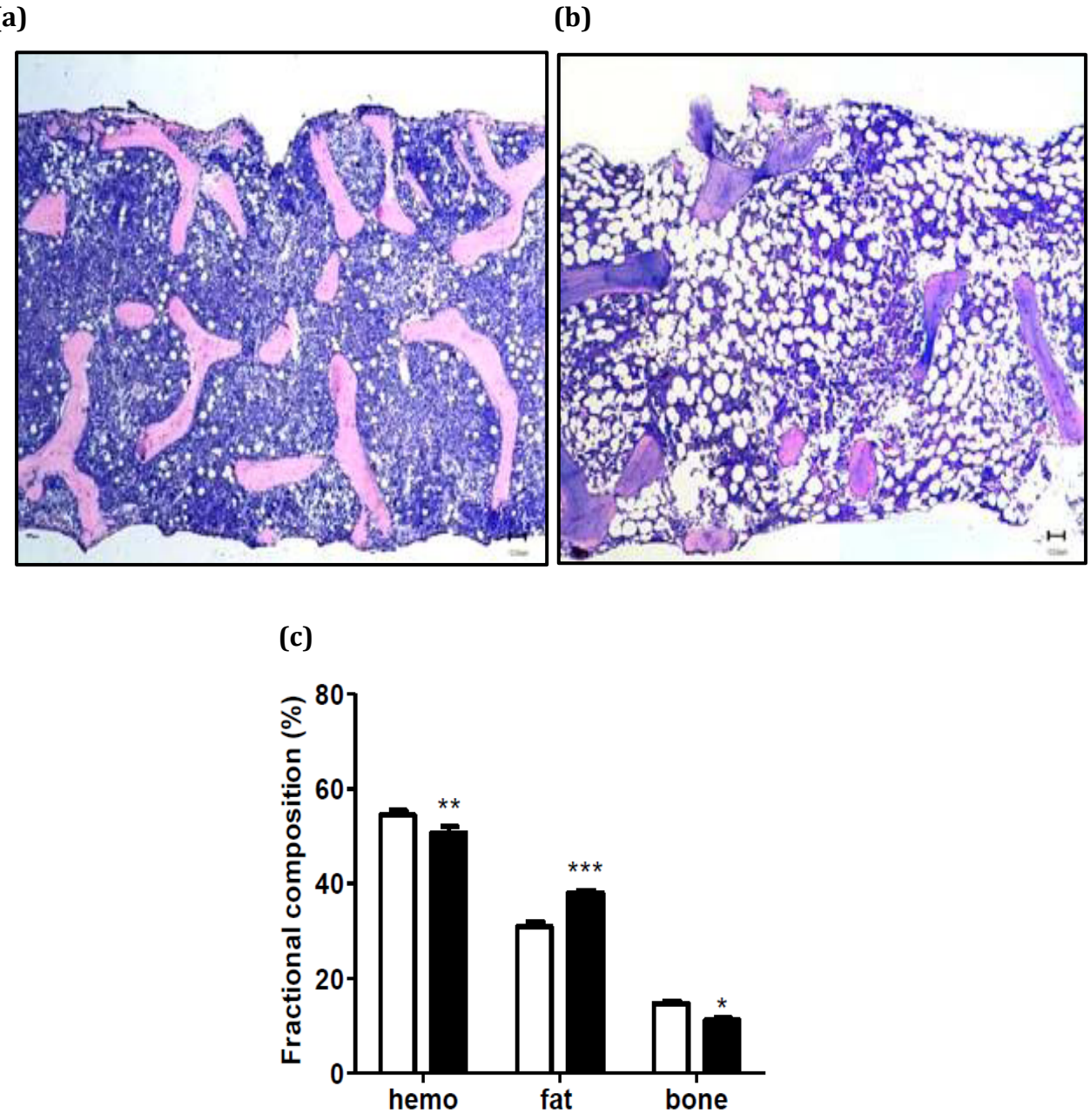

Figure 3: Diabetes significantly alters the microarchitecture of the Bone Marrow. Sections if iliac crest biopsies from patient without (a) and with (b) diabetes (May Grunwald Giemsa). Scale bar 10 μm. Scale bar representing the % in fractional composition between hemopoietic tisse, fat and bone in diabetic and non diabetic individual. N=16, *p<0.05, **p<0.01, ***p<0.001.

Figure 4

(a)

2004-2008: Bone Marrow Transplantation Unit-University of Parma

	Total Mobilization	Non DM	DM
Number	98 (100%)	84 (85.7%)	14 (14.3%)
Good Mobilizers > 20 CD34⁺ cells/uL	81 (82.65%)	79 (94%)	2 (14.3%)
Poor Mobilizers < 20 CD34⁺ cells/uL	17 (17.35%)	5 (6%)	12 (85.7%)

DM: Diabetes Mellitus

Mobilization regiment: chemotherapy + G-CSF

(b)

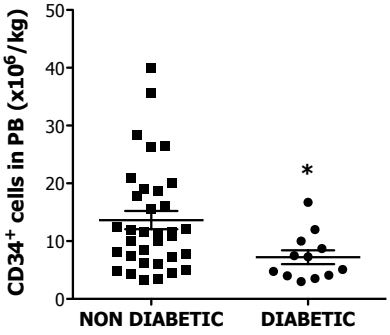

(c)

(d)

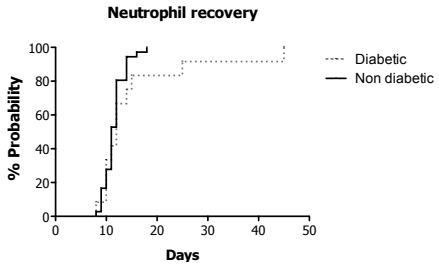

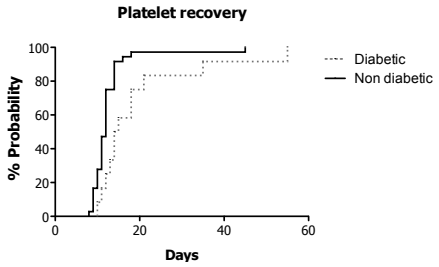

(e)

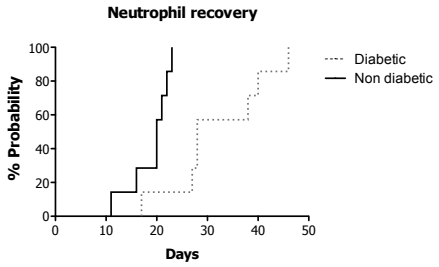

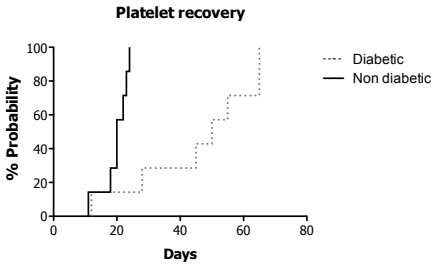

(f)

Patient	Age	Sex	Glucose (mg/dL)	Years of diabetes	HBA1C	Disease	No preTx	Mobilization regimen	CD34⁺ (x10⁶/kg)	BM (x10⁶/kg)	Insulin (U/day)
Diabetic	67	M	100	0.5		MM	2	ICE	7.29		20
	67	F	120	2	8	MM	2	ICE	12		28
	57	F	185	1.4	9.1	MM	2	Cyclophosphamide	4.4		14
	63	M	137	2.2	8.9	MM	2	Cyclophosphamide	16.7		8
	43	M	177	0.8	6.8	MM	2	Cyclophosphamide	7.5		24
	58	M	200	3.4	8.3	MM	2	Cyclophosphamide	3.53		30
	61	M	111	2.8	8.5	L	4	RDHAP	3		20
	49	M	258	0.9		MM	2	ICE	4.1		16
	56	F	290	0.7		L	4	RDHAP	4.75		22
	55	F	213	5.2	8.4	MM	2	Cyclophosphamide	5.05		18
	39	F	165	3.2	7.9	MM	2	Cyclophosphamide	10		14
	62	F	201	5.1		MM	1	Cyclophosphamide	8.7		12
	56	F	110	4	7.6	AL	2	FLAG	FAILURE	180	24
	55	M	230	2.4	8.1	AL	2	DNR-ARAC	FAILURE	214	28
	58	M	140	3.3	8.4	MM	2	Cyclophosphamide	FAILURE	112.5	22
	54	F	134	3.9	7.7	AL	2	DNR-ARAC	FAILURE	160	18
	61	M	245	0.6	6.7	AL	3	DNR-ARAC	FAILURE	257.2	12
	62	F	303	5.3	8.2	AL	2	DNR-ARAC	FAILURE	150	24
	59	M	98	4.8	9.1	AL	3	DNR-ARAC	FAILURE	211	20
Non diabetic	28	M	80			AL	2	DNR-ARAC	28.3		
	51	F	84			MM	2	Cyclophosphamide	8.5		
	60	F	76			MM	2	Cyclophosphamide	15.6		
	69	M	90			AL	2	DNR-ARAC	3.3		
	64	M	80			MM	2	Cyclophosphamide	12.1		
	69	F	92			L	4	DNR-ARAC	10		

Figure 3: Diabetes reduces G-CSF-induced HSPC mobilization and engraftment in humans. (a) Table showing the actual numbers (and percentages) of patients mobilized with more than (good mobilizers) or less than (poor mobilizers) 20 $CD34^+$ cells /uL. Overall 22.6% (14/62) rate of mobilization failure. Frequency of diabetes is 50% (7/14) in poor vs. 25% (12/48) in good mobilizers (p=0.102) (b) Glucose levels (mg/dl) in good mobilizers versus poor mobilizers. Scatter plot showing mean ± s.e.m. Higher glucose levels are found in poor mobilizers (n=62, **p<0.01). (c) Number of $CD34^+$ cells per kg in the PB of patients mobilized with 10 ug/kg/day G-CSF. Scatter plot showing mean ± s.e.m., n=36 non diabetic and n=12 diabetic. Diabetic patients mobilize $CD34^+$ cells more poorly (n=48, * p<0.05), even among good mobilizers. (d) Curves representing probability of neutrophil (left) and platelet (right) engraftment in patients receiving mobilized $CD34^+$ autologous cells. Diabetic patients exhibit trend towards longer neutrophil recovery (n=12, p= 0.146) and longer time to platelet engraftment (p=0.006). (e) Curves representing probability of neutrophil (left) and platelet (right) engraftment in patients receiving BM harvested autologous cells. Diabetes is associated with slower engraftment of both neutrophil and platelet (n=7, p=0.002 and p=0.003 respectively). (f) Details of the human caseload included in the study. Columns represent (from left to right): age; sex; glucose levels at the time of admission; years from the onset of the diabetes; HBA1C: glycate hemoglobin levels (%); hematologic disease; No preTx: number of chemotherapy cycles administered to the patient before the mobilization; type of mobilization regimen; amount of CD34+ cells collected; amount of mononuclear cells harvested from the BM (data applicable just for the poor mobilizers); daily dose of insulin in diabetic subjects.

Figure 5

(a)

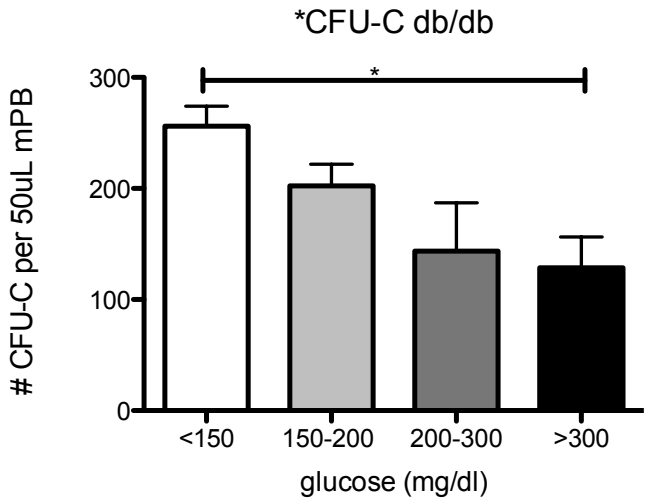

(b)

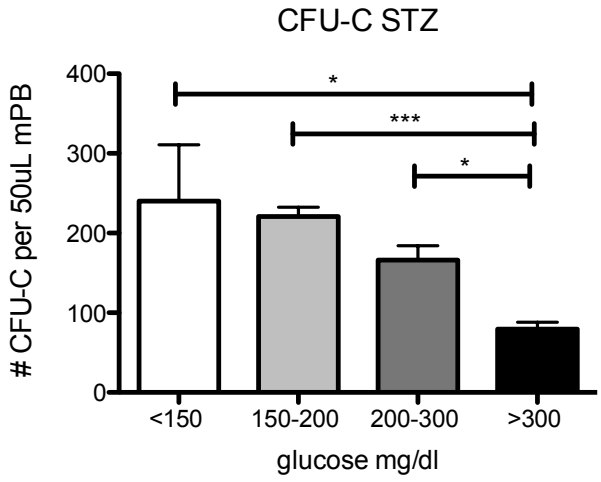

Figure 5: **Diabetes reduces G-CSF-induced HSPC mobilization.** Histogram plot representing the number of CFU-C per 100ul G-CSF-mobilized peripheral blood, obtained from db/db (a) or STZ-treated (b) mice with different glucose leves. Columns represent mean ± s.e.m., n=12, * $p<0.05$, *** $p<0.001$.

Figure 6

(a)

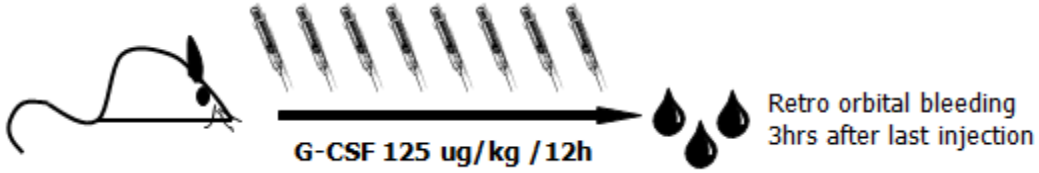

(b) **(c)**

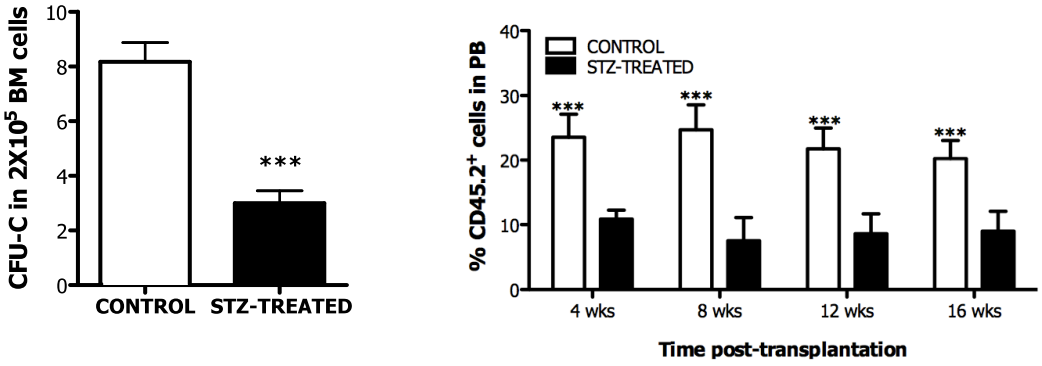

Figure 6: STZ-induced diabetes impairs G-CSF triggered mobilization in mice.

(a) Schematic representation of the experimental procedure for the G-CSF triggered mobilization regiment. (b) Number of CFU-C per 150 ul G-CSF-mobilized peripheral blood cells, obtained from STZ-treated or control mice. Columns represent mean ± s.e.m., n=12, *** $p<0.001$. (c) Percentages of total $CD45.2^+$ donor derived cells in the peripheral blood of lethally irradiated SJL recipients transplanted with 200ul of G-CSF mobilized PB from C57Bl/6 diabetic or control mice as assessed by FACS analysis at regular time intervals. Columns represent mean ± s.e.m., n=12 *** $p<0.001$; ** $p<0.01$.

Figure 7

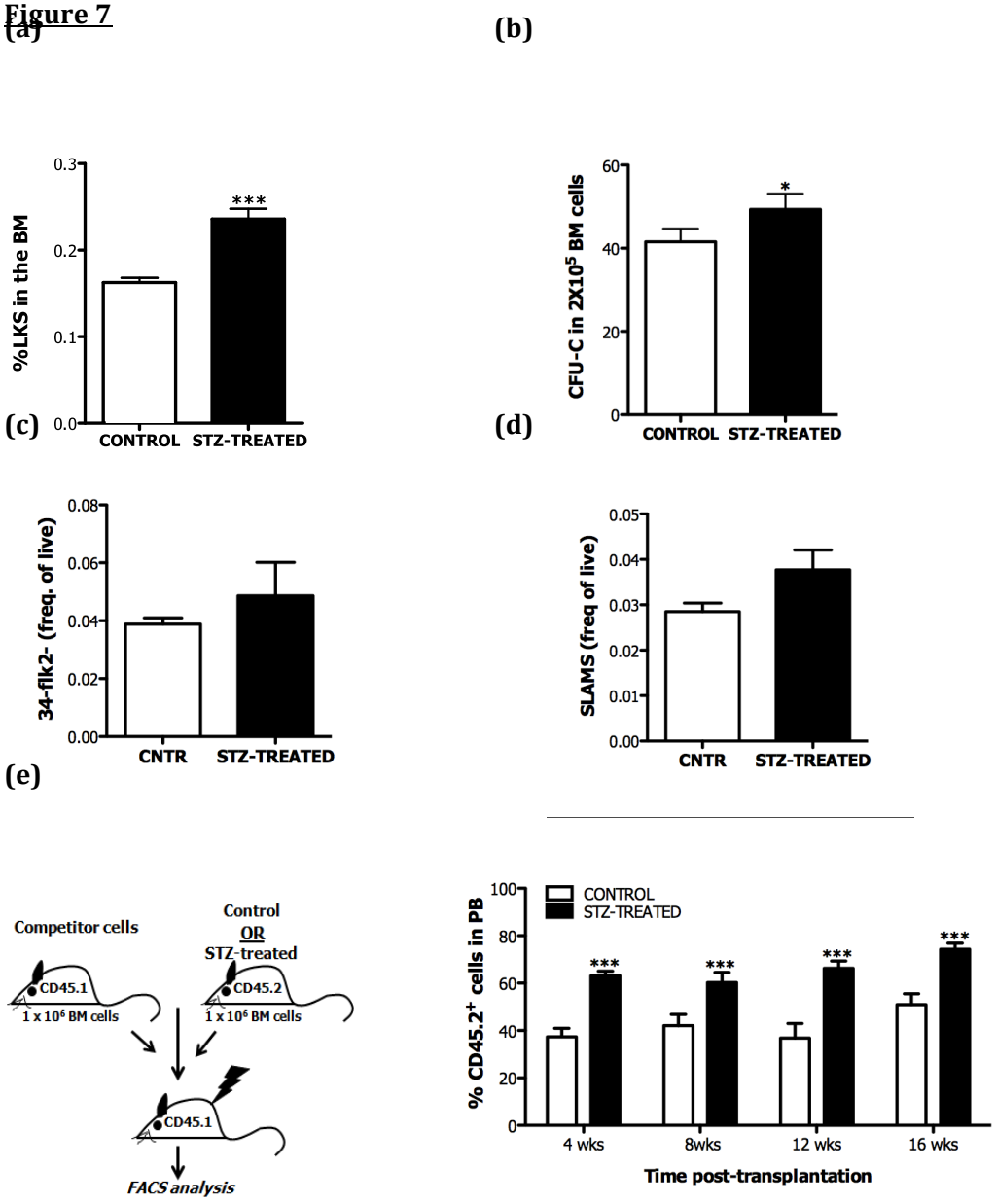

Figure7: Characterization of the haemopoietic compartment in the BM of STZ-treated animals. (a) Immunophenotypic enumeration of the percentages of LSK by flow cytometry in the BM of STZ-treated or control mice. Data are mean ± s.e.m., n=24 *** $p<0.001$. (b) CFU-C numbers of BM cells obtained from STZ-treated and control mice. Data are mean ± s.e.m., n=6, * $p<0.05$. (c) Percentages of LT-HSC $Lin^-Sca^+cKit^+CD150^+CD48^-$ and (d) $Lin^-Sca^+cKit^+Flk2^-CD34^-$ in the BM of STZ-treated or control mice as assessed by flow cytometry. Data are mean ± s.e.m., n=8. (e) Schematic representation of the transplantation experiment to assess the number/functionality of BM cells from STZ-induced diabetic mice. (f) Donor-derived $CD45.2^+$ cell engraftment 4, 8, 12 and 16 weeks after transplantation in the peripheral blood of secondary SJL recipient mice transplanted with bone marrow isolated

from STZ-treated or control mice and mixed with equal amount of CD45.1 competitor cells. Columns represent mean ± s.e.m., *** $p<0.001$.

Figure 8

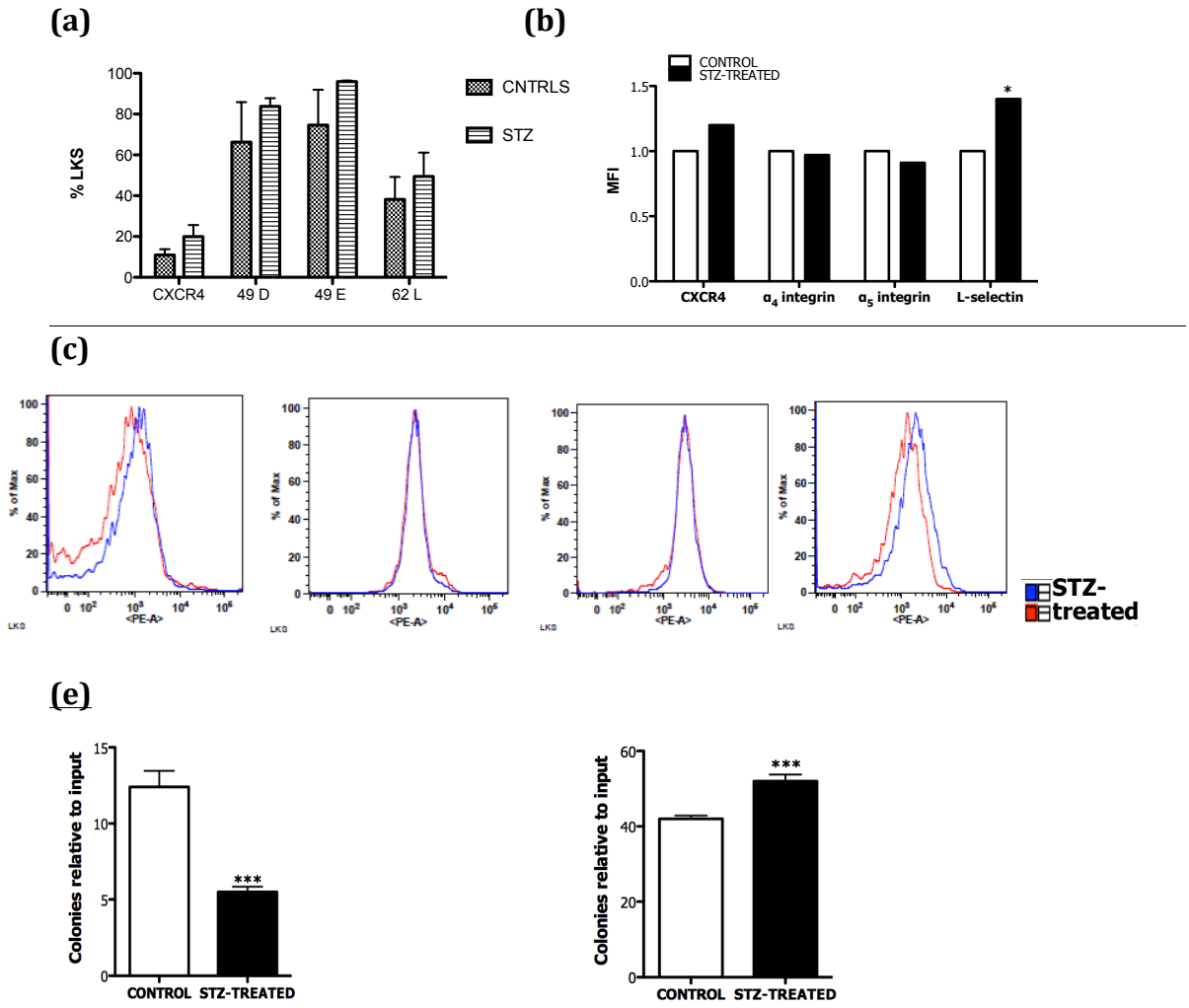

Figure 8: Diabetes alters adhesion, migration and surface molecules expression in BM-HSPCs **(a)** CFU-C relative mean number ± s.e.m from the migrated FACS-sorted LSK from STZ-treated or control mice toward the SDF-1 in a transwell assay, n=6, *** p<0.001. (**b**) CFU-C relative mean number ± s.e.m representing the adhesive LSK content within 4 hours from FACS-sorted LSK from control or STZ-treated mice plated in fibronectin coated 24-well plates. Data are mean number relative to control ± s.e.m., n=6, *** p<0.001. (**c**) % LSK and mean fluorescence intensity values (**d**) of two different experiments showing the expression levels of CXCR4, 49D (α4 integin), 49E (α5 integin), and L-selectin in LSK isolated from STZ-treated and control mice (**e**) representative FACS plots.

Figure 9

(a)

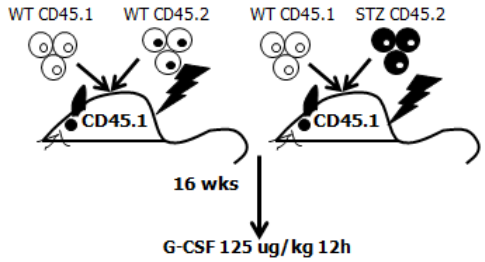

(b)

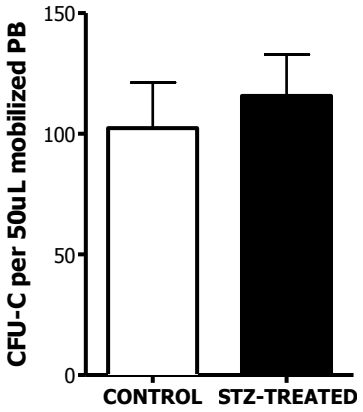

(c)

CONTROL	45.1 baseline	45.1 post G-CSF	45.2 baseline	45.2 post G-CSF
#1	50.8	54.5	45.1	42.7
#2	23.9	22.5	73	76
#3	33.8	44.6	47.6	52.6
#4	38.6	41.6	57.7	56.5
#5	65.4	62.7	29.3	30.8
#6	61.3	62.7	36.4	34.3
#7	41.5	46.8	52.4	50
#8	46.8	37.2	52.3	59.9

STZ	45.1 baseline	45.1 post G-CSF	45.2 baseline	45.2 post G-CSF
#9	23.7	27.2	65.1	70.3
#10	13.3	32.3	81.2	65
#11	13.6	14	83.8	83.8
#12	27.6	27.8	69.5	70
#13	31.4	15.4	66.5	82.3
#14	12.2	12.8	86.1	85.4
#15	30.6	32.9	64	64.5
#16	14.5	15.9	83.7	81.3
#17	20.9	20.4	74.8	76.8

(d)

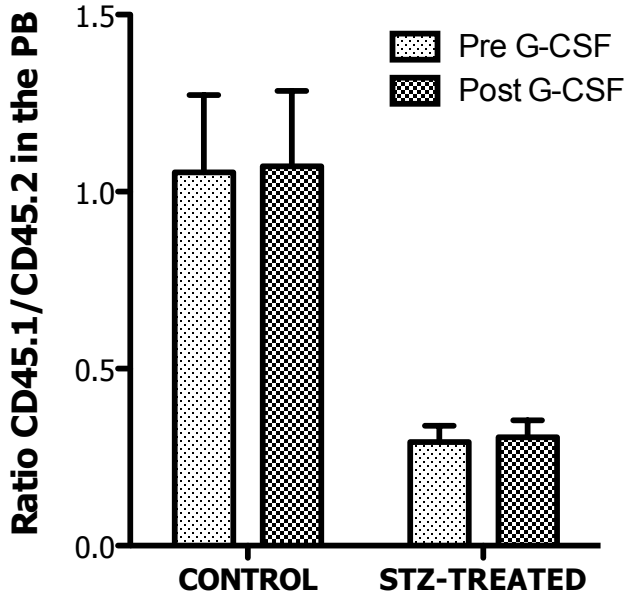

Figure 9: Altered mobilization ability in diabetic mice is not cell autonomous.
(a) Schematic representation of the procedure followed to assess whether the inhibition of mobilization is cell autonomous or microenviroment dependent. Lethally irradiated SJL recipients were transplanted with 200ul mobilized PB from STZ-treated or control mice, along with $1x10^6$ CD45.1 support cells. 16 weeks after transplantation the SJL recipients from the two groups underwent the G-CSF mobilization regiment (eight i.p injections of 125ug/kg G-CSF every 12 hours). (b) Number of CFU-C in the PB of recipients transplanted with STZ-treated or control cells after the induction of mobilization with G-CSF. Columns represent mean ± s.e.m., n=6. (c) Actual numbers and ratio (d) of CD45.1 and CD45.2 positive cells in the peripheral blood of recipient mice transplanted with STZ-treated or control cells before and after mobilization with G-CSF treatment. Columns represent mean ± s.e.m., n=9 and 8 mice respectively.

Figure 10

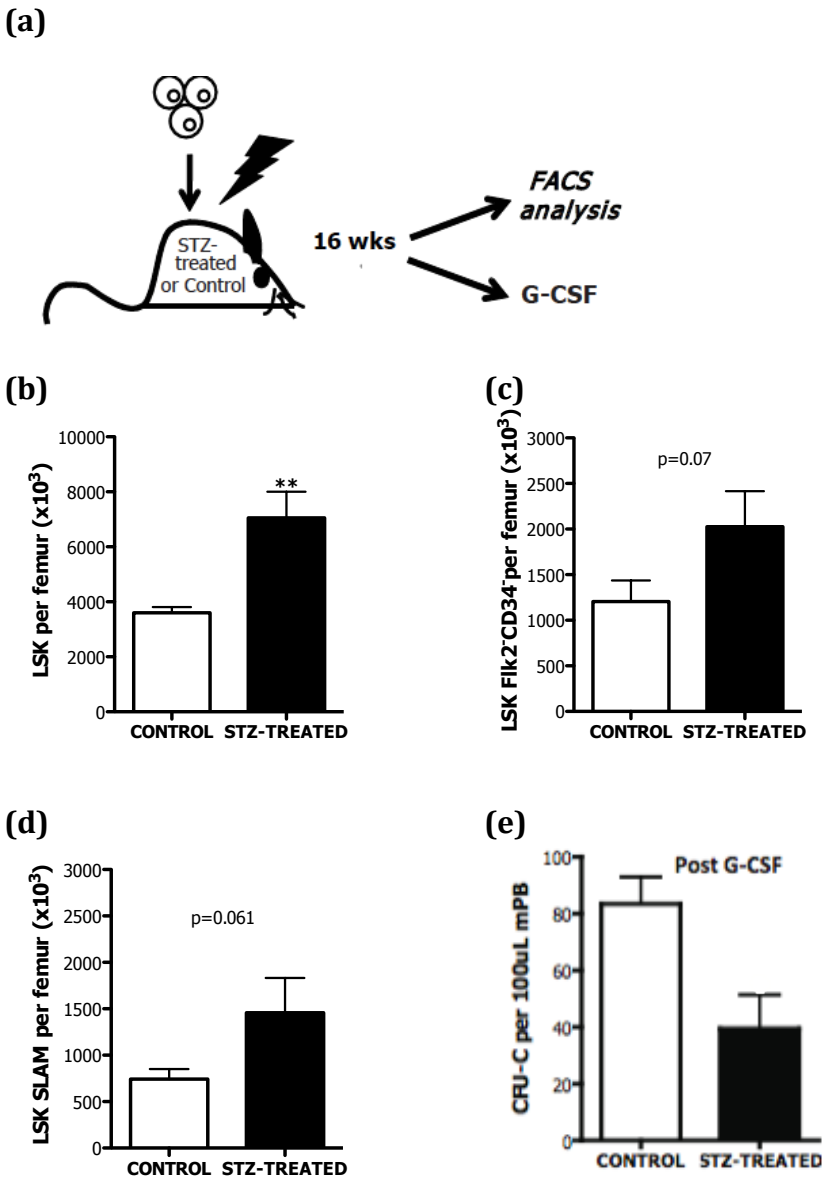

Figure 10: **The defect in HSPC mobilization is host imposed.** (a) Schematic representation of the reverse experiment in which 15 STZ-treated and control C57Bl6 mice were transplanted with wild type CD45.1 whole bone marrow cells. After 16-weeks 10 mice were evaluated for LSK and LT-HSC numbers. 5 mice underwent G-CSF mobilization therapy followed by blood collection and evaluation of CF-U-C number. (b) Graph bars represent number of LKS per femur. Data are mean ± s.e.m., n=10, * $p<0.05$. Number per femur of LT-HSC Lin- $Lin^{-}Sca^{+}cKit^{+}Flk2^{-}CD34^{-}$ (c) and $Lin^{-}Sca^{+}cKit^{+}CD150^{+}CD48^{-}$ and (d) as assessed by flow cytometry. Data are mean ± s.e.m., n=10. (e)Number of CFU-C per 100ul G-CSF-mobilized peripheral blood from STZ-treated and control mice 16 weeks after transplantation, data are mean ± s.e.m., n=5, * $p<0.05$.

Figure 11

(a)

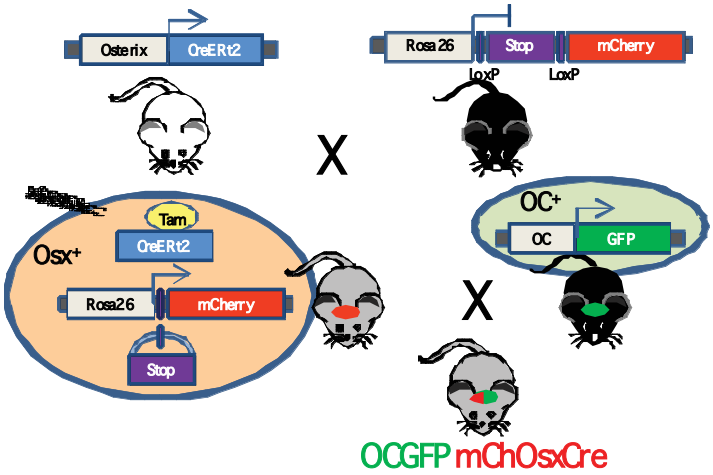

(b)

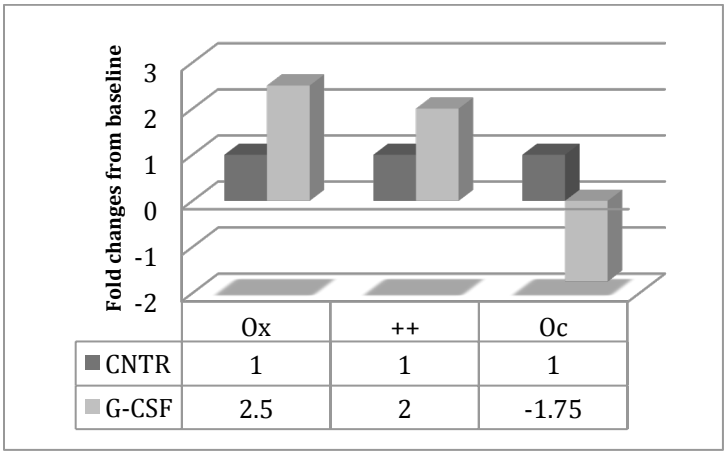

Figure 11: **Among osteolineage cells Osteocalcin subset inhibition is associated with G-CSF treatment**.(a) Schematic of the crosses performed to obtain the triple mouse model. Osterix-Cre (OsxCre) mice were crossed with the Rosa26-loxP-stop-loxP-mCherry reporter mice (mCh), which express mcherry fluorescent protein upon Cre mediated excision of a stop sequence. OsxCre+;Rosa-mCh+ mice were then crossed with the osteocalcin-GFP (OCGFP) mice. In the OsxCre+;Rosa-mCh+;OCGFP+ mice upon tamoxifen injection the osterix positive cells (Osx) and their progeny are labeled red and the osteocalcin-producing cells (OC) are labeled green. Cells that have expressed osterix within the days post tamoxifen injection and are currently producing are double positive for red and green (++) (b) Bar graph are fold changes in the number of osteoblastic cells after G-CSF as measured by flow cytometry. Data are normalized to the number of cells in PBS-treated control mice. n=6. The experiment was performed twice with 3 mice per group.

Figure 12:

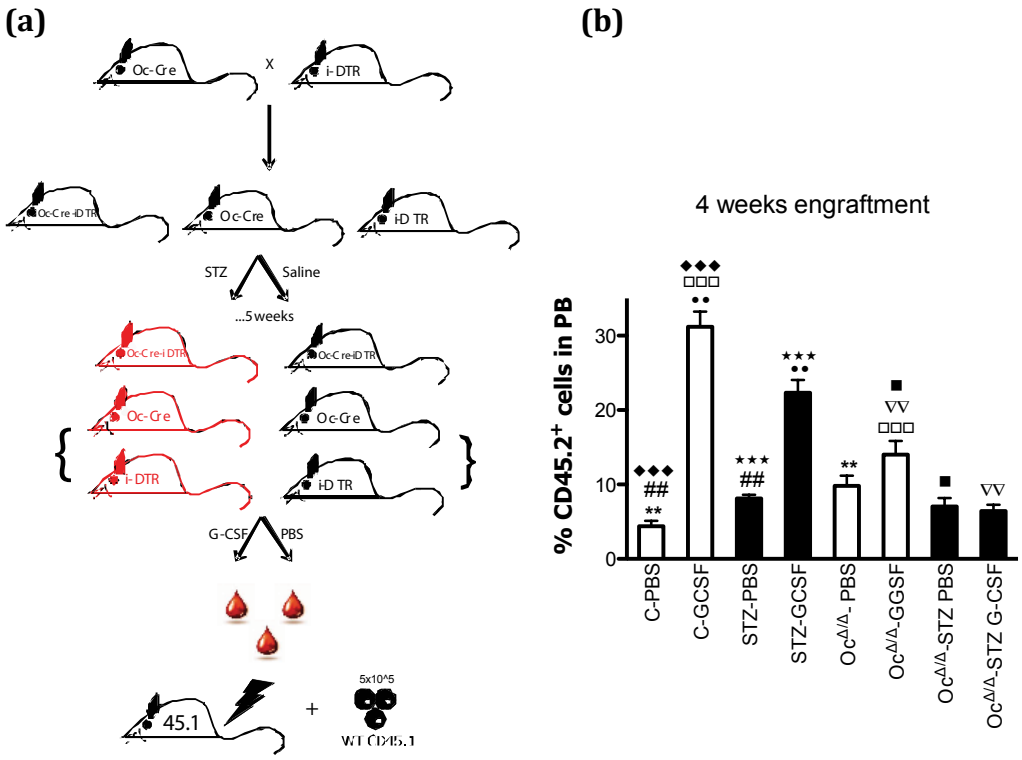

Figure 11: (a) Schematic representation of the experimental design used to selectively disrupt osteoblastic cells (see methods). (b) Donor-derived CD45.2+ cell engraftment 4 weeks after transplantation of mobilized peripheral blood in lethally irradiated SJL recipients. Columns represents mean± s.e.m., n=8 in each group, ◆◆◆, □□□, ★★★ p<0.001 **, ●●, ▽▽, ## p<0.01, ■ p< 0.05

Figure 13

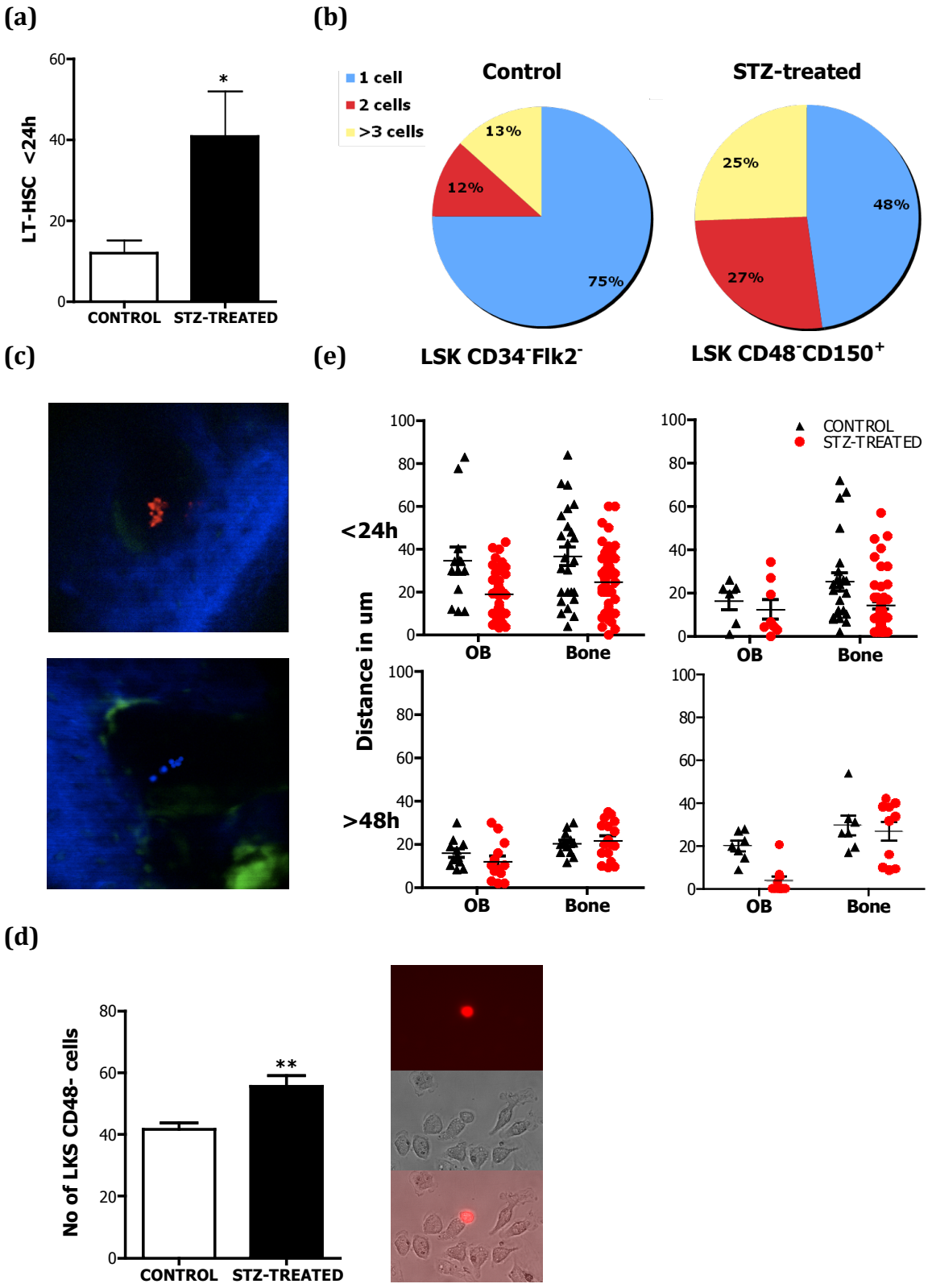
(a)
(b)
(c)
(d)
(e)
LT-HSC <24h
CONTROL
STZ-TREATED
1 cell
2 cells
>3 cells
Control
STZ-treated
13%
12%
75%
25%
48%
27%
LSK CD34-Flk2-
LSK CD48-CD150+
<24h
>48h
Distance in um
OB
Bone
CONTROL
STZ-TREATED
No of LKS CD48- cells

(f) **(g)**

Figure 12: Bone marrow microenvironment from diabetic mice augments adhesiveness of normal stem cells to osteoblasts and increases their proliferation.

(a) Number of LT-HSC from not diabetic mice visualized within 24 hours in the BM cavity of control or STZ-treated recipients with the in vivo imaging. n=4, * $p<0.05$. (b) Percentages of clusters of 1, 2 or 3 and more cells in the BM of control and STZ-treated recipients. (c) Representative pictures of the BM cavity of control and STZ-treated mice injected with equal numbers of DiD and DiI labelled HSCs. Blue=second harmonic generation (bone signal), green=Col2.3GFP OB, red=DiD labeled cells, white=DiI labeled cells. (d) Distance of the $Lin^{-}Sca1^{+}c\text{-}kit^{+}Flk2^{-}CD34^{-}$ and $Lin^{-}Sca1^{+}c\text{-}kit^{+}CD48^{-}CD150^{+}$, 24 and 48 hours after transplantation relative to the Col2.3GFP cells (OB) and the bone measure in um. (e) Number of $Lin^{-}Sca1^{+}c\text{-}kit^{+}CD48^{-}$ after 5 days co-culture with control or STZ-treated BM-originating stroma cells and representative photos showing DsRed a $Lin^{-}Sca1^{+}c\text{-}kit^{+}CD48^{-}$ cell on top of stromal cells (f) Percentage changes in SCF (*kitl*) mRNA levels in sorted $col2.3GFP^{+}$ osteoblastic cells between STZ-treated and control mice normalised to GAPDH ($\Delta\Delta$CTmethod). Columns represent mean ± s.e.m.. n=6, * $p<0.05$ (g) Percentage difference in *Cxcl12* mRNA levels in steady state condition among nestin cells and osteoblastic cells. n=6, ** $p<0.01$

Figure 14

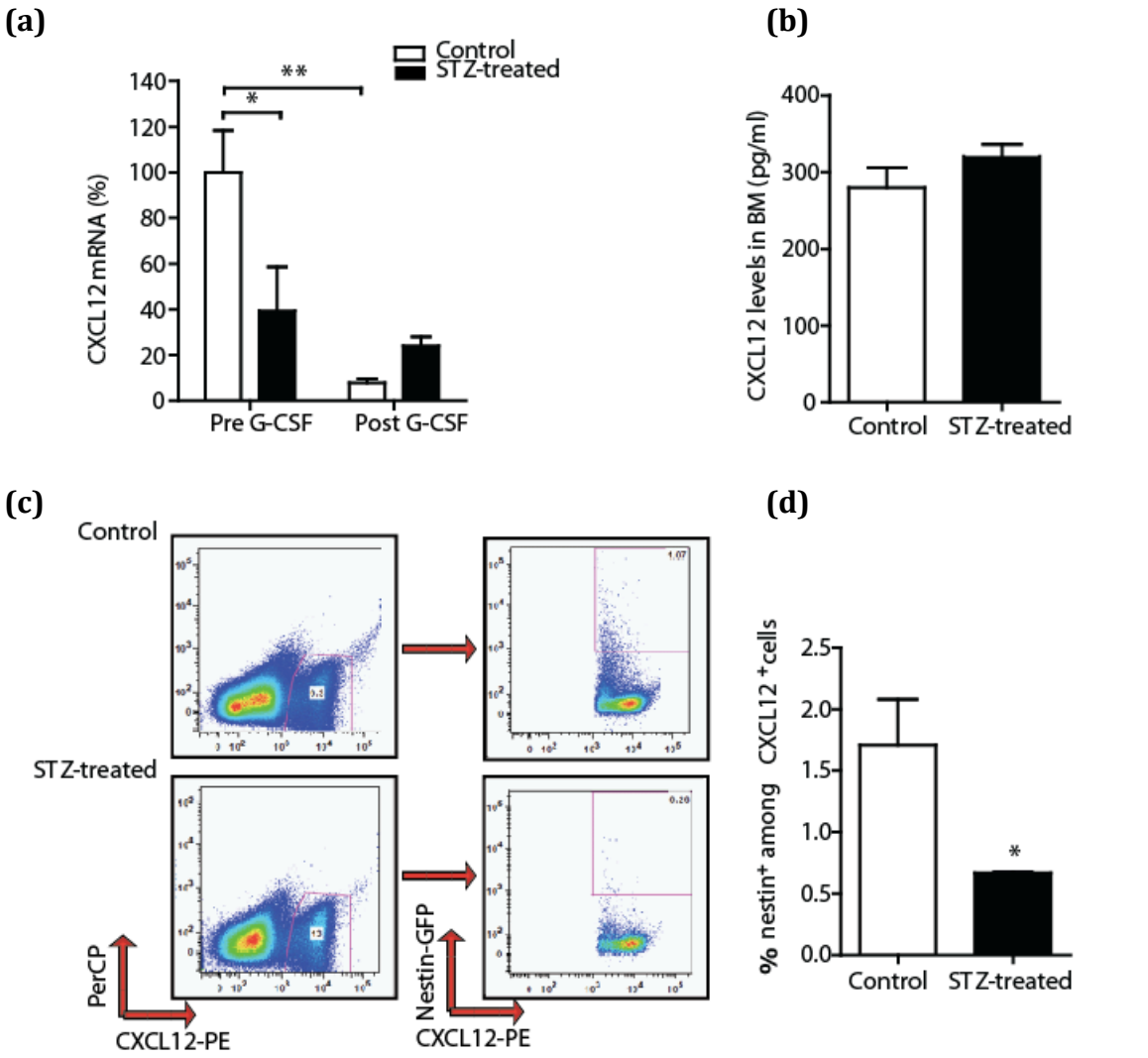

Figure 14: STZ-induced diabetic mice have aberrant expression of niche related molecules. (a) Percent changes in the expression of mRNA levels of *Cxcl12* in FACS sorted nestinGFP$^+$ cells before and after G-CSF treatment relative to control nestinGFP$^+$ cells before G-CSF treatment and normalised to GAPDH (ΔΔCTmethod). Columns represent mean ± s.e.m., n=6 * $p<0.05$ and **$p<0.01$. (B) Representative FACS plots and graph bars showing percentages of CXCL12$^+$ cells among nestin$^+$ cells. Data are mean ± s.e.m., n=6, * $p<0.05$. (C) Concentration (pg/ml) of CXCL12 in BM extracellular fluid from control and STZ-treated mice. Data are mean number ± s.e.m., n=6.2.

Figure 15

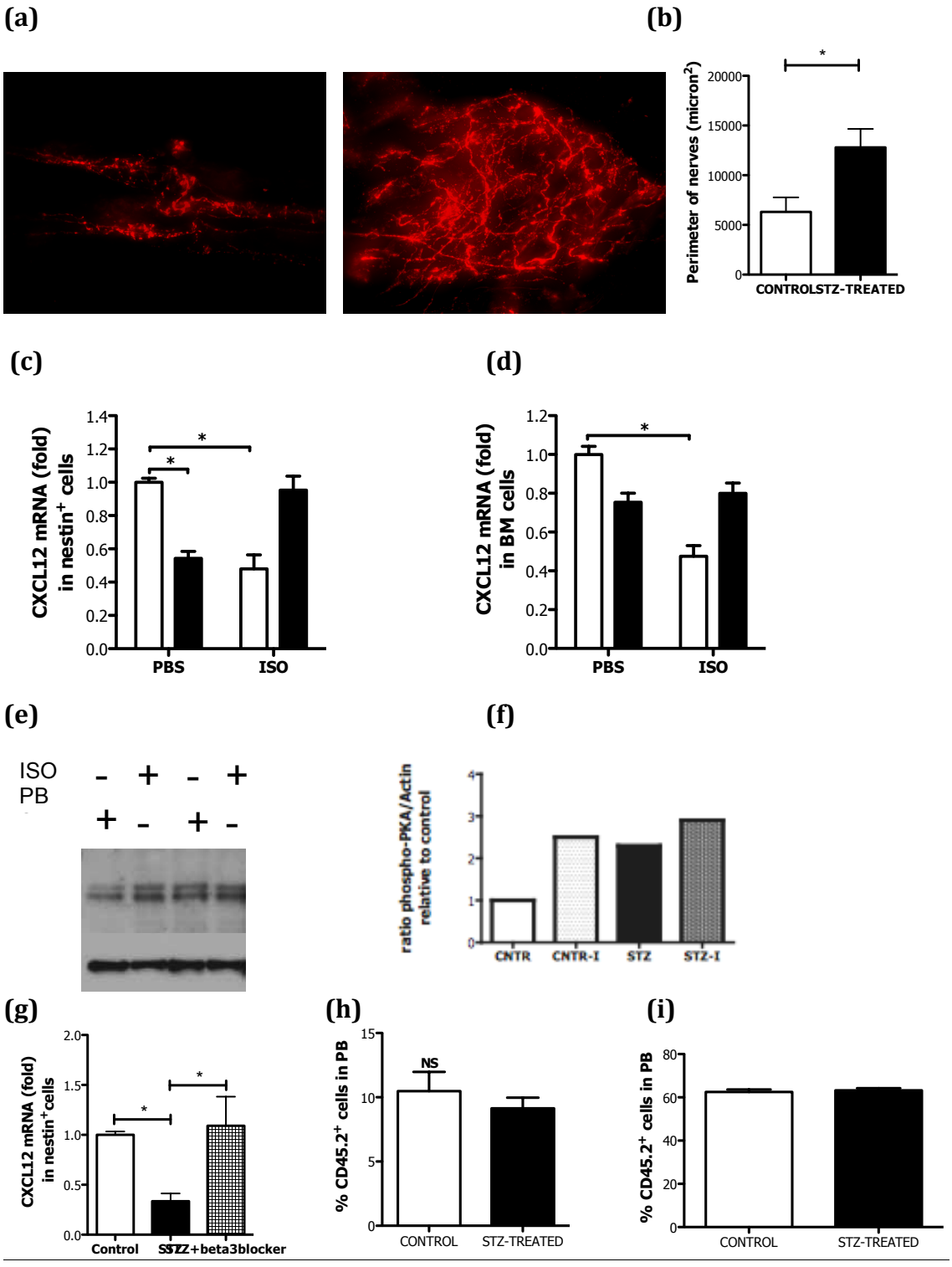
(a)
(b)
Perimeter of nerves (micron²)
20000
15000
10000
5000
0
*
CONTROL
STZ-TREATED
(c)
CXCL12 mRNA (fold) in nestin⁺ cells
1.4
1.2
1.0
0.8
0.6
0.4
0.2
0.0
*
*
PBS
ISO
(d)
CXCL12 mRNA (fold) in BM cells
1.2
1.0
0.8
0.6
0.4
0.2
0.0
*
PBS
ISO
(e)
ISO - + - +
PB + - + -
(f)
ratio phospho-PKA/Actin relative to control
4
3
2
1
0
CNTR
CNTR-I
STZ
STZ-I
(g)
CXCL12 mRNA (fold) in nestin⁺cells
2.0
1.5
1.0
0.5
0.0
*
*
Control
STZ
STZ+beta3blocker
(h)
% CD45.2⁺ cells in PB
15
10
5
0
NS
CONTROL
STZ-TREATED
(i)
% CD45.2⁺ cells in PB
80
60
40
20
0
CONTROL
STZ-TREATED

Figure 15: PNS disautonomy mediates deregulation of CXCL12 gradient. (a) Representative pictures from whole mounting of calvaria of controls (left picture) and STZ-treated mice (right picture). Red signal: tyrosine hydroxilase. Scale bar: 50 mm. Nerve terminal quantification in terms of perimeter (b) in calvaria of STZ-treated versus controls mice n=5 *p<0.05. Fold changes in the expression of mRNA levels of CXCL12 in (c) nestin+ cells (d) bone marrow from control and STZ-treated mice in baseline conditions and 2 hrs after injection of isoproterenol (5 mg/kg i.p) relative to control cells in baseline and normalised to GAPDH (ΔΔCTmethod). n=6, *p<0.5. (e) Left: Western blot showing the amount of phospho-PKA (pPKA) in sorted nestin+ cells from control (+/- isoproterenol) and STZ-treated (+/- isoproterenol) mice. Right: Histogram plot showing ratio in pPKA. (f) Fold changes in the expression of mRNA levels of *Cxcl12* in nestin+ cells from diabetic saline treated and diabetic b3 -blocker treated (5 mg/kg/day for 10 days) animals relative to non-diabetic controls. Data are normalized to GAPDH (ΔΔCTmethod). n=6, *p<0.5. Percentage of donor cell engraftment 4 weeks after transplantation of 150 mL of mobilized-PB from STZ-treated and control mice (along with whole bone marrow support cells) in congenic lethally irradiated recipients. Mice were mobilized with single dose of AMD3100 (g) or single dose of AMD3100 (h) at the end of the G-CSF mobilization regimen (h), n=5.

Figure 16

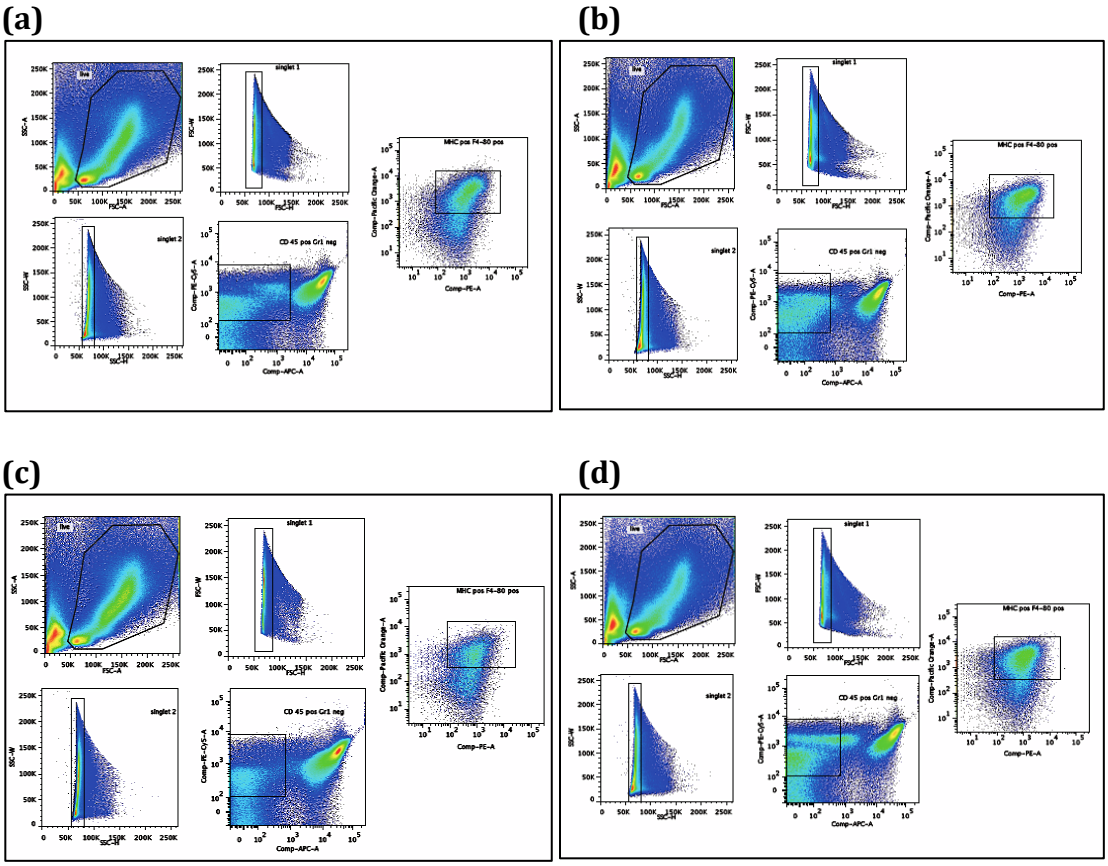

Figure 16: Diabetes increases the amount of BM macrophages. Representative FACS plots of gating strategy used to evaluate the percentages of BM macrophages

in murine BM at baseline in normal (a) or diabetic (b) conditions and after G-CSF treatment in normal (c) and diabetic mice (d). (E) Boxplot representing the % of BM macrophages in the aforementioned conditions. N=3 per group, *p<0.5, **p<0.01, ***p<0.001.

Figure 17

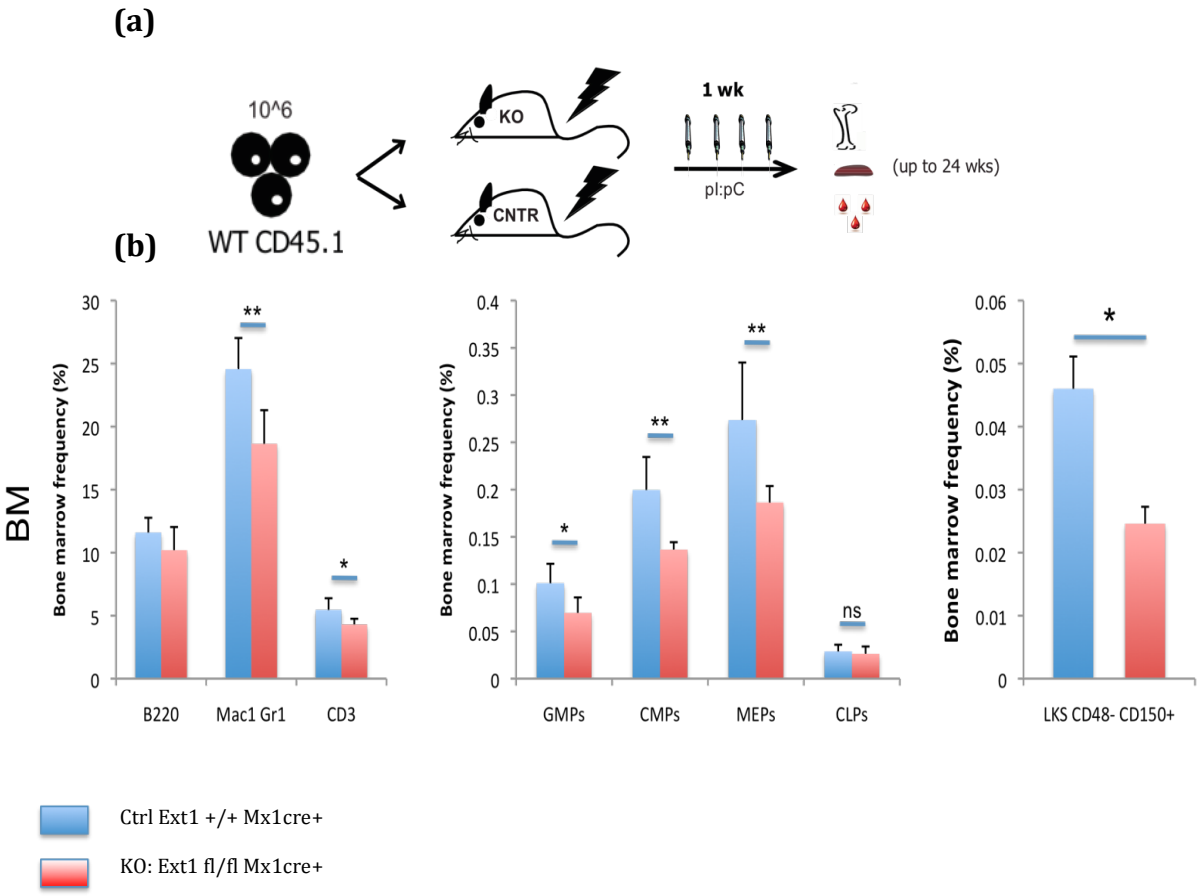

Figure 17: EXT1 influences HSPC localization. EXT1 control (WT) or deleted (WT) animals were evaluated for localization of WT hematopoietic cells 16 weeks following transplantation. These data indicate that EXT1 in the microenvironment is critical for the retention of HSPC and that EXT1 deletion results in HSPC

mobilization. (a) Scheme of experimental design. (b) Bar graph representing hematopoietic compartments at various stages of maturation in WT versus Ext1 KO animals in the BM. (c) Bar graph representing hematopoietic compartments at various stages of maturation in WT versus Ext1 KO animals in the spleen. N=5, * $p<0.05$, * *$p<0.01$, *** $p< 0.001$

Figure 18:

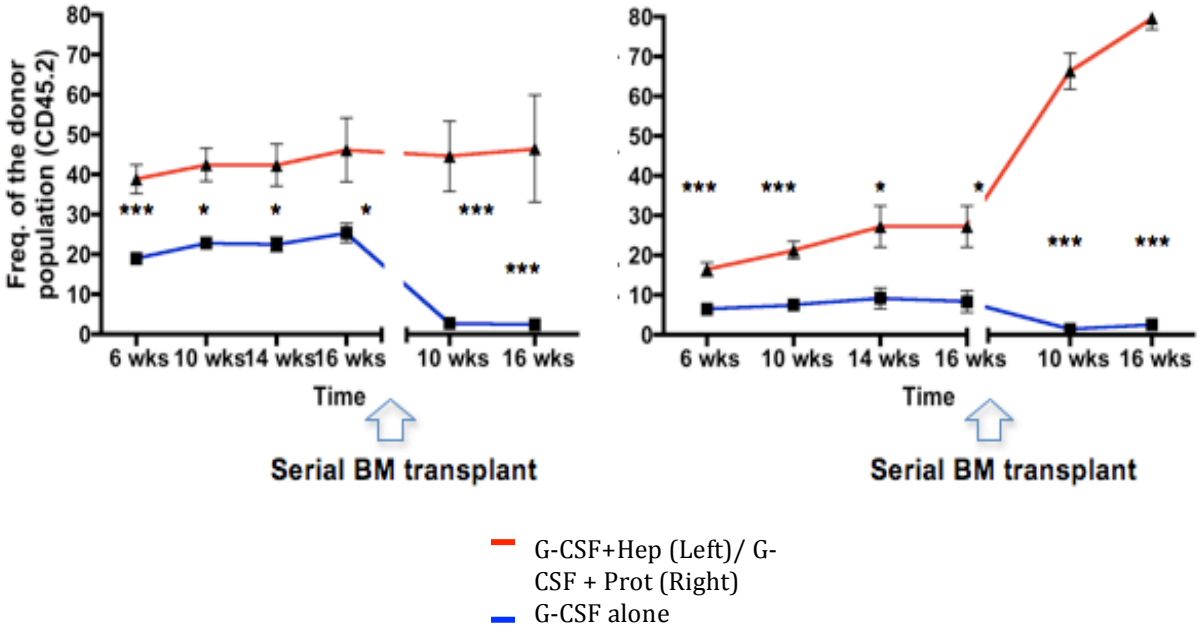

Figure 18: ***Heparan sulfate inhibitors are additive to G-CSF in mobilizing HSPC.*** Results of transplantation with blood from donor undergoing mobilization with either G-CSF alone or in combination with the heparan sulfate inhibitors, heparin or protamine sulfate. Curves representing recipients' engraftment at different timepoints. Advantage in engraftment in groups mobilized with combination of G-CSF with heparin or protamine is even more pronounced in secondary recipients (blue arrow indicates secondary transplant).

Figure 19

(a)

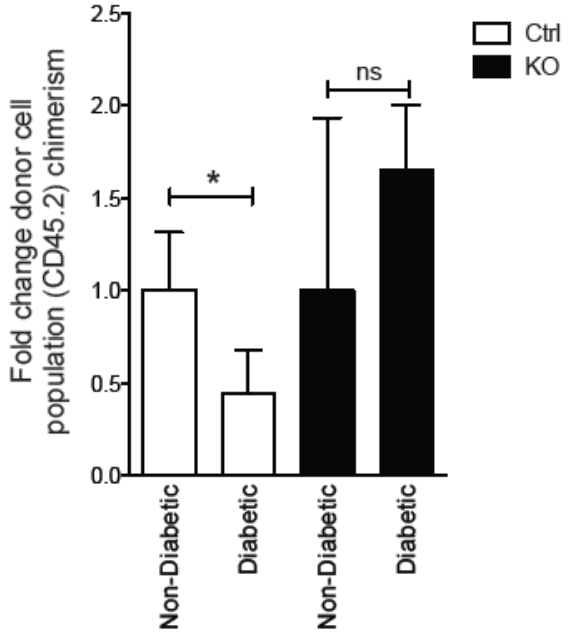

(b)

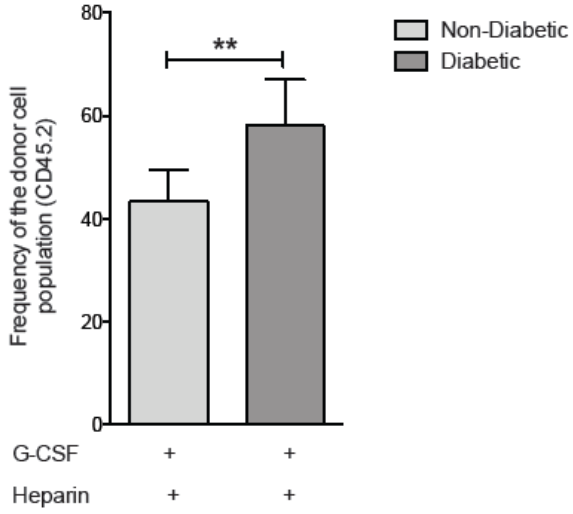

Figure 19: EXT-1 inhibition restores normal mobilization in diabetic mice. (a) Histogram plots representing fold changes in engraftment in mice transplanted with peripheral blood collected from EXT1 KO mice with and without diabetes. N=8,

*p<0.01 (b) Histogram plots representing engraftment in recipient mice transplanted with peripheral blood from mice with and without diabetes mobilized with G-CSF alone or with combination of G-CSF and heparin. N=10, **p<0.01.